INFORMATION TO USERS

This manuscript has been reproduced from the microfilm master. UMI films the text directly from the original or copy submitted. Thus, some thesis and dissertation copies are in typewriter face, while others may be from any type of computer printer.

The quality of this reproduction is dependent upon the quality of the copy submitted. Broken or indistinct print, colored or poor quality illustrations and photographs, print bleedthrough, substandard margins, and improper alignment can adversely affect reproduction.

In the unlikely event that the author did not send UMI a complete manuscript and there are missing pages, these will be noted. Also, if unauthorized copyright material had to be removed, a note will indicate the deletion.

Oversize materials (e.g., maps, drawings, charts) are reproduced by sectioning the original, beginning at the upper left-hand corner and continuing from left to right in equal sections with small overlaps.

Photographs included in the original manuscript have been reproduced xerographically in this copy. Higher quality 6" x 9" black and white photographic prints are available for any photographs or illustrations appearing in this copy for an additional charge. Contact UMI directly to order.

Bell & Howell Information and Learning
300 North Zeeb Road, Ann Arbor, MI 48106-1346 USA
800-521-0600

UMI®

EVALUATION OF FLUID-TO-PARTICLE HEAT TRANSFER COEFFICIENT UNDER TUBE-FLOW CONDITIONS INVOLVING PARTICLE MOTION WITH RELEVANCE TO ASEPTIC PROCESSING

by

Mohammad Reza Zareifard

Department of Food Science and Agricultural Chemistry
Macdonald Campus of McGill University
Montreal, Canada

June, 1999

A thesis submitted to the Faculty of Graduate Studies and Research in partial fulfilment of the requirements for the degree of Doctor of Philosophy

0-612-55397-3

Suggested short Title:

HEAT TRANSFER IN TUBE-FLOW CONDITIONS INVOLVING PARTICLE MOTION

ACKNOWLEDGEMENTS

I am unable to find appropriate words to express my great appreciation and thanks to Dr. Hosahalli Subrayasastry Ramaswamy, the thesis supervisor, for his interest, understanding, advice and guidance throughout this research. Access to financial support from research funding, a well equipped laboratory, as well as encouragement to attend various scientific conferences is really appreciated and never will be forgotten.

Many thanks to all staff members and professors of the Department of Food Science and Agricultural Chemistry for the warm and friendly environment provided; especially to Dr. I. Alli, the Chairman of the department, Dr. F. R. van de Voort and the other professors who have assisted both learning and adaption to the food science program. I am also thankful to the research committee members: Dr. A. S. Mujumdar and Dr. S. O. Prasher.

Technical and scientific discussion, useful suggestions and advice is fully appreciated from Dr. Stefan Grabowski, Dr. Alain le Bail, Mr. Ali Reza Taherian, Dr. George Awuah, Dr. Shyam Sablani, Dr. S. Sreekanth, and Dr. K. Pannu.

Thanks are also extended to all friends involved in the food processing group: Ms. Carla Abbatemarco, Ms. Sarmista Basak, Dr. Sasithorn Tajchakavit, Dr. Michele Marcotte, Dr. Dinna Mussa, Mr. Pramod Pandey, Mr. Harish Krishnamurty, Ms. Mahtab Afaghi, Dr. Tatiana Koutchma, Ms. Nada Houjaij, Ms. Farideh Nourian, Ms. Lawrende Chiu and Mr. Cuiren Chen. I also wish to thank all the Iranian families and friends, who have always given help and moral support during my time at Macdonald Campus of McGill University.

I would like to dedicate this effort to my kind parents for the love and support they gave me all my life, to my wonderful wife Mansooreh and lovely daughters Zahra and Zohre, my dear brothers and sisters for their patience, understanding, support and encouragement, without all of which this study would not have been successfully completed.

ABSTRACT

The convective fluid-to-particle heat transfer coefficient (h_{fp}) is one of the critical factors influencing the process design for multi phase food products, in continuous tube-flow systems. Determination of h_{fp} associated with moving particles poses a unique challenge to investigators because of the difficulty in monitoring the temperature of moving particles without interfering with the particle motion. The majority of the previous studies have been carried out using stationary particles, with only a few exceptions. These techniques generally ignore the contribution of particle motion to heat transfer in tube-flow system. In order to account for this in the present study, two different techniques involving particle motion were developed to evaluate h_{fp} and to study the effects of factors influencing h_{fp}, associated with spherical particles under tube-flow conditions.

In the first technique, a laboratory scale apparatus was fabricated to evaluate h_{fp} under conditions imparting particle oscillatory motion while being heated in a model holding tube. Spherical Nylon particles with centrally located fine-wire flexible thermocouples, were suspended from the upper mid-section of a curved glass tube in order to provide lateral movement of the particle as the tube was subjected to oscillatory motion. A programable servo motor was used to control the frequency and amplitude of the tube, thereby keeping the particle in continuous motion. Time-temperature data were gathered continuously from the time the particle was immersed into a pre-established heating medium. The h_{fp} values were computed based on analytical solution to basic heat transfer equations.

The developed technique was then used to study factors influencing h_{fp}. A full factorial experimental design was studied involving spherical particles made of Aluminum epoxy and Nylon of different diameters (12.7 to 17.5 mm), particle linear velocities (0.06 to 0.21 m/s), heating medium viscosities (0 to 1% Carboxymethyl cellulose, CMC) and fluid temperatures (60 to 80 ^{o}C). Statistical analysis of experimental data indicated that all the above mentioned factors had a significant (p<0.001) effect on h_{fp}. Depending on experimental conditions the values of h_{fp} varied from 350 to 2000 W/m^{2}K. The fluid-to-particle heat transfer coefficient increased with particle velocity, fluid temperature, decreasing CMC concentration and particle size. Overall, h_{fp} values associated with the aluminum epoxy particle were about 30% higher than that for the Nylon particle.

A calorimetric method was developed to evaluate h_{fp} associated with a freely moving particle. The technique consisted of introducing a particle into a holding tube at an upstream location, which allowed circulation of a fluid under pre-stabilized temperature and flow, and its retrieval from a downstream location. The particle was transferred immediately into a specially constructed calorimeter and its bulk temperature was determined upon equilibration. The technique was calibrated using thermocouple equipped particles subjected to various time-temperature treatments. The associated h_{fp} was computed using an iterative numerical technique for the evaluated bulk temperature of the particle.

The calorimetric method was used to evaluate the effect of fluid flow rate, viscosity and temperature, as well as particle size on the associated h_{fp} under tube-flow conditions. Experiments were carried out using different flow rates (9 to 19 L/min), fluid viscosity (0 to 1 % CMC solution) and fluid temperature (50 to 70^{o}C) as well as Aluminum spherical particles of different sizes (19 to 25.4 mm). Values of h_{fp} varied from 650 to 2660 W/m^2K, depending on the experimental conditions, and increased significantly ($p<0.001$) with an increase in fluid flow rate and particle size, whereas a decrease was observed with CMC concentration and temperature.

Dimensionless correlations were investigated for estimating h_{fp} for spherical particles under forced convection heat transfer regimes and tube-flow conditions. The SAS computing program with multiple regression analysis and backward elimination procedures was used to obtain the best model with statistically significant parameters associated with h_{fp}. Correlations between Nusselt number and other dimensionless numbers were developed for the predictive modeling of h_{fp}, using data obtained from the particle oscillatory motion method and the calorimetric approach separately as well as a combination of all the data together. Several correlations were developed in the form of Nusselt number as a function of other influencing dimensionless numbers. Introducing the diffusivity ratio (α_p/α_f), particle-to-tube diameter ratio (d/D) and particle-to-fluid velocity ratio (V_p/V_f) were found to improve model development. Nusselt numbers estimated from the developed equations showed good agreement with the experimental data ($0.88<R^2<0.99$).

RÉSUMÉ

Le coefficient de transfert de chaleur par convection du fluide aux particules (h_{fp}) est un des facteurs les plus critiques pouvant influencer la conception du procédé aseptique pour les produits alimentaires multiphasiques se déplaçant en continu dans des tuyaux. La détermination de h_{fp} associé aux particules en mouvement représente un défi unique pour les scientifiques à cause de la difficulté de mesurer la température des particules en mouvement sans interférence avec le procédé. La majorité des études précédentes ont été réalisées avec des particules stationnaires avec quelques exceptions. Généralement, les techniques développées ignorent la contribution des particules en mouvement au transfert de chaleur dans les tuyaux. Pour tenir compte de ceci, deux techniques différentes ont été développées pour évaluer le h_{fp} et pour étudier les effets des facteurs influençant le h_{fp}, sur des particules sphériques en mouvement dans un tuyau.

Pour la première technique, un appareil de laboratoire a été fabriqué pour évaluer le h_{fp} dans des conditions oscillatoires de mouvement de particules pendant le chauffage dans un tube de retenue modèle. On a utilisé des particules en nylon sphériques dans lesquelles des thermocouples flexibles très fins ont été fixées au centre. Celles-ci ont été suspendues à la mi-section d'un tuyau courbé en verre pour permettre d'obtenir un mouvement latéral de la particule lorsque le tuyau était soumis à un mouvement oscillatoire. Un servo-moteur programmable a été utilisé pour contrôler la fréquence et l'amplitude de tuyau pour garder la particule en mouvement continu. On a enregistré les données de temps/température en continu à partir de moment où on a immergé la particule dans un médium chauffant déjà conditionné. Les valeurs de h_{fp} ont été calculées, par ordinateur, en se basant sur les solutions analytiques des équations de base de transfert de chaleur.

Par la suite, cette technique a été utilisée pour étudier les facteurs influençant h_{fp}. Un plan statistique factoriel complet a servi à l'étude de l'effet des matériaux des particules (aluminium epoxy et nylon) de différents diamètres (12.7 à 17.5 mm), des vitesses linéaires de la particule (0.06 à 0.21 m/s), des viscosités du médium chauffant (0 à 1% CMC) et des températures de fluide (60 à 80°C). L'analyse statistique des données expérimentales a démontré que tous les facteurs mentionnés avaient un effet significatif ($p<0.001$) sur le h_{fp}. En fonction des conditions expérimentales, on a trouvé des valeurs de h_{fp} qui variaient de 350 à 2000 W/m^2K. Le coefficient de transfert de chaleur du fluide aux particules augmentaient avec l'augmentation de la vitesse de la particule et de

la température du fluide et la réduction de la concentration de CMC et de la grosseur des particules. Les valeurs de h_{fp} associées avec les particules en aluminium epoxy étaient 30% plus élevées que celles obtenues avec les particules de nylon.

Une deuxième technique a été développée soit la méthode calorimétrique pour évaluer le h_{fp} associée aux particules libres de mouvement. Cette technique a consisté à introduire une particule dans un tube de retenue à une localisation précise dans un fluide en circulation à une température pré-établie et à la recueillir par la suite. Cette particule est transférée immédiatement dans un calorimètre spécialement construit et sa température globale est déterminée à l'équilibre. La technique a été calibrée en utilisant des particules équipées avec des thermocouples et qui ont été soumises à différents traitements de temps/température. Les h_{fp} ont été calculés en utilisant une méthode numérique itérative pour l'évaluation de la température globale de la particule.

Par la suite, la méthode calorimétrique a été utilisée pour évaluer l'effet des débits du fluide, de sa viscosité et de sa température ainsi que la grosseur des particules sur les valeurs de h_{fp} dans des conditions de mouvement en continu dans des tuyaux. Les expériences ont été réalisées en utilisant différents niveaux de débit (9 à 19 L/min), de viscosité (0 à 1% CMC), de température du fluide (50 à 70°C) et grosseur de particules sphériques en aluminium (19 à 25.4 mm). Des valeurs de h_{fp} ont varié de 650 à 2660 W/m^2K en fonction des conditions expérimentales. Celles-ci variaient significativement ($p<0.001$) avec une augmentation du débit et de la grosseur des particules et une réduction de la concentration de CMC et de la température.

Des correlations adimensionnelles ont été calculées pour l'estimation des h_{fp} pour des particules sphériques sous des conditions de transfert de chaleur en convection forcée et de mouvement en continu dans des tuyaux. La procédure de régression multiple par élimination de SAS a été utilisée pour obtenir le meilleur modèle avec des paramètres statistiquement significatifs pour le h_{fp}. Des correlations entre le nombre de Nusselt et d'autres nombres adimensionnels ont été développées pour la prédiction de h_{fp} en utilisant des données expérimentales générées par la méthode de mouvement oscillatoire des particules et l'approche calorimétrique séparément et ensemble. L'introduction du ratio de diffusivité (α_p / α_f), du ratio du diamètre de la particule par rapport au diamètre du tuyau (d/D) et du ratio de vitesse (V_p / V_f) a permis d'améliorer le modèle développé. On a trouvé une très bonne correspondance entre les nombres de Nusselt estimés par les équations développées et les données expérimentales ($0.88 < R^2<0.99$).

CONTRIBUTION OF AUTHORS

All manuscripts published from the thesis research have been co-authored by M. R. Zareifard and H.S. Ramaswamy. All the experimental work including the design and fabricating the experimental setup, data analysis and manuscript preparation were carried out by the candidate, M. R. Zareifard, under the supervision of the thesis supervisor, professor H. S. Ramaswamy.

LISTS OF PUBLICATION AND SCIENTIFIC PRESENTATIONS RELATED TO THE THESIS

Zareifard M. R. and H. S. Ramaswamy, 1999. Dimensionless correlations for forced convection heat transfer to spherical particles under tube-flow conditions. (*prepared*)

Zareifard M. R. and H. S. Ramaswamy, 1999. Evaluation of factors influencing the tube-flow fluid-to-particle heat transfer coefficient: using a particle oscillatory motion technique Food Research International . (*submitted*)

Zareifard M. R. and H. S. Ramaswamy, 1999. A calorimetric evaluation of factors influencing fluid-to-particle heat transfer coefficient under tube-flow conditions. J. of Food Engineering. *(submitted)*

Zareifard M. R. and H. S. Ramaswamy, 1999. Two techniques for evaluating tube-flow fluid-to-particle heat transfer coefficient involving particles motion. Canadian Institute of Food Science and Technology (CIFST). Kelowna, B.C., June 6-9.

Zareifard M. R. and H. S. Ramaswamy, 1998. A calorimetric approach for evaluation of fluid-to-particle heat transfer coefficient under tube-flow-conditions. Lebensm.-Wiss. u -Technol. *(Accepted)*

Zareifard M. R. and H. S. Ramaswamy. 1998. Fluid-to-particle heat transfer coefficient in tube-flow condition using a calorimetric approach: influence of flow rate, fluid viscosity and ratio of particle to tube diameter. Institute of Food Technologist (IFT). Atlanta, Georgia, June 20-24.

Zareifard M. R. and H. S. Ramaswamy. 1997. A new technique for evaluating fluid-to-particle heat transfer coefficients under tube-flow conditions involving particle oscillatory motion. J. of Food Process Engineering (20):453-457.

Zareifard M. R. and H. S. Ramaswamy. 1996. Evaluation of the effect of particle motion on fluid-to-particle heat transfer coefficient in a holding tube using a new technique involving particle oscillation. Institute of Food Technologist (IFT). New Orleans, LA June 22-26.

Zareifard M. R. and H. S. Ramaswamy. 1995. Fluid-to-particle heat transfer coefficient evaluated under particle oscillatory conditions in a model holding tube. Conference of food engineering (CoFE) . Chicago, IL. November 2-3.

NOMENCLATURE

A	Area (m^2)
a	Radius of sphere (m)
C_p	Heat capacity (J/Kg ^{o}C)
d	Particle diameter (m)
D	Inside tube diameter (m)
f_h	Negative reciprocal slope of the straight line portion of the heating curve on semi-log coordinate (heating rate index) (s)
g	Local acceleration due to gravity (m/s^2)
h_{fp}	Fluid-to-particle heat transfer coefficient (W/m^2 K)
ID	Inside tube diameter (m)
k	Thermal conductivity (W/m K)
L	Length of the tube or distance (m)
m	Mass (kg) or consistency coefficient (Pa. s^n)
n	Number of revolution per minute (rpm) or flow behaviour index
Q	Fluid flow rate (L/min or m^3/s)
r	position along radius of a sphere ($0 \leq r \leq a$) (m)
R	Position of the particle from the centre of rotation (m)
R_t	Radius of the tube
R_p	Radius of the particle
Sd.	Standard deviation
t	Heating or cooling time (s)
T	Temperature (^{o}C)
T_b	Bulk temperature
T_f	Fluid or medium temperature
T_i	Initial temperature
T_m	Mass average temperature
T_p	Particle temperature
U	Dimensionless temperature ratio ($(T_f - T)/(T_f - T_i)$)
V	Linear particle velocity (m/s)
V_f	Fluid velocity (m/s)
V_p	Particle velocity (m/s)
V_s	Slip velocity (m/s)
x	Rectangular coordinate (m)
W	Moisture content (%)

Greek letter

α	Thermal diffusivity (m^2/s)
β	Root of characteristic equation or thermal expansion coefficient (1/K)
δ	Root of the characteristic equation
ρ	Density (kg/m^3)
μ	Dynamic or apparent viscosity ($\mu = \rho \upsilon$) ($N.s/m^2$)
μ_∞	Fluid apparent viscosity at bulk fluid temperature ($N.s/m^2$)
σ	Shear stress (Pa)

υ	Kinematic viscosity (m^2/s)
γ	Shear rate (s^{-1})
ω	Angular velocity ($2\pi n$)

Dimensionless numbers

Bi	Biot number ($h_{fp}\, a / k_p$)
Fo	Fourier number ($\alpha\, t / a^2$)
Fr	Froude number ($v^2 / g\, d$)
Gr	Grashof number ($g\, \beta\, \rho^2 \Delta T\, d^3 / \mu^2$)
Pe	Peclet number ($Re\, Pr$)
Pr	Prandtl number ($\mu\, C_p / k_f$ or υ / α)
Ra	Rayleigh number ($Gr\, Pr$)
Re	Reynolds number ($\rho\, V\, d / \mu$)
Nu	Nusselt number ($h_{fp}\, a / k_f$)

Subscript

q	Equilibrium condition
f	Fluid
fh	Fluid-to-particle
i	Initial
p	Particle
w	Water
s	Surface or slip
∞	Ambient

Abbreviations

ANOVA	Analysis of variances
CMC	Carboxymethyl cellulose
CV	Coefficient of variation (standard deviation/mean)
FC	Fixed particle at the center of the tube
FR	Free particle
FS	Fixed particle at the surface of the tube
GLM	General linear procedure
HTST	High temperature short time
L	Large particle size
LSD	Least significant difference
M	Medium particle size
RPM	Revolution per minute
RTD	Residence time distribution
RV	Relative velocity
S	Small particle size
SS	Sum of squares
SSHE	Scraped surface heat exchanger
TLC	Thermochromic liquid crystal

LIST OF TABLES

LIST OF FIGURES

TABLE OF CONTENTS

CHAPTER 1

INTRODUCTION

Today there is an ever-increasing consumer awareness and demand for flavourful, colourful, inexpensive, conveniently packaged, high-quality, readily available, clearly and informatively labelled, and above all safe food products. The demand for better quality and larger quantities of processed foods continues to increase. These demands require innovative processing techniques involving both safety and quality as primary priorities.

Thermal processing is considered to be one of the most important techniques for producing packaged, shelf stable, food products. While designed to kill spoilage and pathogenic microorganisms, the high temperature treatment also results in some loss of quality factors such as texture, color and nutrients. Early studies by Ball and Olson (1957) and Stumbo (1973) indicate that nutrient and sensory factors are less heat sensitive than hazardous microorganisms, and a given increase in temperature causes a larger increase in the rate of destruction of microorganisms. Such a difference in temperature dependence implies that optimization of quality retention is possible in thermally processed food . The mode of heat transfer in foods plays an important role in the process optimization. For convection heated products, high temperature short time (HTST) processes have been found to be beneficial, since the product heats rapidly and uniformly and microorganisms are destroyed faster than the quality factors. Conduction-heated foods do not benefit from this concept because of slower heating rates. Recent commercial developments have focused primarily on other means of increasing the rate of heat transfer to these products, in order to maximize retention of the quality factor. Aseptic processing, rotary sterilization and processing in thin profile package forms, are developments aimed at promoting better quality retention in processed foods. There is also a considerable amount of scientific work pertaining to the effect of processing on nutritive values together with minimization of quality degradation in thermally processed foods (Teixeira *et al.* 1969a,b; Lund, 1982; Leonard *et al.*, 1986; Ramaswamy and Ghazala, 1990; Ramaswamy and Abdelrahim, 1991; Abbatemarco and Ramaswamy, 1993; Ramaswamy *et al.*, 1993).

Aseptic processing is one of the processing techniques with a tremendous potential for high-quality production (Lopez 1987). As opposed to conventional canning, aseptic processing involves heating, holding, cooling and aseptically packing a food product in a continuous flow system. Aseptic processing and packaging offer high quality, safety, better color and texture of particulate foods. Other advantages include cost reduction, packaging material safety and handling convenience of the flexible and fiber-based aseptic packaging.

Successful aseptic processing of milk-based beverages and fruit juices using a modified Tetra Pack machine (Jairus, 1992 and Buchner, 1993) gave considerable attention to aseptic processing/packaging. Additionally, and most importantly, in February 1981 the US Food and Drug Administration (FDA) approved hydrogen peroxide as a sterilant for polyethylene (Cousin, 1993). Also, ultraviolet light and gamma radiation have also been accepted by the FDA as packaging sterilants (Stevenson and Ito, 1991). Now aseptic containers come in many different sizes and shapes, from small packages to very large bulk storage tanks. During the last two decades there has been a significant growth in the market as well as associated technical development of aseptic processing and packaging of foods.

The potential, growth and development achieved with aseptic processing, led the IFT to name aseptic processing and packaging as the top invention. Following the success of aseptic processing of liquid food, such processing of low acid, liquid foods containing solid particles is currently being evaluated with considerable attendant interest. According to the FDA, the minimum effort to establish a process for continuous heat-hold-cool sterilization of particulate low-acid food should consist of the following four elements: (1) identification and selection of the appropriate sterilization value; (2) development of a conservative model that predicts the sterilization value achieved at the lowest heating zone in a particle by the time the particle reaches the end of the holding tube; (3) quantitative microbiological validation of the lethality delivered; and (4) a list of critical factors and the procedure to be used for controlling them (Dignan *et al.*, 1989). Recently, in workshops conducted jointly by the National Center for Food Safety and Technology (NCFST) and the Center for Aseptic Processing and Packaging Studies

(CAPPS) a case study was developed which served as a framework for a validation study for filing with the FDA. In this study, an aseptic process filing for foods containing particulates, especially diced potato soup, was indicated by FDA's acceptance letter of May 31, 1997 (Palanappan and Sizer, 1997).

Reliable experimental data and mathematical models are required in order to aseptically process particulate foods, which are not over-processed but microbiologically safe. The efficiency of mathematical models in the design of an aseptic processing system depends on the accuracy of the input values either determined experimentally or estimated from the existing empirical equations. However, the continuous processing of a multi- phase system is not yet commercially approved, due to the unknown process parameters. Particle residence time distribution (RTD) and convective fluid-to-particle heat transfer coefficient (h_{fp}) in tube-flow conditions are the main critical parameters under investigation. Both of these depend on the flow behavior of the fluid and also particle motion during processing.

Experimental results of particle to liquid relative velocity or particle residence time distribution (RTD) have been presented in several publications (Sastry and Zuritz 1987; Chandarana 1992; Ramaswamy *et al.* 1992a; Singh and Lee 1992 Sastry 1993; Abdelrahim *et al.* 1993). The results of these studies conclude with some mathematical models which generally indicate that the major factors influencing particle velocity in a stream of the carrier fluid are: viscosity, the temperature and flow rate of the liquid, the relative (particle to fluid) density of solids, the relative (particle to tube) particle size, particle shape and concentration of the solid phase in the fluid (Grabowski and Ramaswamy, 1995).

Aside from the RTD, the design of thermal processes for particulate foods also depends strongly on the value of convective fluid-to-particle heat transfer coefficient (h_{fp}) which is one of the major obstacles in the establishment of aseptic processing. With traditional processing methods, the food temperature can be monitored during heating and simultaneously documented. With discrete particles suspended in a continuously moving fluid, the experimental determination of fluid-to-particle heat transfer coefficients is a very difficult task. Therefore, a conservative approach has been suggested, based on a non-flow stationary particle condition (Dignan *et al.* 1989). A solution to this problem requires the development of techniques to measure and/or predict microbial lethality at the coldest spot of the continuously flowing particle in complex two-phase systems.

Several experimental techniques have been developed for evaluating h_{fp} associated with a liquid-solid mixture (Richardson and Holdworh, 1989; and Sastry, 1992). These methods, which depend on either direct or indirect temperature measurement, include: the relative velocity method (Kramers, 1946; Ranz and Marshal, 1952, Whitaker, 1972); the stationary particle (Chandarana *et al.*, 1989 Chang and Toledo, 1990, Awuah *et al.*, 1995); microbiological history indicators (Hunter, 1972; Heppel, 1985; Weng *et al.*, 1992); a moving thermocouple (Sastry *et al.*, 1989; Zitoun and Sastry 1994b), melting point (Mwangi *et al.*, 1993), use of thermo-chromic liquid crystal material (Stoforos *et al.*, 1989; Moffat, 1990; Balasubramaniam and Sastry, 1994a,b), and use of remote temperature sensors in moving particles (Balasubramaniam and Sastry, 1994 and 1996b).

Although various techniques have been employed for evaluating fluid-to-particle heat transfer coefficient, and the research studies have contributed to understanding of the heat transfer phenomena, they all have certain limitations and only partially simulate the commercial processing situation. None of the above mentioned methods perfectly applies to the evaluation of h_{fp} in the aseptic processing system of particulate foods. Some studies have used aseptic processing conditions, but are limited to a stationary particle. Some others involve a kind of particle motion, but are limited to a transparent carrier medium in a glass holding tube. Although limitations still exist, each technique appears to offer some advantages.

In continuous processing of particulate foods, both RTD and h_{fp} are still subjects open to research and discussion. There is insufficient evidence regarding the boundary layer conditions between fluid and particles; also, the quantification of convective heat transfer coefficient in this complex situation is still at an early stage (Baptista *et al.*, 1997a). Data in the literature are sparse, due to difficulties inherent in measuring the temperature of moving particles. Optimum processing conditions cannot be established without proper assessment of heat transfer in relation to particle/fluid relative velocities, shape, size of particles, pipe diameter, temperature and concentration of carried fluid.

While a number of methods could be used for evaluation of fluid-to-particle heat transfer coefficient in continuous flow, none of them are yet universally applicable. The various approaches can, however, be used to complement and cross-check one another (Sastry, 1992). Thus, there is scope for the development of new techniques which to some extent, would overcome the limitations and help to evaluate the fluid-to-particle heat transfer coefficient under different conditions as affected by influencing factors on h_{fp}.

The objectives of this research were to:

a) to develop and evaluate a new technique, *particle oscillatory motion technique*, for imparting particle motion in a model holding tube in continuous flow systems, while using a thermocouple approach to get time-temperature data and hence calculating h_{fp} using an analytical solution also called heating rate index,

b) to develop and verify an indirect method, *calorimetric technique*, to measure the mass average or bulk temperature of a naturally moving particle in tube-flow conditions for the subsequence evaluation of h_{fp} determination, using a finite difference model,

c) to apply the previously developed techniques for evaluating the effect of different factors such as: fluid flow rate, viscosity and temperature (using both Newtonian and non Newtonian fluids as a carrying medium) as well as particle size, material and velocity on associated h_{fp}, and

d) to develop dimensionless correlations, using dimensional analyses and multiple regression procedures, for the prediction of convective fluid-to-particle heat transfer coefficients under tube-flow conditions using two different methods.

CHAPTER 2

LITERATURE REVIEW

In the food processing industry, most processes involve the operation of heat transfer. Unit operations such as cooling, freezing, thermal sterilization, drying and evaporation involve transfer of heat between a product and some heating or cooling medium. Heating and cooling of food products is necessary for processes that result in preventing microbial and enzymatic degradation. Desired flavor and nutrients also are imparted to foods when they are processed. Thermal processing involves destruction of the microorganisms contained in food so that it can be stored safely for a longer period. The primary objective of thermal processing is the destruction of microorganisms of public health concern, as well as microorganisms and enzymes causing spoilage of food. The main public health concern with low-acid foods is *Clostridium botulinum*, which is a highly heat resistant, rod shaped, spore forming, anaerobic pathogen that produces the deadly botulism toxin. The major purpose of thermal processing of low acid food products is the prevention of the formation of the botulinum toxin. The phrase "minimal thermal process" was introduced by the U.S. Food and Drug Administration in 1977, and defined as "the application of heat to food, either before or after sealing in a hermetically sealed container for a period of time and at a temperature scientifically determined to be adequate to ensure the destruction of microorganisms of public health concern". Heat processing can be achieved by a variety of techniques. Among them continuous tube-flow processing of particulate food is a significant innovation in thermal processing development during the last decade. Today, consumer needs demand more than safe production and shelf-stable foods. High- temperature-short time (HTST) technique have been developed to minimize the severity of heat treatment and to promote product quality. Whatever procedure is employed for thermal processing of food, it is still imperative to improve the design process that delivers the required heat treatment to the food.

Aseptic processing

Aseptic processing and packaging is a challenging alternative compared to conventional methods of canning foods. Compared to other challenging processing techniques such as extruded food technology, freeze drying, controlled atmosphere packaging, and microwave, aseptic processing and packaging is rated the most significant innovation in food science development during the 50-year history of the Institute of Food Technologists (IFT Staff Report, 1989).

An important landmark in the history of food processing was achieved when the aseptic concept was conceived in 1950. Aseptic technology differs markedly from in-container processing where non-sterile products are hermetically sealed in non-sterile containers and subsequently subjected to thermal treatment. Real progress in the commercial development of aseptic processing technology of foods began with the invention of the Martin-Dole process in the late 1940s, in California, by the Dole Engineering Company (Lopez, 1987). The process could be used for the sterilization of any low or high acid fluid. Product heating and cooling was achieved by heat exchangers, based on the principles of high temperature-short time (HTST) sterilization, while the containers were sterilized by super heated steam (Mitchell, 1988). Another historical development was achieved by Loelinger and Regez, from Switzerland, who successfully used hydrogen peroxide (H_2O_2) to sterilize flexible packaging materials for milk products. The primary focus of the Swiss system was to extend the shelf life of fresh milk without refrigeration, whereas obtaining better quality products than conventional processing was the main objective of the Martin-Dole process. The filling of milk was done in a modified Tetra Pack machine which produced tetrahedron packs from paperboard and polyethylene (Buchner, 1993). These developments gave considerable attention to aseptic processing/packaging and most importantly in February 1981 when the US Food and Drug Administration (FDA) approved hydrogen peroxide as a sterilant for polyethylene (Cousin, 1993). Recently, ultraviolet light and gamma radiation have also been accepted by the FDA as packaging sterilant (Stevenson and Ito, 1991). Now aseptic containers come in many different sizes and shapes, from small package to very large bulk storage tanks.

More recently, in workshops conducted jointly by the National Center for Food Safety and Technology (NCFST) and the Center for Aseptic Processing and Packaging Studies (CAPPS) a case study was developed which served as a framework for a validation study for filing with FDA. In this study, an aseptic process filing for foods containing particulates, especially diced potato soup, was accepted by the FDA. Tetra Pack referred to the resulting FDA's acceptance letter of May 31, 1997 to prepare the filing for the commercial production of potato soup (Palanappan and Sizer, 1997). During the last two decades there has been a significant growth in the market as well as the associated technical development of aseptic processing and packaging of foods. The potential, growth and development achieved with aseptic processing, led the IFT to name aseptic processing and packaging as the top invention.

Unit component of aseptic system

Aseptic processing is a high temperature-short time process for the continuous sterilization and packaging of foods offering potential, at reduced costs, for the production of high quality foods. Figure 2.1 shows a schematic of an aseptic system. A typical aseptic process involves sterilization of the product by a heat-hold-cool approach followed by filling and sealing. Using this approach, the food is first heated in a set of scraped surface heat exchangers (SSHE) and held for a pre-determined time in a hold tube, cooled quickly through a second set of SSHEs and then filled and sealed in pre-sterilized containers under aseptic condition.

Conventionally, the aseptic processing system consists of one or more heat exchangers for heating, a holding tube, and one or more heat exchangers for cooling. Lund and Singh (1993) divided the aseptic processing system into six elements including: the product, flow controls, product heating, holding tube, product cooling and packaging. Product heating in aseptic systems can be performed directly (steam injection and steam infusion) or indirectly (plate, tubular or scraped surface heat exchangers) for the pasteurization and sterilization of foods, whereas containers are sterilized by superheated steam, ultraviolet light, gamma radiation and hydrogen peroxide.

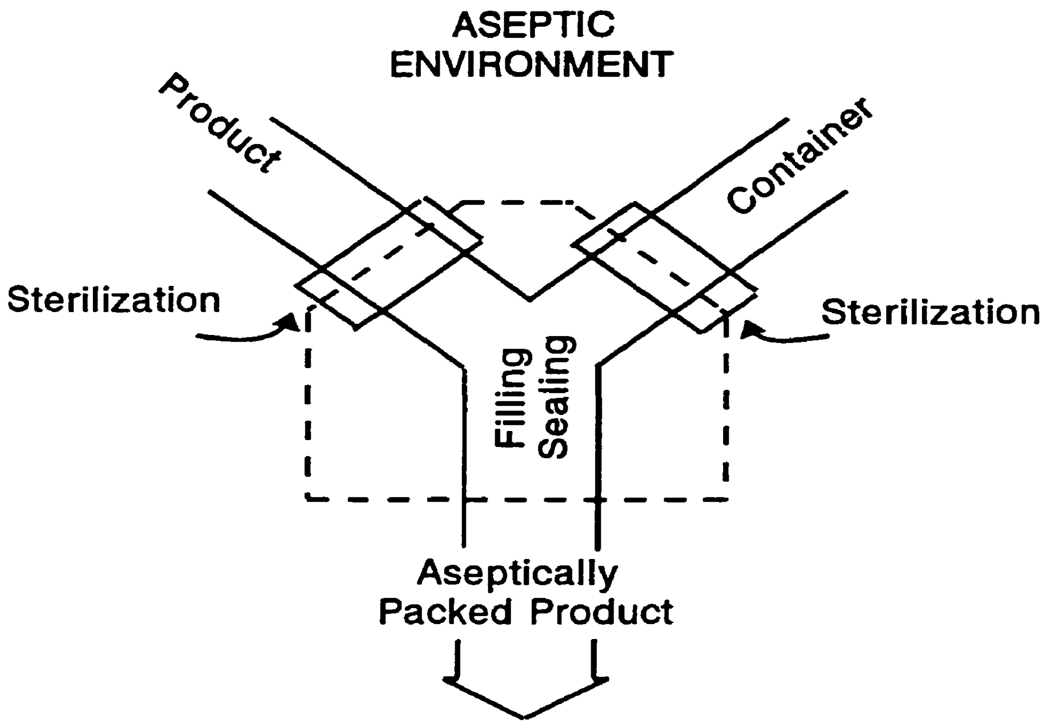

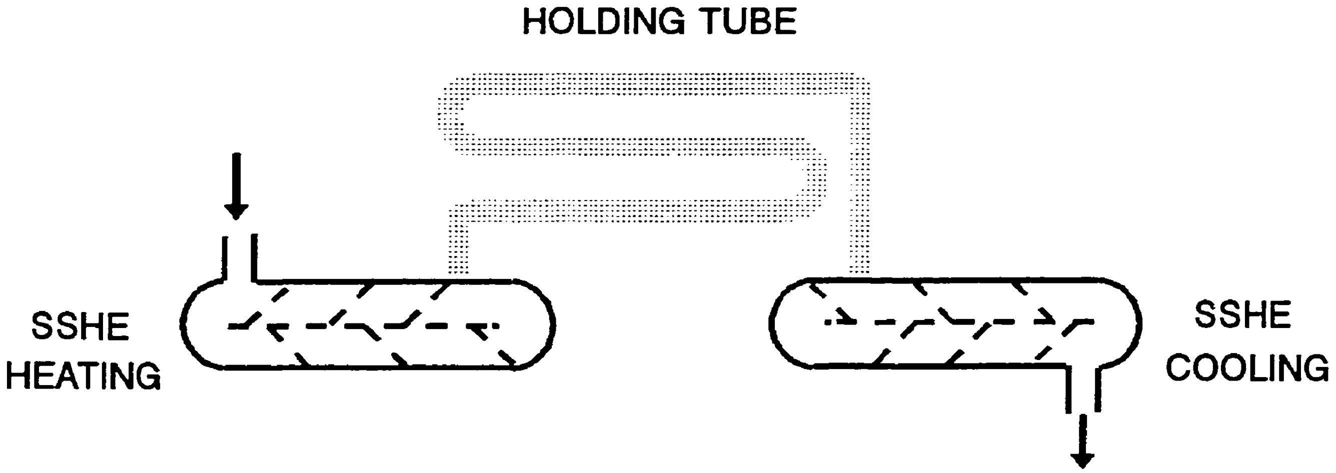

Figure 2.1. Top: schematic of aseptic processing system in which the commercially sterilized product is filled into a pre-sterilized container and sealed hermetically in a sterile environment. Bottom: sterilization unit of the system for the processing of particulate food.

Although the main objective is to achieve commercial sterility, specialized equipment may be needed for specific products. Recent developments in packaging technology allow various forms of packaging materials to be adopted for specific needs. Obviously, the selection of a particular processing/packaging system is product dependent.

Advantages and limitations of aseptic processing

The following advantages are recognized for aseptic processing in comparison to the traditional thermal process. Aseptic processing offers potential for: (1) HTST operation, (2) energy savings, (3) higher efficiency, (4) faster and more uniform heat transfer, (5) reduced variation in process parameters due to the high level of automation employed, and, (6) lower production costs (Chandarana *et al.* 1987). Adaptation to new packaged forms, saving in packaging costs and convenience, are also regarded as major advantages (Toledo and Chang, 1990).

Lund (1977) and Lopez (1987) have mentioned some limitations of aseptic processing system as: (1) the apparent difficulty in destroying heat resistant enzymes, (2) higher initial capital investment, (3) limitations to aseptic product types and (4) the sophisticated instrumentation needed to initiate the process. However, such apparent limitations are outweighed by long term economic returns. Silva *et al.* (1992) indicated that the HTST approach may not be applicable to solids and highly viscous foods, due to the slow heat penetration to the cold spot. The slow heat conduction requires more time for commercially sterilized products, thereby causing severe surface burns.

Aseptic processing of particulate food

Aseptic processing has been used commercially for liquid products and acid foods containing small particulate matters but its use for low-acid foods containing particulates is still under investigation. Conventional thermal processes were established based on the temperature response of the food, which can be easily evaluated during heating and cooling. However, particle temperature cannot be easily measured in continuous flow aseptic processing situations, with discrete particles suspended in a continuously moving fluid. Since implementing traditional routines for process calculations became questionable under such situations, mathematical modeling has been used as an alternative. A major obstacle, for modeling particle temperature history in an aseptic processing unit, is a lack of adequate information on the heat transfer coefficient between the carrier fluid and suspended particles (Heldman, 1989). Considerable effort has gone into finding suitable models for estimation of lethality of low-acid food containing particulate (Sastry, 1986; Chandarana *et* al., 1989; Chang and Toledo, 1990; Larkin, 1990). Dignan *et al.* (1989) listed the critical factors needed in modeling heat transfer and lethality distribution, in continuously processed low-acid particulate foods as: particle size/distribution, the convective heat transfer coefficient and residence time distribution both in the heat exchanger and holding tube.

According to the FDA, the minimum effort to establish a process, for continuous heat-hold-cool sterilization of particulate low-acid food, should consist of the following four elements: (1) identification and selection of the appropriate sterilization value; (2) development of a conservative model that predicts the sterilization value achieved at the lowest heating zone in a particle by the time the particle reaches the end of the holding tube; (3) quantitative microbiological validation of the lethality delivered; and (4) a list of critical factors and the procedure to be used for controlling them (Dignan *et* al., 1989).

Selecting a sterilization value

The first step in the design of any heat-preservation process is to establish the preservative requirements of the product, F value. Lethality (F value) is a measure of the heat treatment or sterilization processes. The F value represents a certain multiple or fraction of D value depending on the type of microorganism. The microbial destruction rate is generally defined in terms of a decimal reduction time (D value) which is the heating time in minutes at a given temperature required to result in one decimal reduction in the surviving microbial population. In other words, D value represents a heating time that results in 90% destruction of the existing microbial population. To ensure commercial sterility, foods must experience a 12 D cycle reduction at the coldest spot based on the kinetic data for *Clostridium botulinum*. In conventional canning, the minimum "bot cook", which refers to a process lethality of 3 minutes at 121°C, is used for low acid foods (Brown, 1991). However, recommended F values have often been larger than necessary, in order to destroy the most heat resistant thermophile capable of causing storage problems. According to Dignan *et* al. (1989), lethality, credited to particulates in the holding tube, should be calculated on the basis of the coldest temperature for the fastest moving particle. This means that lethality, credited to particles, should be that associated with the largest particle having the least residence time.

Mathematical model for aseptic process evaluation

Mathematical models are useful for estimating particle temperatures when developing the process and sizing equipment. Many factors influence the rate of heat transfer to a particle of food. The ability of the mathematical model to predict the rate of heat transfer depends on the accuracy of these factors, which include: particle size, shape and distribution; the residence time distributions for the particles in the heat exchangers and holding tube; the convective heat transfer coefficient at the fluid/particle interface and at the heat exchanger surface; the thermophysical properties of both the fluid and particles; and the configuration of the heat exchangers and holding tube (Dignan *et* al., 1989). The authors indicated that the most important factors among the above mentioned are: the particle size and the fluid-to-particle heat transfer coefficients, both in the heat exchanger and the holding tube.

Earlier published mathematical models (de Ruyter and Brunet, 1973; Manson and Cullen, 1974) have yielded considerable insights on the critical parameters for sterilizing aseptically processed particulate food. Both of these models emphasize the importance of particle size and particle residence time, on the holding time required to achieve commercial sterility at the center of the particles. Unfortunately, both models assume infinite heat transfer coefficients at the particle surface, meaning that there was no resistance to heat transfer in the boundary layer around the particle. Such assumption resulted in an over estimate of the lethality delivered to the particle.

Merson *et* al. (1978) also discussed the limitations associated with Ball's formula method, for estimating holding times for low-acid foods containing particulate. These limitations included: (1) an infinite fluid-to-particle heat transfer coefficient; (2) the necessity of long process times, required to satisfy the first term approximation of the infinite series solution; and (3) the need for a constant medium temperature. Larkin (1989) modified Ball's formula by introducing a hyperbolic function to determine process lethality for particulate products. The author illustrated that Ball's formula method can over-estimate lethality by 241% of the actual value for heating and holding alone.

Sastry (1986) developed a numerical model to calculate the temperature profile of the fluid and individual particle. The author explained that the straight-line curve obtained for conduction heated, canned foods will never exist for particulate products in continuous flow systems, because the particles continue heating in the holding tube at the expense of the fluid temperature, resulting in a decrease in fluid temperature. Therefore, the energy balance equation approach, involving energy input from steam and energy loss from a population of average-sized particles, was used to calculate the temperature profile of the carrier fluid. According to Sastry (1986), the size of the holding tube should be based on the slowest heating particle, the most rapid moving particle in both heat exchanger and holding tube, and the lowest heat transfer coefficient. Chandarana *et al.* (1989), Chang and Toledo (1989), Lee *et al.* (1990a), Yang *et al.* (1992), and Skjoldebrand and Ohlsson (1993 a,b) have also developed computer based models to simulate aseptic processing systems containing particulate foods. Usually, the process calculation procedure in any mathematical model and computer simulation, accounts for product heating in the heaters, particle heating and fluid cooling in the holding tube, and product cooling in the coolers. The model calculates the mean fluid temperature as a first step. Then using this information, the temperature of the fastest-moving particle is calculated. The accuracy of the calculation procedure is primarily dependent on the accuracy of the value determined experimentally or estimated from the existing empirical equations. The model also determines the particle lethality (center point and integrated sterilization value) and fluid lethality (Palaniappan and Sizer, 1997).

Residence Time Distribution in Aseptic Processing

In continuous processing systems, except in the case of the ideal plug flow situation (Singh and Lee, 1992), each flowing element will spend different lengths of time to flow through the heat exchanger or the holding section. This means that the particles have a distribution of residence time. Thus residence time distribution (RTD) can be defined as the length of time that different elements spend in the system. Therefore, each element will receive a different degree of sterility depending upon the length of time that particular element spends in the heat exchanger or holding tube. In order to predict the lethality received by each element of the product, one must be able to determine the length of time that different elements spend in the system (Singh, 1987). The residence time, of the fastest moving particle in the heating and holding sections of the aseptic system, is critical from a public health standpoint. Of equal importance is the determination of mean and maximum particle residence times (Ramaswamy *et al.* 1995). Factors affecting the residence time include: the particle size and its distribution, the characteristics and flow properties of the fluid medium, the velocity profile within the holding tube and heat exchanger, the heating characteristics of the product and the configuration of the holding tube (Heldman, 1989; Sastry, 1989).

Earlier studies on RTD, in continuous sterilization and pasteurization systems, have considered liquid foods but not the two-phase flow system. RTD for a homogeneous liquid can be easily determined with two widely used techniques: radioactive tracers and dyes (Fichtali, 1990). More interest has focused on RTD of liquid foods, containing particles in an aseptic processing system, where the introduction of particulate to liquid makes the flow conditions more complex. The RTD of food particles in the heat exchangers and holding tube of an aseptic system is an integral part of the thermal process establishment, since the temperature at the slowest heating point of a particle is a function of both time and heating rate (Manson and Cullen, 1974).

Residence time distribution of the particles can be described by an E (t) or F(t) function through the introduction of tracer particles at the entrance of the system and enumerating them at the exit (Abdelrahim, 1994). The *E* function gives the RTD of the fluid and particles or exit age distribution for any non-ideal flow. Residence time distribution [E(t)] is defined as the fraction of material in the outlet stream that has been in the system for times between t and t+dt. The *F* function is related to the *E* function by measuring the output response when a step change of tracer is introduced. Therefore, the *F* function represents the accumulation of particles at the exit with a residence time of t seconds.

Singh and Lee (1992) classified typical inputs for the RTD determination as follows: a step function where input concentration is changed from one level to another, a pulse input where a small amount of particles is injected into the feed stream, and a sinusoidal input. The step function and pulse inputs methods are relatively easy to implement compared to the sinusoidal method. The principal reason for employing the step, pulse or sinusoidal inputs in RTD analysis is the convenience and ease of mathematical analysis.

There have been several techniques for studying and investigating the RTD of solid/liquid two-phase flow systems. These methods include: visual observation, photography, laser beam, play-back videotaping, radioactive trace and magnetic response. These different techniques which require the use of different experimental set-ups and various types of particles and liquid media, are fully described in a review of residence time distribution in aseptic processing of particulate foods (Ramaswamy *et al.*, 1995).

Biological validation

Biological verification of an aseptic process for low-acid particulate foods requires some form of biological indicator that can be processed through the aseptic system, retrieved intact, and tested quantitatively for sterility. A variety of bio-indicators, using bacterial spores, have been developed and used in various thermal processes. Several researchers have utilized the thermophilic bacterium, *Bacillus sterothermophilus*, to validate particulate sterility in various food models under aseptic conditions (Brown *et al.*, 1984; Sastry *et al.*, 1988; Hinton *et al.*, 1989; Ronner, 1990; Palanippan and Sizer, 1997).

Biological methods are needed to validate mathematical models, which are used to determine acceptable thermal processes for aseptically produced foods. To confirm the effectiveness of a specific thermal process, an inoculated pack is used to confirm the lethality achieved in canned food (Segner *et al.*, 1989). An inoculated pack test assumes that the food will have the inoculum evenly distributed through the food. The test cans are placed at the lowest-heating position in the retort. This combination of factors guarantees that the inoculated pack will be measuring the worst-case scenario at the coldest point in the slowest-heating container. The conditions achieved in inoculated test packs cannot be replicated in biological challenge studies, in particulate food processed aseptically. In aseptic processing conditions, each particle of the food receives a different thermal process, with one particle receiving the least thermal process. Because it is not possible to identify which particle will receive the least thermal process, a statistically significant number of particles need to be tested (Marcy, 1997). The inoculated pack method requires a relatively large number of particles to ensure that an inoculated particle will be placed in the containers to be incubated (Digeronimo *et al.*, 1997). Care should be taken, in biological validation of an aseptic process, that the particles used for testing should behave in a manner identical to that of the food intended for processing. The test particle should maintain its physical integrity throughout the aseptic process. The physical properties of the test particle should be known before and after thermal processing to ensure that no changes have been made (Sastry,1997).

All microbiological testing for biological validation of a thermal process should be sufficient to achieve commercial sterility. Biological validation of multiphase aseptic foods is used to demonstrate the effect of thermal processing on the particle which would receive the minimum thermal treatment. This is determined after considering which particle was the slowest heating and the fastest moving through the hold tube.

Heat transfer coefficient

In simulated process evaluations, the fluid-to-particle heat transfer coefficients (h_{fp}) in both heat exchanger and holding tube are probably the most important but difficult parameters to be determined experimentally (Dignan *et al.*, 1989; Heldman, 1989). For continuous sterilization of food particulate, de Ruyter and Brunet (1973), and Manson and Cullen (1974) assumed the heat transfer coefficient to be infinite. However, several researchers demonstrated a finite convective heat transfer coefficient at the fluid-particle interface (Sastry, 1986; Chandarana and Gavin, 1989a,b; Chang and Telodo, 1990; Chandarana et al, 1990; Awauh and Ramaswamy, 1995).

A food system is considered as a bi-phasic system especially when particles are suspended in a liquid medium. Therefore, in thermal processing of such products, both the particles and liquid phase need to be sterilized. Since the particles heat up by a slow conduction process, sterilization of the food product will be limited by the size and population of particles in the system (Simpson and Williams, 1974; Chandarana, 1992; Mwangi *et al.* 1992). From the heat transfer point of view, a complex heat transfer phenomena occurs when solid particles are introduced into a liquid medium. Heat transfer to cold spots within the particles will be restricted by the thermal resistance within the product and thermal resistance at the surface. The thermal resistance of the product is a function of thermophysical properties such as: density, specific heat and thermal conductivity. However, the rate of heat transfer is also dependent on the boundary layer surrounding the particle. This boundary layer causes a thermal lag between the particle surface temperature and the ambient fluid temperature.

In convection heat transfer, heat is transferred by the bulk motion of the fluid. Convection heat transfer may be categorized according to the nature of the flow such as: forced convection when the flow is caused by some external means, such as a fan or a pump; and free or natural convection when the flow is induced by buoyancy forces in the fluid. The complexities introduced by heat conduction, fluid dynamics and boundary condition may be lumped together in a single parameter by introducing Newton's Law of cooling, defined as: $q=h_{fp}A\ \Delta T$. The quantity h_{fp}, known as the convective heat transfer coefficient, represents the proportionality factor between heat transferred by convection to a body immersed in a fluid and the temperature difference between the particle and fluid, as well as the surface area. The convective heat transfer coefficient encompasses all the effects that influence the convection mode and also depends on conditions in the boundary layer.

The temperature distribution within the suspended solid particles will therefore strongly depend on the convective heat transfer coefficient (h_{fp}), which characterizes conditions occurring at the fluid particle interface. The significance of the heat transfer coefficient lies in the fact that the temperature history of suspended particles has to be predicted, in order to calculate product sterility. It is also needed to determine the equipment, process design and optimization (Lund and Singh, 1993).

However, h_{fp} is one of the most difficult parameters to evaluate under aseptic conditions (Heldman, 1989), due to the dynamic nature of the particles. Studies on the measurement of h_{fp} are limited, due to difficulties in the measurement of the moving particles without affecting their actual motion. Moreover, many investigations of convection heat transfer have been carried out to study the means of determining h_{fp}. In basic studies of convection heat transfer phenomena, many researchers have developed means and methods to determine the convective heat transfer coefficient. In the forced convection situation, previous studies have been limited to only simplistic approaches using a fixed particle, due to the complexities involved in h_{fp} determination. Although these studies have contributed to the understanding of the heat transfer phenomenon, they do not simulate real aseptic processing conditions in which particles move in a carrier fluid, flowing in the holding tube. Investigators have tried to simulate more realistic situations to determine h_{fp}, by gathering the time-temperature data of moving particles. Although some of these studies simulate the particle motion, they are limited to tests carried out under atmospheric conditions. Others have used the relevant high temperatures and fluid flow, but with a fixed particle. Generally speaking, to date only partial simulations have been carried out.

While a number of methods have been used to determine the fluid-to-particle convective heat transfer coefficient in continuous tube-flow situations, the available data on h_{fp} are not sufficient and consistent in the literature. Thus,the various approaches should be used to complement and cross check one another.

Experimental Methods of h_{fp} Determination

Several experimental techniques have been developed for evaluating h_{fp} associated with liquid-solid mixtures. These methods, which depend on either direct or indirect temperature measurements, include: the stationary particle, moving thermocouple, liquid crystal, relative velocity, liquid temperature calorimetry, microbiological history indicators, melting point and transmitter methods.

Stationary Particle Method

The general approach involves placement of a transducer particle (with known initial temperature) in a flowing fluid stream (at a different temperature) and measurement of particle and fluid temperatures during the experiment. Chau and Synder (1988), Chandarana *et al.* (1989 and 1990), Chang and Toledo (1990), Zuritz *et al.* (1990) and Awuah *et al.* (1995) determined h_{fp} by recording the time temperature data of a stationary particle while the fluid passed over it. This approach is easy to perform and adaptable to a high temperature and opaque (not transparent) fluid medium. However, due to particle restriction in both the transitional and rotational motions, the stationary particle method may not simulate the condition in real situations (Maesmans *et al.*, 1992). However, since fluid/particle relative velocities are low for non-Newtonian fluids in particular (Awauh 1995; Zuritz *et al.*, 1990), and the laminar regime probably dominates in most practical applications, this method may be adopted for a conservative estimation of h_{fp}.

Moving Thermocouple Method

Researchers have also attempted to simulate more realistic situations, by putting the particle in a moving condition in order to evaluate h_{fp}. Sastry *et al.* (1989, 1990) proposed a moving thermocouple method. This method involves the introduction of a hollow, metallic, transducer particle into a constant-temperature, fluid stream. The temperature of the moving particle is measured using the thermocouple that is withdrawn from the downstream end at the same velocity as the particle. In this case, a thermocouple was attached to a motor at a pre-determined speed. The values of heat transfer coefficient were back-calculated using the lumped capacity approach. Using this method, Zitoun and Sastry (1994) studied the heat transfer coefficient for cube shaped particles in a continuous tube flow. One problem is that the presence of the thermocouple results in some unavoidable interference with particle motion. Although free-particle velocities can be duplicated by adjusting the speed of the motor, it is not possible to control particle trajectories with a thermocouple attached. Therefore, studies on the variation of h_{fp} with radial position are not possible with this approach. A further problem is that the experiment is difficult to perform even with one particle. These difficulties are likely to be greatly increased with a multi-particle system,. In addition, the moving thermocouple approach is not readily adaptable to high temperature and pressure, due to difficulties in equipment design. However, major advantages associated with this procedure are: reading the exact temperature of a mobile particle and the possibility of using an opaque carrier fluid.

Thermochromic liquid crystal (TLC) method

Recently, thermochromic liquid crystals (TLC), have been used to get the surface temperature history of a moving particle in order to evaluate the heat transfer coefficient under continuous flow conditions. This involves coating the surface of the particle with temperature-sensitive color-changing crystals and video-taping the color change. Temperature history, and thereby h_{fp}, can be obtained by calibrating the color change. Moffat (1990) provided a detailed discussion on the use of the liquid crystal method. Stoforos and Merson (1991) were the first to employ the method to evaluate the overall and liquid-to-particle heat transfer coefficient for model food particles in a rotating liquid/particulate canned food system. Balasubramaniam and Sastry (1994a,b and 1995) applied the same technique to measure the heat transfer coefficient, but in a continuous flow system. Under the same experimental conditions the liquid crystal method resulted in higher values of h_{fp}, compared to the moving thermocouple method .

This method is non-invasive, rapid and provides a surface temperature measurement which is sensitive to variations in h_{fp}. However, the accuracy of temperature measurement is limited by the range of temperature over which color changes, and the resolution of video image. Also, this method is limited to the use of a transparent carrier medium.

Relative velocity method

The relative velocity method utilizes established, empirical correlations associated with fluid flow, over objects of known geometry. In dimensional analysis, the convective heat transfer coefficient is expressed in terms of the Nusselt number (Nu), which is generally described as a function of the Reynolds (Re), Prandtl (Pr), and Grashof (Gr) numbers:

$$Nu = f\,(Re,\ Pr,\ Gr)$$

Examples of such correlations include those presented by Kramers (1946), Ranz and Marshall (1952), and Whitaker (1972) which relates flow properties and characteristics, as well as particle geometry to the Nu. The flow field around a moving particle can be determined using small tracers within the carrier fluid. If the test particle is videotaped, it is possible to observe the motion of the tracers relative to it. The relative velocity between fluid and particle can then be calculated by determining the time elapsed for a given tracer to pass over a particle.

This method is limited to the use of a transparent fluid and the fact that the accuracy of h_{fp} estimated with this method depends on the reliability of the existing correlations. Balasubramaniam and Sastry (1996a) in a study of liquid to particle heat transfer showed that values of h_{fp}, estimated by the above mentioned correlations, were lower than the values of h_{fp} obtained using the liquid crystal method, and higher than those obtained using the moving thermocouple method under the same experimental conditions.

Liquid temperature calorimetry method

This method determines the convective heat transfer coefficient by adding a number of low-temperature particles to a hot liquid and monitoring the temperature of the liquid as time progresses. The energy loss found in the liquid indicates the energy gained by the particles. With knowledge of the thermophysical properties of both the particle and liquid, the number of particles and their surface area, the average h_{fp} value can be calculated for the group . Although this method is simple in principle and provides h_{fp} values for bulk particles, even in an opaque carrier medium, it is difficult to adapt this approach to process temperatures and pressure. In addition, individual variations in h_{fp} values are not determinable.

Microbiological history indicators method

Indirect methods of h_{fp} determination have also been proposed which are based on locating heat-labile substances such as enzymes or microbial spores at the center of simulated food particles. This procedure involves immobilization of a test microorganism within test particle. The particles are processed in a continuous flow heat-hold-cool system and the survivors are enumerated. The heat transfer coefficient is then back calculated from a mathematical model. Hunter (1972) and Hepple (1985) were the first to use microorganisms suspended in beads. This approach prompted further research with the use of chemical indicators (Weng *et al.* 1992).

Generally, the microbiological method predicts average h_{fp} over the entire aseptic processing unit rather than individual components such as the heat exchanger or holding tube section. Obviously, this approach has the advantages of being non invasive, usable at process temperatures, and applicable to opaque carriers. However, sample-to-sample variation in a microbial population can cause problems with replicated data. Also, the immobilization process may alter particle characteristics due to the indicator used or differences in materials used to hold the microorganisms. Hence, the choice of experimental materials and location of bacterial spores are important.

Melting point method

The melting point method utilizes polymers which change color at specific temperatures. It is then possible to use polymers of various melting points within transparent particles, and to determine the time required to achieve melting. Mwangi *et al.* (1992) mobilized a melting point indicator, with temperatures ranging from 51 to 80°C, at the center of transparent polymethylmethacrylate spheres. The particles were introduced into a holding tube of an aseptic simulator containing a glycerin/water mixture. As melting point is reached, the surface of the indicator changes color, and the time is recorded. Using a number of different particles, the heat transfer coefficient is back calculated from time-temperature data after careful calibration of color change with temperature. This method is also non-invasive but limited to a transparent particle and carrier liquid.

Transmitter method

In principle, this technique involves the placement of a miniature sensor at the coldest spot of concern, in order to relay time-temperature data to a logging system. In a recent study with this method, Balasubramaniam and Sastry (1996c) used a remote temperature sensor which transmitted magnetic signals to an external receiver, which converted the magnetic signals to temperature readings. The heat transfer coefficient was then back calculated from the time-temperature data using a finite difference program. The device currently available is, in its contact form, of a density considerably greater than real food particles.

Theoretical background for h_{fp} determination

If a solid body is suddenly subjected to a change in environment, some time must elapse before an equilibrium temperature condition will prevail in the body. This equilibrium condition situation is referred to as the steady state, and the temperature distribution and heat transfer can be calculated by applying the Laplace equation, assuming constant thermal conductivity.

$$\frac{\partial^2 T}{\partial x^2} + \frac{\partial^2 T}{\partial y^2} + \frac{\partial^2 T}{\partial z^2} = 0 \qquad (2.1)$$

In the transient heating or cooling process, which take place in the interim period before equilibrium is established, the analysis must be modified to take into account the change in internal energy of the body with time. The boundary conditions must also be adjusted to match the physical situation, which is apparent in the unsteady state heat transfer problem (Holman, 1990). The unsteady state heat transfer analysis is obviously a significant practical interest because of the large number of heating and cooling processes which must be calculated in industrial applications. Different procedures based on either analytical or numerical solutions have been proposed for the unsteady state heat transfer problems.

Analytical solutions for h_{fp}

The heating rate of food particles, suspended in a liquid food, is function of the boundary layer surrounding the particle, which cause a thermal lag between particle surface temperature and heating liquid temperature. The presence of solid particles in the liquid results in a complex heat transfer system. The critical parameter is the convection surface heat transfer coefficient between the fluid and the particle surface (h_{fp}). The time-temperature distribution in a particle, with constant thermophysical properties, is obtained by solving the transient heat transfer equation for conduction. In cartesian coordinates this is given as follows:

$$\frac{\partial T}{\partial t} = \alpha\left(\frac{\partial^2 T}{\partial x^2} + \frac{\partial^2 T}{\partial y^2} + \frac{\partial^2 T}{\partial z^2}\right) \qquad (2.2)$$

with the initial condition as $T = T_i$ at $t = 0$ and boundary conditions as:

$$k_p \frac{\partial T}{\partial n} = -h_{fp}\,(T_p - T_f) \qquad (2.3)$$

The above mentioned convective boundary condition is obtained by equating at the surface, the fluxes given by Newton's law defined as:

$$q = h_{fp}\,A_p\,(T_p - T_f) \qquad (2.4)$$

to Fourier's equation:

$$q = -\,k_p\,A_p\,(\partial T/\partial n) \qquad (2.5)$$

where A_p is the surface area , k_p is the thermal conductivity, α is the thermal diffusivity, and T_p is the surface temperature of the particle; T_f is the fluid temperature, h_{fp} is the heat transfer coefficient at the fluid-to-particle interface, and $\partial T/\partial n$ is the temperature gradient along the normal direction to the surface. Relevant assumptions made in solving the partial differential equation (Incropera and de Witt 1985; Chapman, 1989; Weng *et al.*, 1992) are: 1) constant thermal and physical properties; 2) homogeneous and isotropic particle; 3) pure conduction heating within particle; 4) no phase change in the fluid and particle during processing and 5) uniform initial temperature for both liquid and particle.

The one-dimensional unsteady state, heat conduction differential equation governing heat transfer to isotropic objects, suddenly transferred into a constant temperature medium is expressed as:

$$\frac{\partial U}{\partial t} = \alpha \left(\frac{\partial^2 U}{\partial r^2} + \frac{n}{r} \cdot \frac{\partial U}{\partial r}\right) \tag{2.6}$$

with n = 0, 1, and 2 corresponding to slab, cylinder, and sphere respectively.

The analytical solution to the above equation for a sphere, under convective boundary conditions, is given below as detailed in Carslaw and Jaeger (1959) and Luikov (1968):

$$U = 2Bi \sum_{n=1}^{n=\infty} \frac{[\delta_n^2+(Bi-1)^2]\sin(\delta_n)}{\delta_n^2(\delta_n^2+Bi(Bi-1))} \cdot \frac{\sin(\delta_n r/a)}{(r/a)} \exp(-\delta_n^2 Fo) \tag{2.7}$$

where δ_n is the nth positive root of

$$Bi = 1 - \delta\cot(\delta) \tag{2.8}$$

The series solution converges to the first term beyond an Fo value of 0.2 (Heisler, 1947). Using δ as the first root of Eq.(2.7), and abbreviating all parameters behind the exponential term as A, Eq.(2.7) can be re-written as:

$$U = A \exp(-\delta^2 Fo) \tag{2.9}$$

By taking the logarithm on both sides of the above equation, transforming the logarithm to base 10, and expanding Fo as $\alpha t/a^2$, Eq.(2.8) can be written as:

$$\log U = \log A - \left(\frac{\delta^2 \alpha t}{2.303\ a^2}\right) \tag{2.10}$$

Heating rate index (f_h)

Equation 2.10 represents the straight line portion of the heating or cooling curve obtained by a plot of log U vs t. The slope index of such a curve is called the heating rate index, f_h, which is related to δ in the following form:

$$f_h = \frac{2.303\ a^2}{\alpha \delta^2} \tag{2.11}$$

The slope index, f_h, is dependent on δ, particle size and thermal diffusivity (α), but independent of the location. Therefore, using this method, it is not necessary to know the exact location of the thermocouple within the sample. Knowing a, α and f_h, which can be evaluated from experimental data, δ can be calculated using Eq.(2.10). Using δ in Eq.(2.7), the corresponding Bi and hence, the heat transfer coefficient, h, can be calculated [$h = Bi\ (k/a)$].

Lumped capacity approach

Lumped-heat-capacity approach can be used to determine the heat transfer coefficient, while the temperature of the immersed particle is assumed to be uniform. Obviously, such a condition is idealized because a temperature gradient must exist in a material if heat is to be conducted into the material. In general, the smaller the physical size of the particle, the more realistic the assumption of a uniform temperature. Clearly, the temperature distribution in the particle depends on the thermal conductivity of the particle and the convective heat transfer coefficient from the surrounding fluid to the particle. A reasonable uniform temperature distribution should be obtained in the particle if the resistance to heat transfer by conduction was small compared with the convection resistance at the surface ($Bi < 0.1$), so that the major temperature gradient would occur through the fluid layer at the surface. The rate of heat gain by the particle is equal to the rate of heat transferred by convection. Thus, the energy balance equation can be written as:

$$q = h_{fp} A (T - T_f) = -m C_p (dT/dt) \tag{2.12}$$

with the initial condition of $T = T_o$ at $t = 0$. Therefore, the solution to the above equation is (Incropera and de Witt, 1985):

$$\frac{T_p - T_f}{T_i - T_f} = \exp -(h_{fp} A / mC_p) t \tag{2.13}$$

In the above equation T_p is the bulk temperature of the particle at time t. The heat transfer coefficient (h_{fp}) can be calculated, with knowledge of the initial temperature of the particle (T_i), constant fluid temperature (T_f), surface area, mass and heat capacity of the particle. However, the bulk temperature of the particle at a given time should be determined using the following energy balance equation between the processed particle retrieved from the carrier fluid and transferred to a thermos flask containing a certain amount of a liquid to achieve equilibrium condition:

$$(mC_p)_p (T_p - T_{eq}) = (m C_p)_l (T_{eq} - T_{il}) \tag{2.14}$$

Numerical solution for h_{fp}

A number of analytical solutions for conduction and convection heat transfer problems have been reported in the literature. Even so, in many practical situations the geometry or boundary conditions are such that an analytical solution has not been obtained at all, or if the solution has been developed, it involves such a complex series solution that the numerical evaluation is difficult. Numerical approaches based on finite-difference or finite-element techniques have been developed for such situations.

The governing partial differential equation for one dimensional, unsteady state heat conduction and a spherical geometry is:

$$\frac{\partial T}{\partial t} = \alpha \left(\frac{\partial^2 T}{\partial r^2} + \frac{2}{r} \cdot \frac{\partial T}{\partial r}\right) \tag{2.15}$$

and the initial and boundary condition is:

$$T(r, 0) = T_i \quad @ \quad t = 0 \tag{2.15a}$$

$$\partial T/\partial r = 0 \quad @ \quad r = 0 \; , \; t > 0 \tag{2.15b}$$

$$-k\,A\,\frac{\partial T}{\partial r} = h_{fp}\,A\,(T_f - T_{ps}) \quad @ \quad r = a \; , \; t > 0 \tag{2.15c}$$

In order to determine h_{fp}, the partial differential equation (with associated initial and boundary conditions) can be solved using a finite difference method as detailed in many books (Holman, 1990; Chandra and Singh, 1995). Usually, the numerical procedure involved with a finite difference technique. The transient temperature distribution in a particle can be computed for a given condition using a computer program and inverse conduction heat transfer approach. Using this approach, transient surface temperature of the particle (T_{ps}) is computed with the knowledge of fluid temperature (T_f), initial temperature (T_i), radius (a), thermal conductivity (k), thermal diffusivity (α) of the particle and assuming a value for h_{fp}. Thus, using an iterative technique the value of h_{fp} changes sequentially to minimize the differences between the computed and experimentally measured particle temperature.

Literature data on fluid-to-particle heat transfer coefficient

The convective heat transfer coefficient is not a material property, such as thermal conductivity or specific heat, but rather a complex function of the composition of the fluid, the geometry of the particle, and the hydrodynamics of the fluid motion past the surface (Chapman, 1989). Heat transfer associated with the immersed particle is most likely to be influenced by factors including: the geometry of the particle (size and shape), its position, the proximity of other bodies, flow rate and fluid properties, fluid-to-particle relative velocity and the diameter of the particle in relation to that of the tube (Gunn and Narayanan, 1981). Some of these factors have been studied by different investigators using various techniques. The results of these studies have been reviewed by Ramaswamy *et al.* (1997) and the summary of published data on h_{fp} in relation to some of the above factors, are given in Table 2.1.

Factors influencing the fluid-to-particle heat transfer coefficient

Initially a conservative approach, based on a stationary condition, was proposed to estimate the fluid-to-particle heat transfer coefficient. However, experimental h_{fp} obtained by several researchers in tube-flow conditions indicated that this approach is very conservative, due to the fact that both fluid and particles usually exhibit different velocities (Sastry *et al.*, 1990 and Palmieri *et al.*, 1992). Ramaswamy *et al.* (1997), in a comprehensive review paper, summarized that the convective fluid-to-particle heat transfer coefficient is influenced by several factors such as: particle size and shape, particle and fluid thermophysical properties, particle location in the tube-flow condition, fluid-to-particle relative velocity, the ratio of particle to tube diameter and fluid viscosity and temperature. Baptista *et al.* (1997), also pointed out that the particles often present a rotational movement that affects the boundary layer and probably increases the h_{fp} values. Chakrabandhu and Singh (1998) proved that values of h_{fp} were significantly higher for rotating particles as compared to those for the stationary particle. Influencing factors on h_{fp} are mainly divided in two sections: either related to the particle or the fluid.

Parameters associated with particles: In recent years a number of experimental approaches have been used to investigate the effect of parameters associated with particles on h_{fp} in continuous tube-flow systems, resulting in a growing body of literature on the subject. Particle size and geometry are the most important factors to be considered because the flow behavior around the particle can be significantly different.

Table 2.1. Published data on convective fluid-to-particle heat transfer coefficient (h_{fp}).

Particle material	Shape and size	Type of fluid	Flow conditions	h_{fp} (W/m^2 K)	Reference
Potato	Cube 1-2 cm	Water	0.36-0.86 cm/s	239-303	Chang and Toledo (1989)
Potato	Cube 1-2 cm	35% sucrose solution	-	146	Chang and Toledo (1989)
Silicone Rubber	Cube 2.54 cm	Water	Static	51-63	Chandarana (1988)
Silicone Rubber	Cube 2.54 cm	Water	0.26-0.88 cm/s	65-107	Chandarana *et al.* (1988)
Silicone Rubber	Cube 2.54 cm	Starch dispersion	Static	8-36	Chandarana *et al.* (1989)
Silicone Rubber	Cube 2.54 cm	Starch dispersion	0.26-0.88 cm/s	56-90	Chandarana *et al.* (1988)
Aluminium	Sphere 23 .9 mm	Water	4.3-11 gal/min	2039-2507	Sastry *et al.* (1989)
Aluminium	Mushroom shaped 3 sizes	CMC solution	0.08-0.29 kg/s	548-1175	Zuritz *et al.* (1990)
Aluminium	Sphere 1.33-2.39 cm	Water	2.1-12.7 gal/min	688-3005	Sastry *et al.* (1990)
Alginate Gel	Sphere 3.4 mm	Water	Re=5250-50,000	2180-7870	Heppel (1985)
Alginate Gel	Sphere 3.4 mm	Starch dispersion	Re=30	930	Heppel (1985)
Aluminium	Mushroom shaped	Water	Static(heating)	652-850	Alhamdan *et al.* (1990)
Aluminium	Mushroom shaped	Water	Static(cooling)	384-616	Alhamdan *et al.* (1990)
Aluminium	Mushroom shaped	CMC solution	0.05-0 9 (heating)	75-310	Alhamdan and Sastry(1990)

Table 1. Continuation.

Particle material	Shape and size	Type of fluid	Flow conditions	h_{fp} (W/m^2 K)	Reference
Aluminium	Mushroom shaped	CMC solution	0.05-0.9 (cooling)	22-153	Alhamdan and Sastry (1990)
Boron nitride	Cylinder	CMC solution	2.0-5.0 gal/min	134-669	Balasubramaniam Sastry (1994)
Gellan Gel	Cubes 0.96 cm	Water	1.3-3.8 x10^{-4} m^3/s	2000-4500	Gratzek and Toledo (1994)
Polymethyl methacrylate	Sphere 8-12.7 mm	Glycerine/ Water	Re=73.1-369	58-1301	Mwangi *et al.* (1993)
Lead	Sphere 8 mm	Silicone oil	Static	287-448	Astrom and Bark (1994)
Alginate Gel	Sphere 8 mm	Silicone oil	Static	231-360	Astrom and Bark (1994)
Turnip	Sphere 17 mm	Starch dispersion	Static	156-177	Astrom and Bark (1994)
Transmitter sensor	Cylinder 22.6 mm	CMC	Re<2	108-195	Bhamidipati and Singh (1995)
Aluminum	Sphere, Cube Cylinder	Water, CMC	Static	183-1800	Kelly *et al.* (1995)
Potato Teflon	Cylinder 25.4 mm	Water CMC	6-12 L/min	100-700	Awuah *et al.* (1996)
Sodium Alginate	Sphere	Starch	Re<106	165-2376	Chen *et al.* (1997)
Aluminum	Sphere Hollow	CMC	Re=7-284	334-1497	Baptista *et al.* (1997)
Potato-alginate	Cube	CMC	Re=0.9-33 Rotational	120-4300	Chakrabandhu and Singh (1998)
Potato	Cube 9-19 mm	Starch	7-21 L/min	600-3000	Kantt *et al.* (1998)

In a conventional canning process for lead particles of different sizes, Lenz and Lund (1978) found that the heat transfer coefficient increased with increasing particle dimensions. Hassan (1984) reported a reverse trend to that of Lenz and Lund (1978) where the h_{fp} was higher for smaller potato particles processed in water as compared to bigger particles. Sablani and Ramaswamy (1998) found agreement with Hassan (1984), in a heat transfer study with end-over-end agitation of cans found both the overall and fluid-to-particle heat transfer coefficient decreased with increasing particle size.

In continuous flow systems, the effect of particle size or particle to tube diameter ratio (d/D) on the heat transfer coefficient also appears to be nonconclusive, because different authors have reported contradictory results. Sastry *et al.* (1990), using a moving thermocouple method for spherical particles, reported that h_{fp} increased with increasing particle size. The authors pointed out that as the particle size increases, the presence of the wall becomes a contributing factor, since part of the particle comes into contact with the slow-moving fluid within the laminar sub-layer, whereas other portions stay with the faster-moving fluid. However, this is in contrast to the result of Zitoun and Sastry (1994b) who, using the same technique but with cubical particles, reported the opposite trend and assigned it to differences in flow regime and particle shape. Balasubramaniam and Sastry (1994b) reported an increase in h_{fp} with increasing particle size, using a liquid crystal technique, but reported that particle size effects were not so clear cut while using the moving thermocouple method due to the lack of control over the radial location. Zuritz *et al.* (1990) also reported an increase in heat transfer coefficient with an increasing spherical particle size, whereas Chandarana *et al.* (1988) found the heat transfer coefficient to decrease with increasing cube size. Using finite cylinders (diameter ranging from 15.9 to 25.4 mm and 25.4 mm length) in two holding tube of diameters 50.8 and 76.2 mm, Ramaswamy *et al.* (1996) found no clear-cut effect of particle-to-tube diameter. However, in this instance, the heat transfer coefficient was found to increase with decreasing particle size. Kelly *et al.* (1995) evaluated convective heat transfer in an open channel flow condition and concluded that particle shape did not significantly affect h_{fp}, when using the characteristic length to describe the particle.

With respect to the particle properties, Measmans *et al.* (1992) pointed out that as particle properties such as density and surface roughness do not affect particle-fluid motion, the type of particle material may not influence the magnitude of the convective fluid to particle heat transfer coefficient. However, the fluid-to-particle heat transfer coefficients determined by Hassan (1984) were higher for potato than that for Teflon particles processed in water. Stoforos (1988) also reported different values for aluminum and Teflon spheres under similar experimental conditions. Chandarana *et al.* (1989) reported higher values of h_{fp} from water and starch solutions for the food particles, potato and carrot, than silicone dices. Astrom and Bark (1994) investigated the effects of influencing factors on h_{fp} in aseptic processing simulation, and found differences in h_{fp} using spherical particles of various materials. The authors stated that although the convective heat transfer coefficient is primarily a function of the fluid properties, it could also be expected that the heat capacity and thermal conductivity of the particle material can have some influence on h_{fp}. Higher thermal conductivity and thermal diffusivity of particles resulted in faster heat conduction, thus keeping the particle surface temperature lower as compared to that of the insulated material. The difference between fluid temperature around the particle, the boundary layer, and particle surface temperature probably altered the interfacial characteristics that caused different heat transfer coefficients (Astrom and Bark, 1994). Using potato and Teflon particles processed in water and CMC solution, Awuah *et al.* (1996) observed similar trends in relation to the effect of fluid temperature, concentration and flow rate on h_{fp} for both materials. However, slightly higher values of h_{fp} were reported for potato particles as compared with Teflon particles. In another study, comparing h_{fp} evaluation based on two analytical methods (rate and ratio methods), using transient time-temperature data obtained from regular objects, Awuah *et al.* (1995) reported different values of h_{fp} for particles of different shapes and material, but of the same size.

Parameters associated with carrier medium: Heat transfer to the particulate strongly depends on the rheological properties of the carrier fluid as well as the fluid flow rate around the particle in the tube-flow systems. Depending on fluid characteristics, fluid can be classified as either Newtonian or non-Newtonian. Most liquid foods used in industry are non-Newtonian fluids and can be described by a power law model (Rao, 1992):

$$\sigma = m\, \dot{\gamma}^{n} \tag{2.16}$$

where σ is the shear stress, γ is the shear rate, m is the consistency coefficient, and n is the flow behavior index. With Newtonian fluids, the shear stress is directly proportional to the shear rate, within the laminar flow range (Bourne, 1982) and the constant of proportionality called viscosity. Viscosity and density are both dependent on the process temperature, and therefore a variation in temperature will affect the flow behavior. The rheological parameters (m and n) for all non-Newtonian fluids are also temperature dependent.

The effect of fluid viscosity on h_{fp} for forced convection has been reported in several studies (Chnadarana *et al.*, 1988; Zuritz *et al.*, 1990; Gaze *et al.*, 1990; Balasubramaniam and Sastry 1994a,b; Kelly *et al.*, 1995; Bhamidipati and Singh 1995; Awuah *et al.*, 1995 and 1996; Ramaswamy *et al.* 1996; Chen *et al.* 1996; Baptista *et al.*, 1997 and Mankad *et al.* 1997). The higher the viscosity of a fluid, in which a particle is immersed, the more heat transfer will be hampered, at least when low turbulence decreases the effective relative particle-to-fluid velocity at the interface (Maesmans *et al.* 1992).

With respect to the temperature effect, it is generally recognized that viscosity decreases as the fluid temperature increases. The expected result is an enhanced convective heat transfer coefficient. Since viscosity decreases at higher temperature, it should be apparent that there is direct relationship between h_{fp} and viscosity, with higher values associated with higher viscosity. However, it should also be recognized that there may be other factors or interactions which may counter-balance the temperature effect on h_{fp}. For example, the particle velocity and/or particle-to-fluid relative velocity, which are a function of fluid viscosity, also influence h_{fp}. Higher particle velocities and higher particle-to-fluid relative velocities will result in higher value of h_{fp}.

Dutta and Sastry (1990) suggested that the most critical factor affecting particle velocity, and hence h_{fp}, is the fluid viscosity. The higher particle linear velocity also tends to increase the particle angular velocity (number of rotation per unit time, ω=v/r), which contributes to a further enhancement the heat transfer coefficient (Baptista *et al.*, 1997). Chakrabandha and Singh (1998) also reported that the rotational velocity of a particle significantly increased with fluid viscosity and fluid flow rate, but decreased as the fluid temperature increased, due to lowering of viscosity. Studying the effect of temperature and viscosity together is somehow confusing and more complicated. Particle velocity is viscosity dependent and viscosity is temperature dependent. The more viscous the fluid, the higher the particle velocity. Concomitantly, the higher the temperature, the lower the viscosity. Hence, at higher temperatures, h_{fp} is expected to decrease as a result of lower particle velocity while at the same time there is an expected increase due to lower viscosity. With only a few exceptions, most references in the literature, concerning h_{fp} evaluation, have been carried out at a constant fluid temperature. Alhamdan and Sastry (1990) studied the effect of fluid temperature in natural convection (with no particle motion); Awuah *et al.* (1996) studied the temperature effect with a stationary particle (hence no particle velocity was involved); and Bhmidipati and Singh (1995) studied the effect of temperature at very low values of h_{fp}(108-195 W/m^2K). Alhamdan and Sastry (1990) reported that the h_{fp} values increased with fluid temperature, with the lower viscosity fluids, but not so much with the higher viscosity fluids. They also pointed out that higher viscosity tends to overshadow the influence of temperature.

In addition to fluid viscosity, fluid flow rate is another important factor which can affect particle velocity and hence the associated convective heat transfer coefficient, in a continuous tube-flow system containing particulate. The effect of flow rate on h_{fp} is consistent in the literature, no matter which technique or what carrier fluid has been used: the higher the fluid flow rate, the higher the h_{fp}.

Dimensionless correlations

Successful temperature prediction for aseptically processed particulate food requires data on the fluid-to-particle heat transfer coefficient, h_{fp}, besides the relevant thermo-physical properties. Dimensional analysis is a useful method to generalize experimental data in the form of dimensionless numbers, grouped from physical variables. This analysis gives more insight to the physical phenomena and can also be used for scale-up. Different forms of correlations have been proposed for free and forced convection. In free convection, the convective heat transfer coefficient is usually correlated in the form of Nusselt number with other dimensionless numbers such as of Grashof and Prandtl. Whereas in forced convection condition Nusselt number is expressed as a function of Reynolds and Prandtl. These dimensionless numbers are defined as follows:

Nu =(Dimensionless measure of convection heat transfer coefficient) = $(h/k_f)d$
Re = (Inertia force/Viscous force) = $\rho\ V\ d\ /\ \mu$
Gr = (Buoyancy force/ Viscous force) = $g\ \beta\ d^3 \Delta T\ /\upsilon^2$
Pr =(Diffusion of momentum/ Diffusion of heat) = υ/α

Free convection for a single sphere has not been studied as extensively as those involving cylinders and plates. However, Whitaker (1976) proposed the following equation for free convection from a single sphere when $(Gr)^{0.25}\ (Pr)^{0.33}$ is less than 200:

$$Nu = 2 + 0.6\ (Gr)^{0.25}\ (Pr)^{0.33} \tag{2.17}$$

Kramers (1946) and Ranz and Marshal (1952) were probably the first who presented the following equations for the forced convection condition:

$$Nu = 2 + 1.3\ Pr^{0.15} + 0.66\ Pr^{0.31}\ Re^{0.5} \tag{2.18}$$

$$Nu = 2 + (Re)^{0.5}\ (Pr)^{0.33} \tag{2.19}$$

Whitaker (1972) presented a more general correlation for the flow of gases and liquids across a single sphere in the form:

$$Nu = 2 + (\ 0.4\ Re^{0.5} + 0.06\ Re^{2/3}\ )\ Pr^{0.4}\ (\mu_\infty\ /\mu_W\ )^{0.25} \tag{2.20}$$

which is valid for Re between 3.5 and 80000, Pr between 0.7 and 380, and $\mu_\infty\ /\mu_W$ between 1 and 3.2.

The most conservative approach (Sastry *et al.*, 1989) is to assume that the particle and fluid travel at identical velocities through the aseptic system, so that the Re number becomes zero, according to the above mentioned equations, yielding a relationship:

$$Nu = 2 \tag{2.21}$$

Studies by Chang and Toledo (1989) indicated that the Nu number may range from 10-20 at zero fluid velocity. According to Hunter (1972) a process designed on the basis of Nu=2 may result in over-heating of the product.

Many recent studies (Chandarana *et al.*, 1988; Zuritz *et al.*, 1990; Sastry *et al.*, 1990; Mwangi *et al.*, 1993; Zitoun and Sastry, 1994a,b; Sablani and Ramaswamy, 1995; Bhamidipati and Singh, 1995; Kelly *et al.*, 1995; Awuah and Ramaswamy 1996; Baptista *et al.*, 1997; Mankad *et al.*, 1997; Chakrabandhu and Singh, 1998) have developed modified forms of these equations which are specifically valid for a certain range of dimensionless numbers. To improve the model prediction, making it dependent on the experimental conditions, some other group of dimensionless numbers, such as: Froud number (V^2/gd), Peclet number (Re.Pr), the ratio of particle-to-tube diameter (d/D), the ratio of particle-to-fluid thermal diffusivity (α_p/α_f), the ratio of particle velocity to slip velocity (V_p/V_s), and the ratio of Gr/Re^2 have been also included in the empirical equations. Most of these works were carried out with non-Newtonian fluids, therefore a generalized form of Re, Gr and Pr numbers was used in the developed correlations, where the fluid viscosity (μ) is defined as a function of rheological parameters as follow:

$$\mu=2^{n-3}\ m\ (3n+1/n)^{n}\ (d_p/V_s)^{1-n} \tag{2.22}$$

where, m and n are the consistency and flow behavior indices, d_p is the particle diameter and V_s is the slip velocity.

PREFACE TO CHAPTER 3

With just a few exceptions, most of the previous work related to h_{fp} determination have been carried out using stationary particle methods. Therefore, one of the main objectives of this work was to develop and evaluate a new technique by imparting particle motion during processing. An innovative experimental setup was designed and fabricated to satisfy this purpose, in order to record the time-temperature of a non-stationary particle. An oscillatory approach was used for imparting particle motion in a model holding tube. The experimental setup was designed to permit easier investigation of the effects of some parameters affecting h_{fp}. This setup allowed better control of such factors as particle velocity and particle location inside the tube.

The results of this study were presented partially at two scientific conferences: Conference on Food Engineering (CoFE), 1995 and Institute of Food Technologist (IFT), 1996; and were also published in a paper entitled as: "A new technique for evaluating the fluid-to-particle heat transfer coefficient under tube-flow conditions involving particle oscillatory motion" in the Journal of Food Process Engineering, 1997, volume 20 (6): 453-475 (Zareifard and Ramaswamy, 1997).

Experimental work and data analysis were carried out by the candidate, under the supervision of professor H. S. Ramaswamy. This will fulfil the first objective of the thesis, and a modified version of the paper is presented here as the third chapter of the thesis.

CHAPTER 3

A NEW TECHNIQUE FOR EVALUATING FLUID-TO-PARTICLE HEAT TRANSFER COEFFICIENTS UNDER TUBE-FLOW CONDITIONS INVOLVING PARTICLE OSCILLATORY MOTION

ABSTRACT

Fluid-to-particle heat transfer coefficient between the fluid and the particles (h_{fp}) is one of the critical parameters for the modelling of particle temperature profiles, in the continuous processing of particulate foods in a carrier liquid. A laboratory scale apparatus was fabricated to evaluate h_{fp} under conditions imparting particle oscillatory motion, while being heated in a model holding tube. Spherical particles ($d = 12.7 \times 10^{-3}$ m) with centrally located fine-wire flexible thermocouples ($d = 7.62 \times 10^{-5}$ m) were suspended from the upper mid-section of a curved glass tube ($ID = 50.8 \times 10^{-3}$ m) in order to provide lateral movement of the particle as the tube was subjected to an oscillatory motion. A variable speed reversible motor, in conjunction with an electronic circuit board, was used to control the frequency and amplitude of the tube, thereby keeping the particle in continuous motion. Time-temperature data were gathered continuously from the time the particle-mounted oscillatory unit, was initially set at room temperature, for the desired amplitude and frequency, and then transferred to a heated sucrose solution (0, 30 and 50 % w/w) at 70 or 90^{o}C. The h_{fp} values were calculated from the evaluated heat rate index, f_h, at three particle velocities (0.09, 0.16 and 0.26 m/s), under three oscillatory amplitudes (90, 180 and 270^{o}). Values of h_{fp} increased with the amplitude of oscillation and particle velocity, and decreased with the sucrose concentration. Values of h_{fp}, associated with the fixed particles, were higher than those for particles which were free to move.

INTRODUCTION

Aseptic processing has been used commercially for liquid products and acid foods containing small particulate matters, but its use for low-acid particulate foods is still under investigation. Conventional thermal processes are established based on the temperature response of the food, which can be easily evaluated during heating and cooling. However, in continuous flow aseptic processing situations, with discrete particles suspended in a continuously moving fluid, particle temperature cannot be easily measured. Since implementing traditional routines for process calculations become questionable under such situations, mathematical modeling has been used as an alternative. A major obstacle for modeling particle temperature history, in an aseptic processing unit, is the lack of adequate information on the heat transfer coefficient between the carrier fluid and suspended particles (Heldman, 1989). Considerable effort has gone into establishing suitable models for estimation of lethality of low-acid foods containing particulate (Sastry, 1986; Chandarana *et al.*, 1989; Chang and Toledo, 1990; Larkin, 1990; Sablani and Ramaswamy 1995; Kelly *et al.*, 1995; Balasubramaniam and Sastry 1996a). Dignan *et al.* (1989) listed the critical factors needed in modeling heat transfer and lethality distribution, in continuously processed low-acid particulate foods, as: the particle size/distribution, the convective heat transfer coefficient and residence time distribution, both in the heat exchanger and holding tube.

In process evaluation through simulations, the fluid-to-particle heat transfer coefficients in both heat exchanger and holding tube are probably the most important, but difficult, parameters to be determined experimentally (Dignan *et al.*, 1989; Heldman, 1989). For continuous sterilization of food particulate, de Ruyter and Brunet (1973), and Manson and Cullen (1974) assumed the heat transfer coefficient to be infinite. However, several researchers have demonstrated a finite convective heat transfer coefficient to be associated at the fluid-particle interface (Sastry, 1986; Chandarana and Gavin, 1989a,b; Chang and Toledo, 1990; Chandarana *et al.*, 1990; Zitoun and Sastry 1994a,b; Bhamidipati and Singh 1995; Awuah and Ramaswamy 1996).

Determination of h_{fp} poses a unique challenge to the investigators because of the difficulty in monitoring the temperature of moving particles, without interfering with particle motion. Chau and Synder (1988), Chandarana *et al.* (1989 and 1990), Chang and Toledo (1990), Zuritz *et al.* (1990) and Awuah *et al.* (1995) determined h_{fp} by recording the time-temperature data of a stationary particle in a flowing stream of carrier fluid. Researchers have also attempted to simulate more realistic situations, placing the particle in moving conditions, while evaluating h_{fp}. Sastry *et al.* (1989) suggested a moving thermocouple method in which the temperature of a particle attached to a thermocouple could be monitored, while the thermocouple wire is withdrawn from the downstream end at the same speed as that of the particle. Using this method, Zitoun and Sastry (1994b) studied the heat transfer coefficient for cube shaped particles in a continuous tube flow.

Recently, thermo-chromic liquid crystal, which undergoes color changes with temperature, has been used to get the surface temperature history of moving particles. This enable the evaluation of heat transfer coefficients under continuous flow conditions. This method involves coating the moving particle with a specific liquid crystal and recording the color changes on the particle surface as a function of time. Time-temperature data are then obtained from previously established color-temperature calibrations. Stoforos and Merson (1991) were the first to use the liquid crystal material to evaluate the overall and liquid-to-particle heat transfer coefficient for model food particles, in a rotating liquid/particulate canned food system. Balasubramaniam and Sastry (1994a,b and 1995) applied the same technique to measure the heat transfer coefficient in a continuous tube-flow system. They observed that the liquid crystal method resulted in higher values of h_{fp}, compared to the moving thermocouple method under the same experimental conditions. Other methods, involve techniques such as measuring the relative velocity between the fluid and particle, and back-calculating h_{fp} using published dimensionless correlations (Zitoun and Sastry 1994a; Balasubramaniam and Sastry 1994b). Alternatively, indirect methods of h_{fp} determination have also been proposed which are based on locating heat-labile substances, such as enzymes or microbial spores, at the center of simulated food particles (Weng *et al.*, 1992), or the use of remote temperature sensors in moving particles (Balasubramaniam and Sastry 1996b).

Although the various techniques employed for evaluating the fluid-to-particle heat transfer coefficient have contributed to understanding of the heat transfer phenomena, they all have limitations and only partially simulate the commercial processing situation. Some studies have used aseptic processing conditions, but are limited to a stationary particle. Some others involve particle motion, but are limited to a transparent carrier medium in glass holding tubes. The objective of this study was to develop a technique which, to some extent, overcomes some of the associated problems. An oscillatory approach was used for imparting particle motion in a model holding tube, while using the conventional thermocouple approach for measuring h_{fp} in tube-flow systems. The particle was held in a section of a circular tube, which was subjected to an oscillatory motion, while immersed in a constant temperature water bath. The particle velocity in a relatively stationary fluid could thus be defined by controlling the amplitude and frequency of oscillations.

MATERIALS AND METHODS

Experimental setup

Two transparent glass tubes (ID = 50.8×10^{-3} m) were bent to give radii of curvatures of 0.15 and 0.25 m, and an arc was cut to a length representing about one quarter of a full circle. On the upper midpoint of each tube a hole was cut to pass thermocouples through a connector. Two such units were nested together facing each other in diametrically opposite locations. The four bent tubes were secured on an aluminium cross bar to form two diametrically opposite, open ended quarters of circular tubing (Figure 3.1).

Nylon spheres ($d=12.7\times10^{-3}$ m) were used as test particles and the thermophysical properties of the particles were experimentally evaluated using procedures described elsewhere (Sablani and Ramaswamy, 1996). The thermophysical properties were: density (ρ)=1128 kg/m^3, thermal diffusivity (α)=1.58×10^{-7} m^2/s, and heat capacity (C_p)=2073 J/kg K. Thermal conductivity (k) was calculated as 0.369 W/m K ($k=C_p\rho\alpha$).

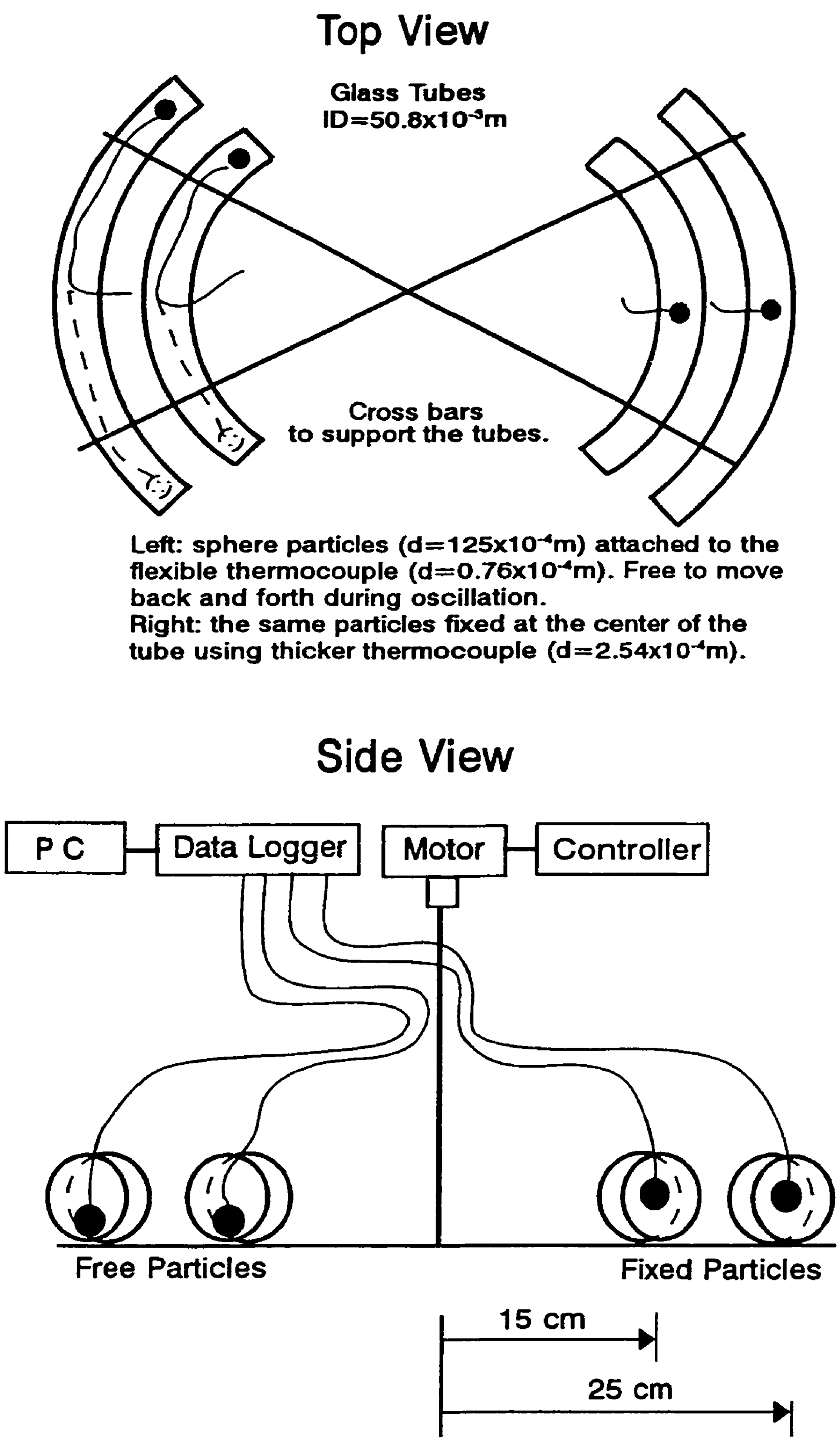

Left: sphere particles (d=125×10^{-4}m) attached to the flexible thermocouple (d=0.76×10^{-4}m). Free to move back and forth during oscillation.
Right: the same particles fixed at the center of the tube using thicker thermocouple (d=2.54×10^{-4}m).

Figure 3.1. Schematic diagram of experimental setup: the particle oscillatory motion method.

The spherical particles were carefully drilled to the geometric center using a one millimeter drill bit. A very fine and flexible Teflon coated type-T copper-constantan thermocouple of 7.62 x 10^{-5} m diameter (Omega Engineering Inc., Stamford, CT) was made and inserted to the center of each Nylon sphere. The gap between the thermocouple wire and the particle was filled with glue (epoxy resin and hardener 50/50). Then one of the particles was located inside the tube with some extra lead of thermocouple wire in order to let the particle move inside the tube during oscillation. In the parallel assembly, on the other side, a thicker gage thermocouple of 25.4x10^{-5} m diameter was used in order to hold the particle rigidly at the center or bottom surface of the tube. All thermocouples were calibrated against an ASTM standard mercury-in-glass thermometer with a temperature resolution of ±0.05°C. Thus, there were two fixed particles at 0.15 and 0.25 m radial distances from the center, and two other particles which were free to move inside the tube at the same radial distance but on the other side. During the oscillations, the fixed particle would move along with the tube thus undergoing a programmed velocity in a relatively stationary liquid phase. On the other hand, the particle that was actually "free" to move remained partly stationary, while the tube slid below it during the oscillations.

The whole assembly was supported by a shaft connected to the output of a 100W electric DC motor. An electronic circuit, in conjunction with two micro-switches which reversed the direction of rotation, was designed in such a way that the shaft could be rotated at different speeds (rpm) and amplitudes (the distance between the two micro-switches could be adjusted to give different amplitudes). Therefore, changing the position of the micro-switches provided different amplitudes of oscillation, and changing the power level provided different revolutions per minute, and hence frequency. In this way, the assembly of the particle equipped glass tubes could be subjected to controlled oscillations. A schematic diagram of the experimental setup is shown in Figure 3.1.

The whole assembly was kept in a water tank at room temperature for equilibration of temperatures in the test particles, and an appropriate oscillatory motion was designed with a specified frequency and amplitude. While the tubes were in a steady oscillatory condition, the assembly was transferred to a stainless steel insulated tank, containing a heating medium at the desired temperature. The heating tank was previously heated using steam injection and controlled to a constant set-point temperature ± 1 °C. Time-temperature data were gathered at 5 s time intervals using a data logger (Dash-8, Metra-Byte Corp. Taunton, Ma) connected to a personal computer.

Experimental procedure

Several experiments were carried out using water and Nylon particles of different sizes in order to evaluate the experimental set-up. To work in the lower range of Biot numbers, it was necessary to restrict the particle size to $d = 12.7 \times 10^{-3}$ m. The sucrose solutions were used as additional heating media providing a higher viscosity. Sucrose solution was prepared in a 0.6 x 0.6 x 0.9 m stainless steel tank and heated to the desired temperature (70° or 90°C). The temperature of the medium was continuously monitored and was found to be stable within ± 1°C during a given test run. The concentration of the solution was monitored using a refractometer and kept constant during the experiment by the addition of small amounts of a higher concentration syrup or water as needed..

Experiments were carried out in water as well as in 30 and 50% (w/w) sucrose solutions, with three different amplitudes of 90, 180 and 270° (angle of oscillation) and two temperatures (70 and 90°C). The rotation speed of 6 and 10 rpm provided three linear velocities for the particle at 0.09, 0.16 and 0.26 m/s with respect to their position from the center of rotation ($V = R\omega = 2\pi Rn$). The number of replications was at least three for each experimental condition. In the majority of experiments, the fixed particle was positioned at the central axis of the tube, while in others it was located along the bottom surface for comparative purposes.

Analytical solution for h_{fp} evaluation

The unsteady state heat conduction differential equation governing heat transfer to an isotropic spherical particle, suddenly transferred into a constant temperature medium is expressed as:

$$\frac{\partial U}{\partial t} = \alpha \left(\frac{\partial^2 U}{\partial r^2} + \frac{2}{r} \cdot \frac{\partial U}{\partial r}\right) \tag{3.1}$$

The details of the analytical solution to the above differential equation is given in chapter 2. Briefly, a simplified form of the analytical solution [Eq. (2.10)] represents the straight line portion of the heating curve. The slope of such a curve is called the heating rate index (f_h) which can be obtained from the plot of the log of temperature difference, between the heating medium and the particle being processed, versus time. The slope index (f_h) is dependent on the thermo-physical properties of the particle and the positive root of the Biot number function (δ), but independent from the location of the thermocouple inside the particle. Therefore, using this method, it is not necessary to know the exact location of the thermocouple within the sample. Knowledge of the particle size, thermal diffusivity and thermal conductivity as well as the heating rate index (f_h), which can be evaluated from the experimental data allows the calculation of the corresponding Biot number and hence, the heat transfer coefficient (h_{fp}) can be calculated as: [h_{fp} = Bi (k/a)].

RESULTS AND DISCUSSION

Typical time-temperature curves for all four particles in a given test run are shown in Figure 3.2, which illustrates the slightly rapid heating behavior of the fixed particles, as compared to the free particles in both radial locations (0.15 and 0.25 m from the central axis). Semi-logarithmic plots of temperature difference (medium temperature minus center point temperature of the particle) versus time are shown in Figure 3.3. Heating rate indexes (f_h) were calculated from these plots as negative reciprocal slopes of the straight portion of the heating curves.

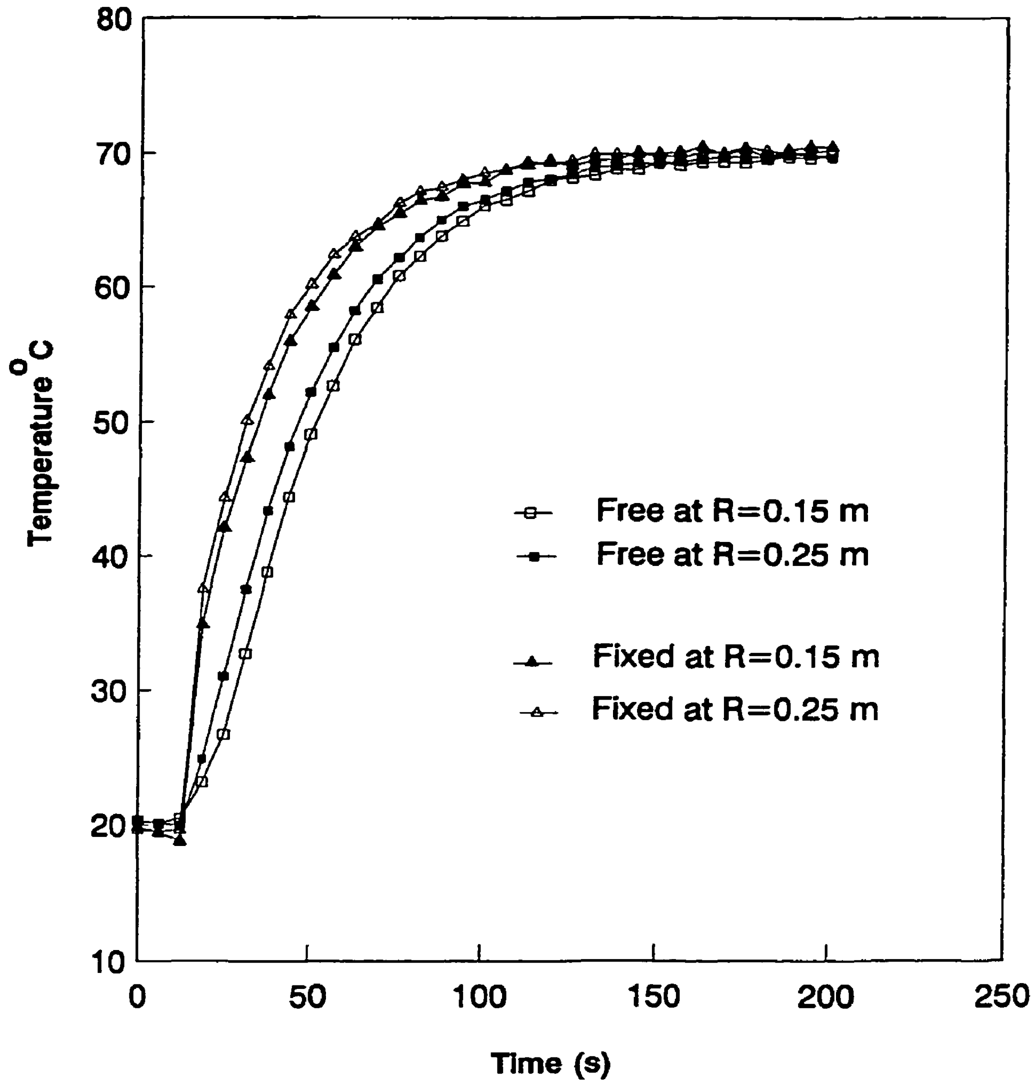

Figure 3.2. Typical time-temperature curves for free and fixed particles at two radial distances from the center of rotation.

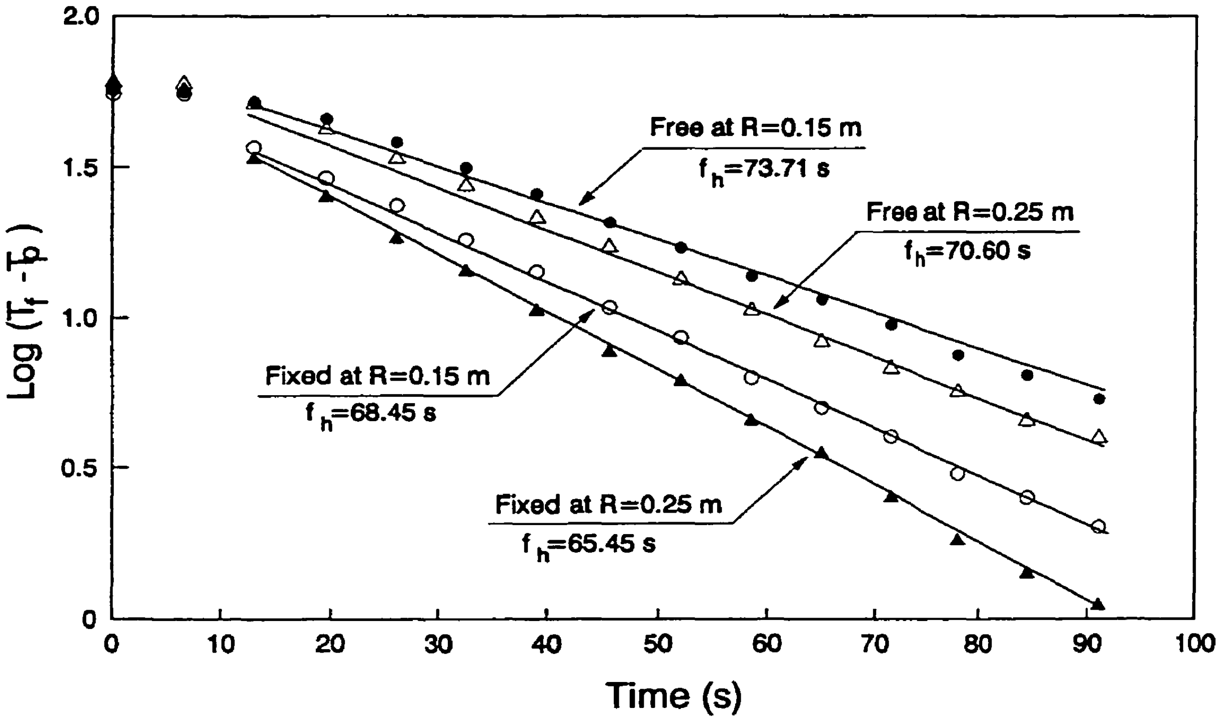

Figure 3.3. Semi-logarithmic plots of temperature difference versus time for free and fixed particles (negative reciprocal slope of the linear portion of the curve was calculated as f_h).

Generally, a Fourier number greater than 0.2 is taken to assure convergence of the series solution for the heat conduction differential equation (Eq. 2.2) to the first term. However, the actual number depends on particle shape and associated Biot numbers. Observation of the spherical particles used in the experimental conditions showed convergence (linearization of the semi-logarithmic plot) generally from a Fourier number as low as 0.1, as indicated by Figure 3.3 (Fo = 0.1 at t~25 s).

Typical data shown in Table 3.1 indicates almost identical values of the calculated slope index (f_h), between Fo values of 0.1-0.4 and 0.2-0.4 (maximum difference was about 1.5%). The evaluated f_h is used as input for calculating the associated heat transfer coefficients. Average values of the fluid to particle heat transfer coefficients and their associated coefficients of variations are presented in Tables 3.2 and 3.3, for the free and fixed particles under various conditions.

Effect of oscillation amplitude on h_{fp}

An initial set of experiments was performed with the purpose of evaluating the effect of the degree of amplitude of oscillation. At any given rotation speed (rpm), the frequency of oscillation (cycles per minute) would be different at each of the three selected degrees of oscillations. For example, at 6 rpm rotation speed, the number of oscillations per minute is 24, 12 and 8, respectively, at amplitudes of 90, 180 and 270^o. Therefore, the lower the angle of amplitude, the higher the frequency of oscillation. Results of these experiments are shown in Figure 3.4 for both the "free" and "fixed" particles at different velocities, for experiments carried out in a 30% sucrose solution. Similar results were observed for experiments conducted in water. The linear velocity of 0.09 m/s for the "fixed" particle is the result of 6 rpm at 0.15 m radius of rotation, while 10 rpm at 0.25 m radius of rotation gives 0.26 m/s; the intermediate value of 0.16 m/s is for 6 rpm at 0.25 m or 10 rpm at 0.15 m. For the "free" particle, these should be taken as "nominal" values because observation showed that the particle remained stationary for a portion of the oscillatory motion, as the tube changed the direction of oscillation. During this "stationary phase", the tube actually slid below the particle until the free-lead distance of the thermocouple wire (about one half of the tube length) was covered by the oscillation.

Table 3.1. Typical data for comparison of f_h for Fo < 0.2 and Fo > 0.2for a spherical geometry.

Fo	f_h (s)	R^2	Difference %	f_h (s)	R^2	Difference %
0.12 - 0.39	73.21	0.998	1.2	72.13	0.999	1.3
0.20 - 0.39	72.32	0.999		71.22	0.999	
0.13 - 0.40	73.16	0.996	0.6	72.47	0.997	1.3
0.21 - 0.40	73.59	0.998		73.40	0.998	
0.12 - 0.38	70.07	0.995	0.5	71.95	0.998	1.3
0.20 - 0.38	69.71	0.988		72.90	0.997	
0.12 - 0.40	69.19	0.999	0.7	70.09	0.999	1.3
0.20 - 0.40	69.67	0.998		71.05	0.998	
0.15 - 0.42	67.32	0.997	0.3	70.22	0.999	1.5
0.20 - 0.42	67.09	0.996		71.28	0.999	

Table 3.2. Associated fluid-to-particle heat transfer coefficents for free particles under different tube-flow conditions.

Heating Medium (^{0}Brix)	Temp (^{0}C)	Rotation Speed (n) (rpm)	Radial Location (R) (m)	Linear Velocity (V) (m/s)	Amp. (deg)	Rep.	h_{f_p} (W/m^2 K)	CV (%)	Bi	Nu
0	70	10	0.15	0.16	270	3	750	8.4	13.0	14.3
0	70	10	0.25	0.26	270	3	790	8.7	13.7	15.1
0	70	10	0.15	0.16	180	3	520	14.9	9.0	9.9
0	70	10	0.25	0.26	180	4	570	8.8	9.8	10.8
0	70	10	0.15	0.16	90	6	560	9.5	9.6	10.6
0	70	10	0.25	0.26	90	6	590	7.1	10.2	11.2
30	70	6	0.15	0.09	270	3	610	9.9	10.5	14.0
30	70	6 , 10	0.25 , 0.15	0.16	270	9	670	14.6	11.6	15.4
30	70	10	0.25	0.26	270	8	840	7.4	14.5	19.3
30	70	6	0.15	0.09	180	5	480	14	8.2	10.9
30	70	6 , 10	0.25 , 0.15	0.16	180	10	520	9	8.9	11.9
30	70	10	0.25	0.26	180	11	590	10	10.1	13.5
30	70	6	0.15	0.09	90	8	450	11.5	7.7	10.2
30	70	6 , 10	0.25 , 0.15	0.16	90	9	470	6.5	8.0	10.7
30	70	10	0.25	0.26	90	8	530	7	9.1	12.2
50	70	10	0.15	0.16	90	6	430	8.3	7.3	11.2
50	70	10	0.25	0.26	90	6	440	7.6	7.6	11.5
30	90	10	0.15	0.16	90	4	460	2.3	7.9	10.2
30	90	10	0.25	0.26	90	4	510	3.9	8.8	11.4
50	90	10	0.15	0.16	90	5	460	4.3	7.9	11.7
50	90	10	0.25	0.26	90	5	480	4.7	8.2	12.1

Amp. : Amplitude, Rep. : Replicates

Table 3.3. Associated fluid-to-particle heat transfer coefficents for fixed particles under different tube-flow conditions

Particle Position	Heating Medium (^{0}Brix)	Temp (^{0}C)	Rotation Speed (n) (rpm)	Radial Location (R) (m)	Linear Velocity* (V) (m/s)	Amp. (deg)	Rep.	h_{fp} (W/m^2 K)	CV (%)	Bi	Nu	Re**
FS	0	70	10	0.15	0.16	270	3	1240	6.4	21.3	23.6	4900
FS	0	70	10	0.25	0.26	270	3	1370	6.9	23.5	26.0	8000
FS	0	70	10	0.15	0.16	180	3	1000	19.6	17.3	19.1	4900
FS	0	70	10	0.25	0.26	180	3	1200	7.2	20.5	22.7	8000
FS	0	70	10	0.15	0.16	90	3	840	16	14.5	16.0	4900
FS	0	70	10	0.25	0.26	90	3	1060	17	18.2	20.1	8000
FC	0	70	10	0.15	0.16	90	3	660	15	11.4	12.6	4900
FC	0	70	10	0.25	0.26	90	3	850	3.6	14.6	16.2	8000
FC	30	70	6	0.15	0.09	270	3	890	7	15.3	20.4	1250
FC	30	70	6 , 10	0.25 , 0.15	0.16	270	7	1140	5	19.6	26.0	2250
FC	30	70	10	0.25	0.26	270	3	1260	3	21.6	28.7	3650
FS	30	70	10	0.15	0.16	270	4	1250	6.1	21.6	28.7	2250
FS	30	70	10	0.25	0.26	270	3	1440	12	24.8	33.0	3650
FC	30	70	6	0.15	0.09	180	3	750	6.8	12.9	17.1	1250
FC	30	70	6 , 10	0.25 , 0.15	0.16	180	4	890	5.3	15.4	20.4	2250
FC	30	70	10	0.25	0.26	180	3	960	4	16.6	22.1	3650
FS	30	70	10	0.15	0.16	180	4	950	3	16.4	21.8	2250
FS	30	70	10	0.25	0.26	180	4	1100	8.2	19.0	25.3	3650
FS	30	70	6	0.15	0.09	90	3	630	12	10.8	14.4	1250
FS	30	70	6 , 10	0.25 , 0.15	0.16	90	3	820	16	14.0	18.6	2250
FS	30	70	10	0.25	0.26	90	3	1090	15	18.7	24.9	3650
FC	30	70	6	0.15	0.09	90	3	580	10	10.0	13.3	1250
FC	30	70	10	0.25	0.26	90	4	690	6	11.9	15.9	3650
FC	30	70	6 , 10	0.25 , 0.15	0.16	90	5	640	7	11.1	14.7	2250
FC	50	70	10	0.15	0.16	90	4	560	6.4	9.7	14.8	850
FC	50	70	10	0.25	0.26	90	4	600	9.5	10.4	15.9	1350
FC	30	90	10	0.15	0.16	90	5	710	10	12.1	15.7	3150
FC	30	90	10	0.25	0.26	90	4	820	4.1	14.1	18.2	5150
FC	50	90	10	0.15	0.16	90	3	770	1.1	13.3	19.7	1400
FC	50	90	10	0.25	0.26	90	3	810	1.6	13.9	20.5	2250

FS: Particle fixed at surface, FC: Particle fixed at center, *V=2πRn, Amp: Amplitude, Rep: Replicates, **Particle Re no.

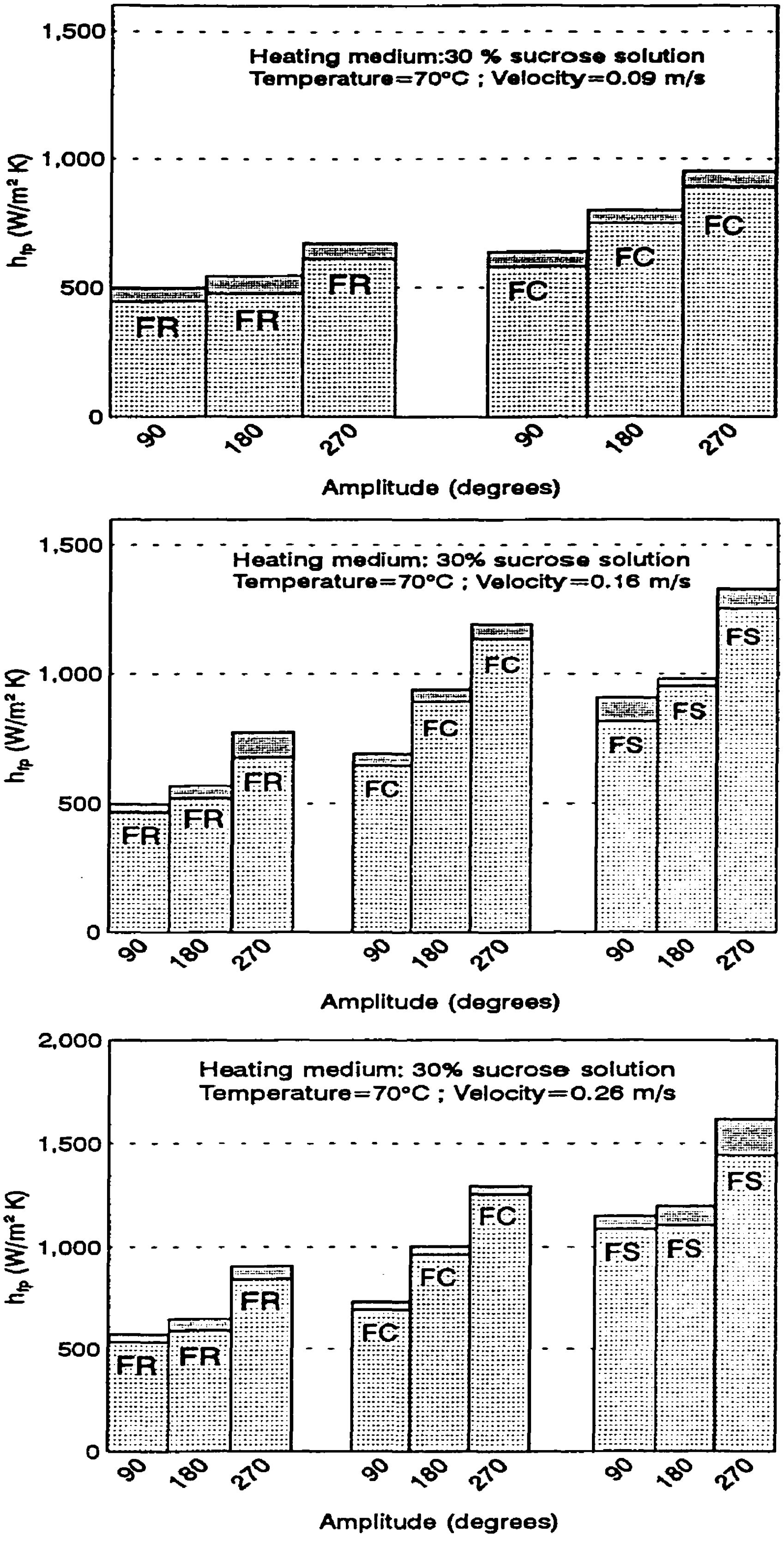

Figure 3.4. Effect of oscillation amplitude on h_{fp} values in 30% sucrose solution at 70°C, for free particle (FR), fixed at the center (FC) and fixed at the surface (FS), for different amplitude and velocities.

As shown in Figure 3.4, the values of h_{fp} consistently increased with the amplitude of oscillation at each condition (with a steeper change at 270^{o}). With the free particle, the increase in h_{fp} was about 40% and with the fixed particle the increase was 50 to 100%. With the fixed particle, this increase in h_{fp} is ascribed to a longer exposure of the particle to steady flow conditions at higher amplitudes. With the free particles, this is consistent with the shift of the particle flow behavior from "stationary" toward "moving" (dragging situation), as the amplitude of oscillation was increased. With the 90^{o} amplitude the particle remained "stationary" for about 50% of the oscillation time, while at 180^{o} and 270^{o} amplitudes the stationary phase accounted for 30% and 20%, respectively.

Effect of temperature and viscosity on h_{fp}

The effect of temperature on the associated h_{fp} in 30 and 50% sucrose solutions, at an oscillation velocity of 0.26 m/s, are shown in Figure 3.5. A similar plot was also obtained at the other velocity of 0.16 m/s. With the fixed particle, the associated h_{fp} values at $90^{o}C$ were clearly higher than at $70^{o}C$. Although a similar trend also existed with the free particles, the difference in h_{fp} between the two temperatures was much smaller. As will be further evident from the discussion of viscosity effects detailed below, this higher value of h_{fp} could be due to lower viscosities associated with the heating medium at higher temperatures.

The average values of h_{fp} and their standard deviations, as influenced by the sucrose concentration (0, 30 and 50%), are shown in Figure 3.6 at two velocities (0.16 and 0.26 m/s), while the medium temperature was maintained at $70^{o}C$ and the amplitude of the oscillation was fixed at 90^{o}. Values of h_{fp} for the free particle varied from 590 ± 35 W/m^2K in water to 440 ± 33 W/m^2K in 50% sucrose solution, with 30% sucrose giving intermediate values. For the particle fixed along the central axis, the values were 850 ± 53 W/m^2K in water and 560 ± 57 W/m^2K in 50% sucrose solution, again with intermediate values in 30% sucrose solution. The values of h_{fp} decreased with sucrose concentration for both fixed and free particles. This was expected because of the increasing viscosity of the medium at higher sucrose concentration.

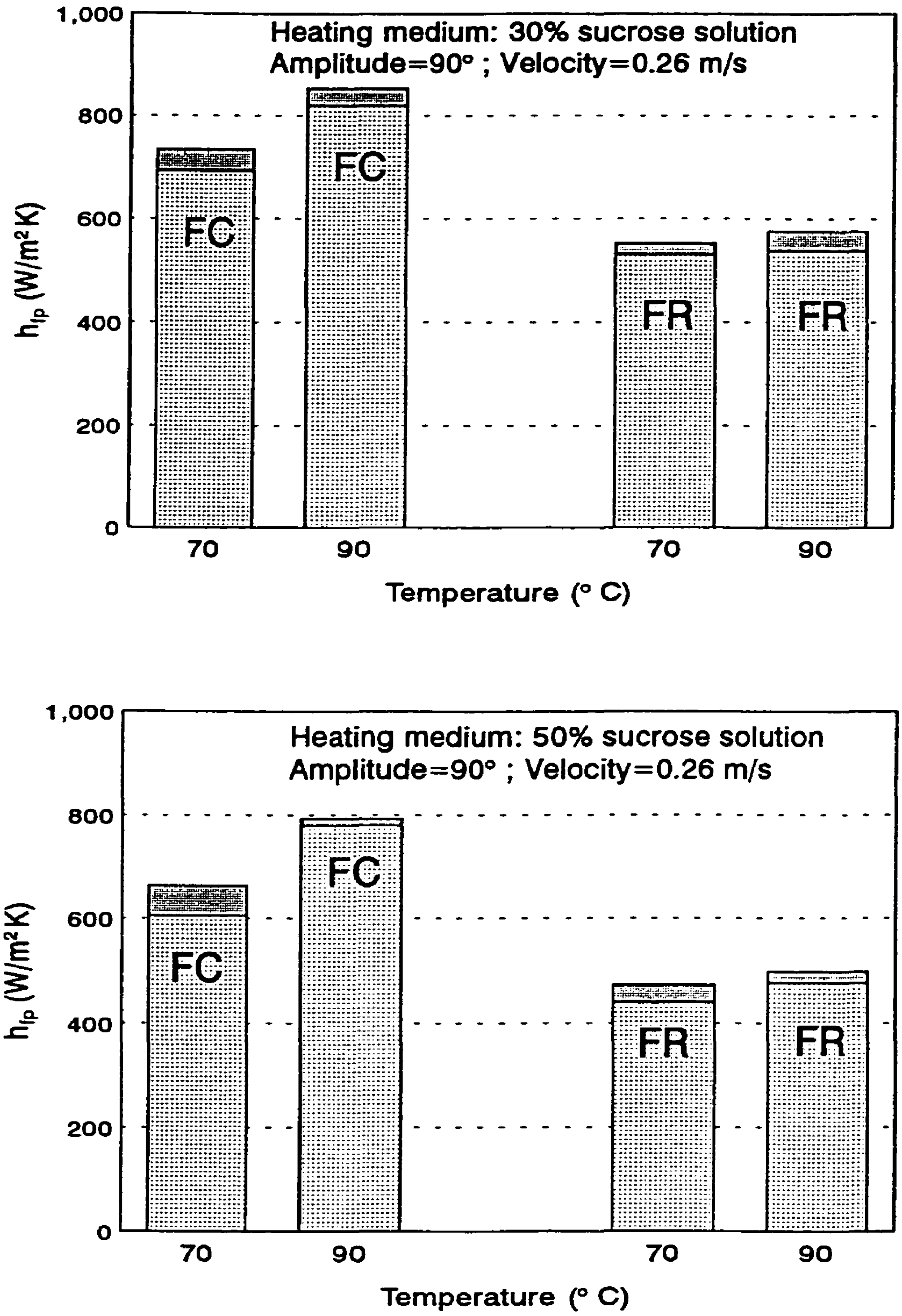

Figure 3.5. Effect of temperature on h_{fp} values in 30% and 50% sucrose solution, for free particle (FR) and particle fixed at the center (FC).

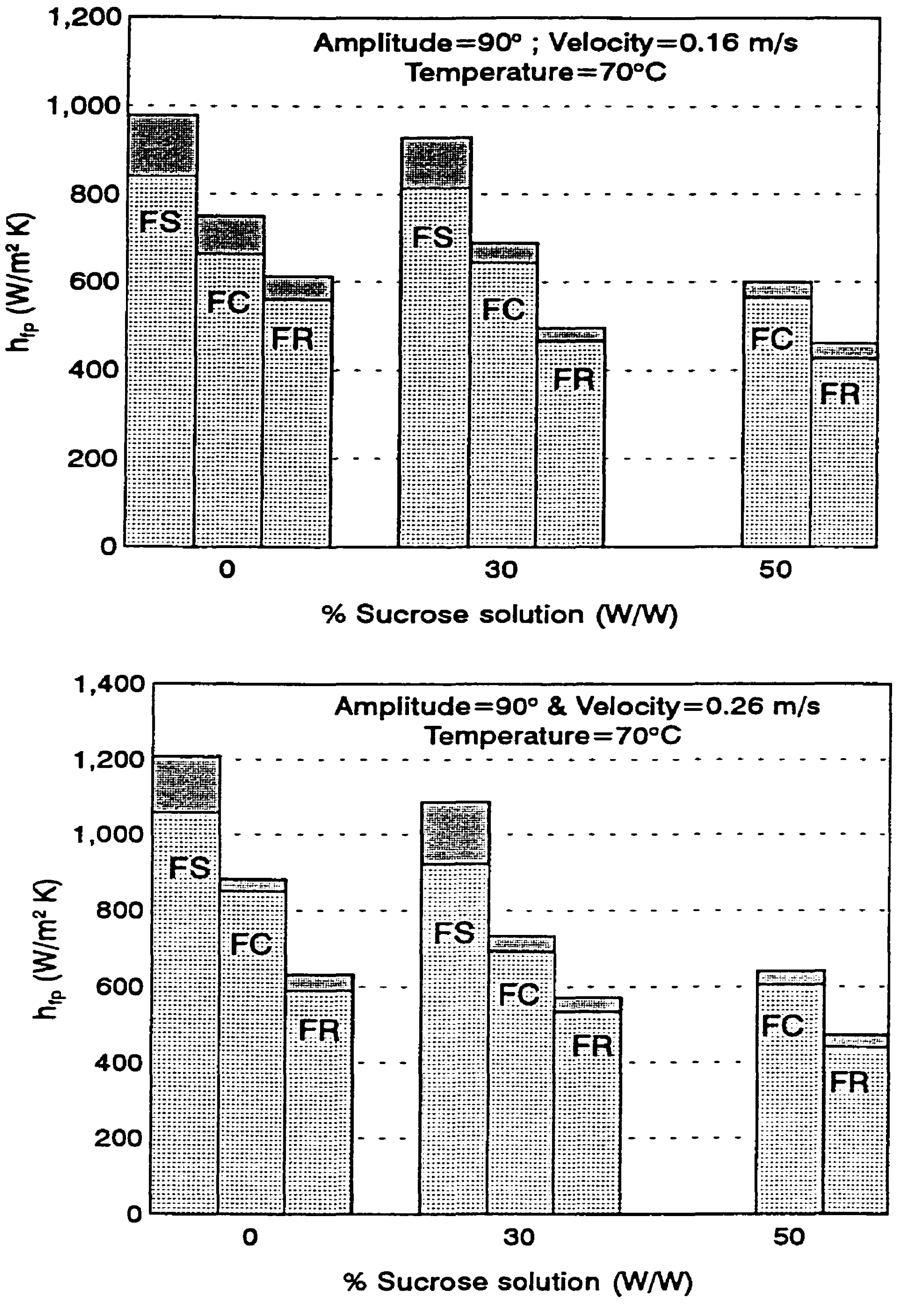

Figure 3.6. Effect of the viscosity on h_{fp} values for free particle (FR), and particle fixed at the center (FC) and at the surface (FS), at 70°C and velocities of 0.16 m/s and 0.26 m/s.

A lower value of h_{fp} has been reported by several researchers for the more viscous fluid. Lenz and Lund (1978) found significantly lower h_{fp} for particles processed in a 60% aqueous sucrose solution, than for solids processed in water. Chandarana *et al.* (1989) noticed that heat transfer coefficient values were larger in water when it passed over solid particles, than in high viscous fluid under the same condition. Also Zuritz *et al.* (1990), Gaze *et al.* (1990), Dutta and Sastry (1990), Awuah et al. (1996) as well as Sablani and Ramaswamy (1998) confirmed the same trend. The high viscosity of the fluid in which the particulate is immersed, hampers heat transfer, at least where the lower turbulence decreases the effective relative particle-to-fluid velocity at the interface.

Effect of velocity (particle oscillation frequency) on h_{fp}

To evaluate the effect of the particle velocity on h_{fp}, experiments were carried out at two rotation speeds (6 and 10 rpm) and different radial distances (0.15 and 0.25 m), giving three different linear velocities for the particles depending on their position (0.09, 0.16 and 0.26 m/s; the combination of 10 rpm at 0.15 m radial distance giving the same linear velocity of 0.16 m/s as 6 rpm at 0.25 m). As noted before, these values apply mainly to the relative velocity of the fixed particle. Since the free particles remain stationary for periods ranging from 20 to 50% of the oscillation time, the velocities indicated should only be considered as "nominal". A detailed analysis was performed while quantifying the effect of the "velocity" component of the "free" particle. In this study, the free particles were found to have relative velocities 20 to 50% lower than their fixed counterparts. In Figure 3.7, data on the means and standard deviations of heat transfer coefficient values are shown, as influenced by linear velocity of the particles in water (0% sucrose) and 30% sucrose solution, respectively. The temperature of medium was kept constant at 70^{o}C and the amplitude of oscillation was again fixed at 90^{o}. The h_{fp} values were found to increase by increasing the particle velocity. Overall, a three fold increase in velocity (from 0.09 to 0.26 m/s) increased the h_{fp} value by a factor of 1.15 for the free particle, 1.25 for the particle fixed in the center, and 1.75 for the particle fixed at the surface. The increase in h_{fp} for the "free" particle are in the range of values observed by Sastry *et al.* (1989 and 1990) in a study of h_{fp} using the moving thermocouple method.

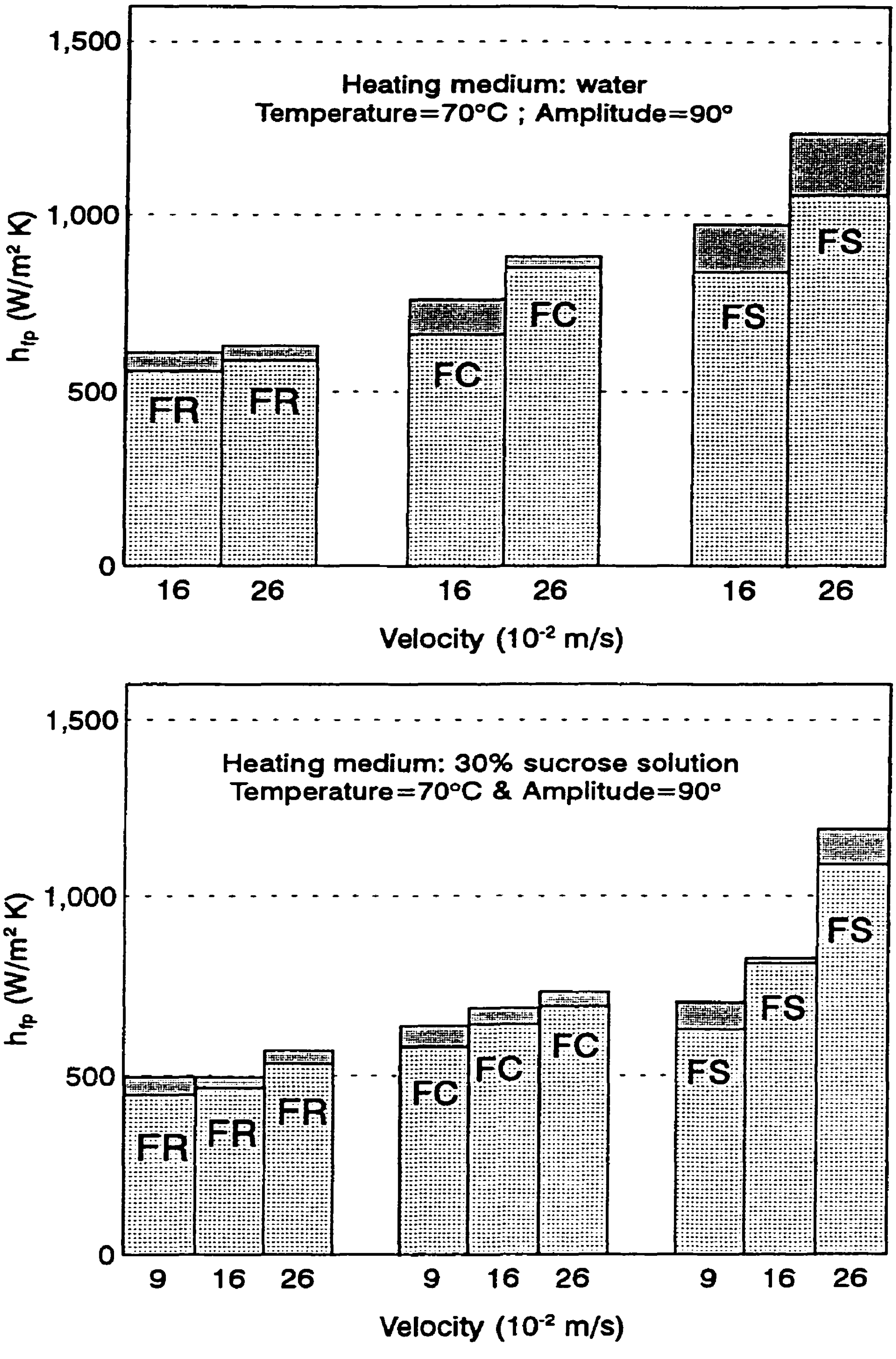

Figure 3.7. Effect of the particle velocity on h_{fp} values for the free particle (FR), and particle fixed at the center (FC) and at the surface (FS), in water as well as 30% sucrose solution at 70°C.

Up to a 150% increase in h_{fp} values was also reported for the stationary particle, by increasing the relative velocity almost three times (Maesmans *et al.*, 1992).

Comparison of h_{fp} for "Fixed" versus "Free" particle

The difference in associated h_{fp} values between free and fixed particles can be seen in Figures 3.4 to 3.7 (also Tables 3.2 and 3.3), under various conditions. Overall, observations indicate that the fluid to particle convective heat transfer coefficient was always higher for the fixed particles than that for the free particles. The difference in h_{fp} values between free and fixed particles was about 20% on the lower side and 100% on the higher side, probably because of the higher fluid-to-particle relative velocity associated with fixed particle situations. This is an important observation, which needs further investigation, and may have implications with respect to studies involving heat transfer coefficients evaluated with fixed particles. Thus, the h_{fp} values would be overestimated, although carried out at comparable fluid-to-particle relative velocities.

Comparison of h_{fp} for fixed particle: center versus surface location

The differences in the associated h_{fp} values between a particle fixed at the central axis, versus that at the bottom surface, can be observed in Figures 3.4 to 3.7. In general, the h_{fp} values associated with the particle at the surface were relatively higher than that found at the center. Although this may appear, at first, to be contradictory to common knowledge, it can be explained. The fixed particle at the center will have a symmetrical fluid flow behavior around the particle, and hence would be placed in a fluid with a relatively "smooth" or less "turbulent" flow regime. The particle fixed along the surface would face a fluid stream of considerably varying velocity profiles, trying to pass through the narrow clearance between the spherical particle and the tube surface thereby creating "rough" or more "turbulent" flow conditions, which would result in an enhanced heat transfer. Free particles under such conditions would also tend to roll (which is somewhat restricted in the present set-up because of attachment of thermocouples), which could also result in an enhanced heat transfer.

CONCLUSIONS

Interest in the aseptic processing of particulate foods demands the measurement of fluid-to-particle heat transfer coefficient (h_{fp}). An oscillatory approach was used to impart motion to particles in a model holding tube, immersed in an appropriate heating medium, while allowing time-temperature data gathering and evaluation of heat transfer coefficient using conventional techniques. Evaluated heat transfer coefficients under different conditions confirmed the conventional trends of increasing with velocity and temperature, and decreasing with fluid viscosity. Further, it was observed that the h_{fp} values for the fixed particle could be about 20-100% higher than that for the free particles, depending on the experimental condition. This implies that the h_{fp} values determined using a stationary particle in a moving fluid, as employed in several studies, may not be conservative.

The experimental set-up design permits an easier investigation of the effect of several parameters affecting h_{fp}, because of better control on factors such as particle velocity and particle location inside the tube. Easy maintenance of a stable medium temperature and the ability to use an opaque medium/tube are added advantages of the oscillatory method. Use of a conventional thermocouple approach to obtain the temperature history, makes the gathered data more authentic than that collected from other indirect methods.

In this section some experiments were conducted involving different temperatures, fluid viscosities, particle velocities etc with the primary purpose of evaluating the suitability of the technique under these conditions. More detailed study on the influence of various factors on the associated h_{fp} are addressed in the next chapter.

PREFACE TO CHAPTER 4

An oscillatory technique for maintaining particle motion was designed and developed to evaluate fluid-to-particle convective heat transfer coefficient (h_{fp}) under tube-flow conditions. The method was described in detail in the previous chapter. The technique for oscillating the setup was further improved by using a more precise programable motor, also additional insulation was added to the heating section to ensure better control of the system.

Heat transfer modeling requires a large amount of data covering a wide range of related parameters. This chapter deals with an additional experiment using the oscillatory technique to obtain data under different experimental conditions. Such conditions included: different particle sizes, materials and velocities, as well as different concentrations of carboxymethyl cellulose (CMC) solution at various temperatures.

A manuscript entitled: "Evaluation of factors influencing the tube-flow fluid-to-particle heat transfer coefficient, using a particle oscillatory motion technique" was submitted for publication in the Food Research International (M. R. Zareifard and H. S. Ramaswamy, 1999). Experimental work and data analysis were carried out by the candidate under the supervision of professor H. S. Ramaswamy.

CHAPTER 4

EVALUATION OF FACTORS INFLUENCING THE TUBE-FLOW FLUID-TO-PARTICLE HEAT TRANSFER COEFFICIENT USING A PARTICLE OSCILLATORY MOTION TECHNIQUE

ABSTRACT

The previously developed particle oscillatory motion technique, with direct temperature measurement of particles in motion, was used to study the effect of several influencing factors associated with h_{fp}. A full factorial experimental design was employed involving spherical particles made of aluminum epoxy and Nylon of different sizes (12.7 to 17.5 mm), different particle linear velocities (0.06 to 0.21 m/s), heating medium viscosities (0 to 1% concentration of carboxymethyl cellulose solution, CMC) and fluid temperatures (60 to 80 ^{o}C). Statistical analysis of experimental data indicated that all factors investigated had a significant ($p<0.001$) effect on h_{fp}. The fluid-to-particle heat transfer coefficient increased with particle velocity and fluid temperature, and decreased with CMC concentration and particle size. A T-test grouping analysis showed that mean values of h_{fp} were different ($\alpha=0.05$) among the levels of the various factors. Overall, values of h_{fp} associated with the aluminum epoxy particle were about 30% higher than that for the Nylon particle of the same size.

INTRODUCTION

Continuous processing of particulate foods needs information concerning both the thermophysical properties of the material being processed as well as the convective fluid-to-particle heat transfer coefficient (h_{fp}). The former material properties can be easily determined using the standardized methods , whereas the later h_{fp} is more complicated and needs more care and special techniques for evaluation (Mohsenin 1980). The convective heat transfer coefficient is one of the most difficult parameters to evaluate under practical conditions (Heldman, 1989). The introduction of particulate into a mobile fluid complicates the dynamic of flow phenomena. Heat transfer to cold spots within particles will be restricted by the thermal resistance within the product as well as at the surface; in turn this is related to the heat transfer coefficient. This coefficient is a complex function of the composition of the fluid, the nature of the geometry of the particle surface, and the hydrodynamics of the fluid motion passing the surface (Chapman, 1989). The heat transfer associated with the immersed particle also depends on the position of the object, the proximity of the other bodies, as well as the flow rate and fluid properties (Burfoot and James, 1988).

During the last decade, the challenge has been h_{fp} evaluation under conditions that simulate continuous aseptic processing of food containing discrete particles. Zuritz *et al.* (1990) studied the effect of particle size, flow rate and fluid concentration on h_{fp} using a stationary particle approach. Values of 548 to 1175 W/m^2K were reported for h_{fp} under low flow rates ($0.12<Re<1.94$) in experimental conditions. It was observed that h_{fp} increased with increasing particle size and fluid flow rate, and decreased with viscosity.

Sastry *et al.* (1990) studied the effects of flow rate and particle-to-tube diameter ratio on h_{fp}, during continuous tube flow, using a moving thermocouple approach with hollow aluminum spherical particles. They reported values of 688 to 3005 W/m^2K over a fluid Reynolds number range from 7300 to 43600, and found an increase in h_{fp} as the fluid flow rate and particle-to-tube diameter ratio increased. Their experimental results contradicted existing dimensionless correlations, such as Ranz and Marshal (1952). Alhamdan and Sastry (1990) reported values of 75 to 310 W/m^2K, for natural convection heat transfer between a non-Newtonian fluid and an irregularly shaped particle; they also observed that h_{fp} values decreased with an increasing viscosity. They have also reported that h_{fp} increased with an increasing initial temperature difference between the medium and the particle. However, this trend was observed only with the lower viscosity fluids.

Using the thermo-chromic liquid crystal method, with different flow rates and fluid concentrations and particle sizes of brass cubes, Balasubramaniam and Sastry (1994a) reported h_{fp} values of 986 to 2270 W/m^2K ($2174<Re<16422$). The heat transfer coefficient was reported to increase with flow rate and decrease with viscosity. With respect to particle size, a decrease of h_{fp} was reported as the particle-to-tube diameter ratio increased, using Ranz and Marshal (1952) or Incorpera and DeWitt (1990) correlations; however, a clear trend was not observed with experimental data. In another study, Balasubramaniam and Sastry (1994b) applied the same technique for aluminum spherical particles of different sizes and concluded that h_{fp} increased with particle size. The authors explained that the effect of particle size was not clear cut, using the relative velocity or moving thermocouple approach, due to a lack of control over the radial locations. Zitoun and Sastry (1994) also used the liquid crystal method to study the influencing factors on h_{fp}, using hollow cubic particles made of aluminum sheet. Values of h_{fp}, in the range of 287 to 930 W/m^2K were reported for laminar flow conditions ($41.2<Re<477.5$). The authors reported that h_{fp} increased with increasing flow rate and decreasing viscosity, as expected. But, for the particle-to-tube size ratio, h_{fp} values were reported to decrease when the particle size increased, somewhat contradicting the earlier results from the same lab.

Ramaswamy *et al.* (1996) also studied the influence of particle characteristics on h_{fp}. Spherical and finite cylinder particles were used in a stationary position in a pilot scale holding tube simulator. They reported h_{fp} values of 60 to 1000 W/m^2K for a wide range of Biot number ranging from 6 to 60. Contrary to Zuritz *et al.* (1990), Ramaswamy *et al.* (1996) found that h_{fp} increased with decreasing particle size and that the effect of the particle-to-tube diameter ratio was not clear-cut.

Recently, Kantt *et al.* (1998), applied a new technique, magnetic resonance imaging or MRI, for evaluating h_{fp} in the heat exchangers and holding tubes under aseptic processing conditions, by temperature mapping of moving particles. Cubic potato particles of different sizes were used in a carrier fluid at a 20% w/w concentration. They reported h_{fp} values varying from 600 to 2500 W/m^2K for the large, and over 3000 W/m^2K for smaller particles. The authors indicated that variability in h_{fp} is likely contributed by unknown residence time distribution, and that the technique may not be ideal for h_{fp} determination unless the particle residence time is accurately known.

Other researchers also tried to investigate the effects of the influencing factors, including both system and product parameters such as: holding tube diameter, fluid flow rate, fluid viscosity and temperature, particle size, shape and material on the associated fluid-to-particle heat transfer coefficient, under tube-flow conditions, using different means and methods (Chandarana *et al.*, 1988; Sastry et al. 1989; Dutta and Sastry 1990; Mwangi et al., 1993; Astrom and Bark, 1994; Awuah *et al.* 1995 and 1996; Chen *et al.*, 1996; Chakrabandhu and Singh 1998). Maesmans et al., 1992 and Ramaswamy *et al.*, 1997 reviewed the heat transfer studies in the aseptic processing of a liquid/particle mixture. The authors mentioned that information on the factors influencing h_{fp} is still lacking in the literature. Especially, in the case of processing of the multi-phase system, where both fluid and solid particles are processed together, the convective fluid-to-particle heat transfer coefficient is not yet clear even, although many researchers have attempted to study factors influencing h_{fp}. The authors concluded that available data, in the literature of h_{fp} associated with continuous flow systems is generally scarce and often inconsistent, or even contradictory and therefore non-conclusive.

The objective of this study was to evaluate the effect of some of the influencing factors such as: particle size, particle material, particle velocity and fluid concentration, as well as fluid temperature, on the associated tube-flow fluid-to-particle heat transfer coefficient, h_{fp}, using the previously established "particle oscillatory motion" method. The oscillatory approach described in chapter 3 showed good potential for evaluating h_{fp} in tube-flow conditions.

MATERIALS AND METHODS

Experimental setup

Full description of the experimental procedure for the particle oscillatory motion technique is given in (Zareifard and Ramaswamy, 1997). Briefly, the setup consisted of two sets of transparent glass tubes (ID=50.8 mm) bent into the radii of curvatures of 0.15 and 0.25 m (Figure 3.1). The four tubes were cut to one quarter of the full circular tubing. The two similar tubes (same radius of curvature) were placed facing each other in diametrically opposite locations to form arcs of a circle and were fixed on an aluminium frame. The whole assembly was connected to a motor using an aluminum shaft. Instead of the previously used 100 W electric DC motor, a more sophisticated programable servo motor (Hoover Precision Products, Inc. Sault Ste. Marie, MI) was used in this setup. The system was equipped with an electronic board to enable programming the motor to run at any pre-set speed and acceleration, with oscillatory motion at a desired amplitude. Of course, a special gearbox unit was used to reduce the number of revolutions per minute (RPM) of the motor, to a range of less than 10 RPM.

Spherical Nylon particles (Small Parts Inc., Miami Lake, Fl, USA) of three different sizes (12.7, 16 and 17.5 mm in diameter) as well as spherical particles (17.5 mm in diameter) made of aluminum epoxy (Soudotec Inc. Lachine, Quebec, Canada) were used as test particles. Aluminum epoxy is a combination of aluminum powder and epoxy material in a soft form. It is a hand-kneadable, non-rusting, aluminum reinforced compound that mixes together to provide any desired shape and size. This industrial product cures tough and hard within half an hour. After its final cure, it can be drilled or machined. To make a spherical particle of a given diameter, the required amount of aluminum epoxy was calculated, based on the density and required volume ($m= \rho V= 4/3\pi r^3$). The calculated amount was kneaded to a uniform color for approximately one minute. It was then rounded uniformly to get the spherical shape of desired size. The thermophysical properties of the particle were experimentally evaluated as follows, using procedures described elsewhere (Sablani and Ramaswamy 1996): density (ρ) = 1128 and 1750 kg/m^3, thermal diffusivity (α) = 1.58×10^{-7} and 4.7×10^{-7} m^2/s, and heat capacity

(C_p) = 2073 and 1370 J/kg K for Nylon and aluminum epoxy, respectively. The thermal conductivity (k) was calculated as 0.369 W/m K for Nylon and 1.13 W/m K for aluminum epoxy ($k = \rho\ C_p\ \alpha$).

The particles were carefully drilled to the geometric center using a one millimetre drill bit. A Teflon coated type-T copper-constantan thermocouple (AWG 40, wire diameter is 0.007 mm) (Omega Engineering Inc., Stamford, CT, USA) was made and inserted in to the center of each particles. The gap between the thermocouple wire and the particle was filled with a glue (epoxy resin and hardener 50/50). Since the thermocouple wires were very fine, easy to break, and not strong to support the particle at a constant position during oscillatory motion, the thermocouple wires were passed through a 20 gage Teflon tube (0.8 mm inside diameter), (Small Parts Inc., Miami Lake, Fl, USA). Each particle was fixed at the center of a given tube in such a way that the two larger particles of the same size (d=17.5 mm, referred to large), but of different materials, were located in the outer tubes, and the other two particles of the same material, but different sizes (d=12.7 and 16 mm, referred to small and medium respectively), were located in the inner tubes. Thus, each pair of the particles were in the same condition with respect to the particle velocity, while carrying out the experiments under different conditions.

The whole assembly, containing the particles, was kept in a water tank at 5 °C for the equilibration of temperature in the test particles, and for achieving an appropriate oscillatory motion (programmed with specific angular velocity, acceleration, frequency and amplitude). Then, the assembly was transferred to another tank containing a heating medium at a pre-set temperature. The heating tank was made of a double jacket stainless steel material (0.6 x 0.6 x 0.9 m), and heated with steam injection by a set of pipes evenly laid at the bottom of the tank. The steam inlet was equipped with a thermostat, as well as a by-pass system, in order to achieve temperature control. Therefore, the bath temperature could be kept constant with a maximum variation of about ±1 °C during the experiments. Time-temperature data were gathered at 3 s time intervals using a data logger (Dash-8, Metra-Byte Corp, Taunton, Ma, USA) connected to a personal computer.

Water, as well as two concentrations (0.5 and 1 % w/w) of commercial carboxymethyl cellulose, CMC (Sigma, St. Louis, MO, USA), were used as heating media. CMC solutions were prepared by slowly adding a known amount of CMC powder to distilled water, using an electric portable hand mixer. The required amount of distilled water was then added, to bring it to the desired concentration and it was thoroughly mixed using a variable speed mixer (Hobert Model D-300, Hobert Canada Inc., Mississauga, ON) to complete the dissolution of CMC lumps. Thereafter, the solution was left for 24 hours to release air bubbles and also to ensure total dispersion of the powder.

Evaluation of fluid-to-particle heat transfer coefficient

The theoretical background, related to the unsteady state conduction heat transfer and differential equations governing heat transfer to an isotropic spherical particle, which suddenly transferred into a constant temperature, has been detailed in chapter 2. Fluid-to-particle convective heat transfer coefficients (h_{fp}) were estimated, based on the analytical solution to the differential equation, using the so called "rate method", which utilizes the heating rate index (f_h) estimated from the straight line portion of the semi-logarithmic plot of temperature difference against time, for back calculating the h_{fp}. Additional details, concerning the evaluation of the heat transfer coefficient by the rate method, can be found in Ramaswamy *et al.* (1983). In this method, the heating rate (f_h) is related to δ, the positive root of a Biot number function ($Bi=1-\delta \cot \delta$), particle size (a) and thermal diffusivity (α) of the particle ($f_h=2.303\ a^2 / \alpha\ \delta^2$). Therefore, knowing a, α, and f_h, which can be evaluated experimentally, δ can be calculated. The corresponding Bi, and hence the heat transfer coefficient h_{fp}, can thus be calculated as $h_{fp}=Bi\ (k/a)$, where k is the thermal conductivity of the particle. The particle oscillatory technique detailed in chapter 3 was employed for the evaluation of h_{fp}.

Experimental conditions

To study the effects of influencing factors such as: particle material, particle size, and particle velocity as well as medium viscosity and medium temperature, experiments were carried out with particles of different materials and sizes in water and CMC solutions. The data were analyzed, considering two full factorial experimental designs, as follows:

a) The first one was a full factorial design with four factors: particle material, particle velocity, medium concentration and temperature. Particles of the same size (d=17.5 mm) were fixed at the same position (center of the outer tubes). Particle materials were Nylon and aluminum epoxy. Particle linear velocities (V_p) were 0.10, 0.16 and 0.21 m/s, resulting from 4, 6 and 8 RPM, respectively ($V_p = r\ \omega$, where r is the radius of curvature and ω is the angular velocity, $\omega = 2\pi n$). Medium concentrations and temperature were 0, 0.5,and 1% CMC and 60, 70, 80 ^{o}C respectively. Experiments were repeated four times for each condition.

b) The second design was also a full factorial design, with three levels of CMC concentrations and temperatures as mentioned above. However, in this design the particles were made from the same material, Nylon, but of different sizes: small (d=12.7 mm) and medium (d=16 mm) were fixed at the same position (center of the inner tubes). Therefore, the particle linear velocities were also different: 0.06, 0.09 and 0.12 m/s resulting from 4, 6 and 8 RPM respectively.

Statistical Analysis

The SAS computer program (SAS Institute Inc. 1997) and the generalized linear modeling (GLM) procedure were used to study the effects of individual influencing factors (particle size, material and velocity, as well as fluid concentration and temperature) and their interactions on the associated fluid-to-particle heat transfer coefficients, by analysis of variance (ANOVA). Also, using the same statistical program, least-significant-difference (LSD) grouping tests were performed to see if there were statistically significant differences among the means of the various variables levels under investigation.

RESULTS AND DISCUSSION

Data acquisition and heating rate index (f_h) calculation

Typical time-temperature curves for the Nylon and aluminum epoxy particles of the same size (d=17.5 mm), heated in 1% CMC solution are shown in Figure 4.1. The initial temperature for both particles was the same, at about 5 ^{o}C; the heating medium was kept at 60 ^{o}C in this case. The center point temperature of the aluminum epoxy particle reached the medium temperature in about 90 seconds, while the Nylon particle of the same size, under the same experimental condition, took almost 170 seconds to reach the medium temperature, due to its lower thermal conductivity. Semi-logarithmic plots of temperature difference (medium temperature minus center point temperature of the particle) versus time are also shown in Figure 4.1. The heating rate indexes (f_h) were calculated as the negative reciprocal slopes of the straight portion of the semi-logarithmic plots. Comparison of these plots clearly illustrates the slower heating behavior of the Nylon particle. Also, a larger initial lag was seen for the center point temperature of the Nylon particle. It was shown earlier (Zareifard and Ramaswamy, 1997) for the spherical particles, linearization of the semi-logarithmic plot (which indicates convergence of the series solution of the unsteady state heat conduction differential equation to the first term) was generally observed from a Fourier number as low as 0.1. Generally, Fo numbers ($\alpha t/d^2$) greater than 0.2 ($t>30$ second and $t>90$ second for the aluminum epoxy and Nylon particle, respectively) were considered to calculate the slope of the plots or f_h, to assure convergence of the series solution (Holman, 1990).

Typical time-temperature curves and semi-logarithmic plots for the Nylon particles of different sizes (small and medium), heated in 1% CMC solution, are shown in Figure 4.2. Obviously, the figures show the faster heating rate of the smaller particle. The center point temperature of the small particle reached the heating medium temperature in about 90 seconds, while the medium size particle required about 150 seconds. To calculate the f_h, $t>50$ s and $t>80$ s were considered for small and medium particles respectively, to satisfy the condition Fo> 0.2.

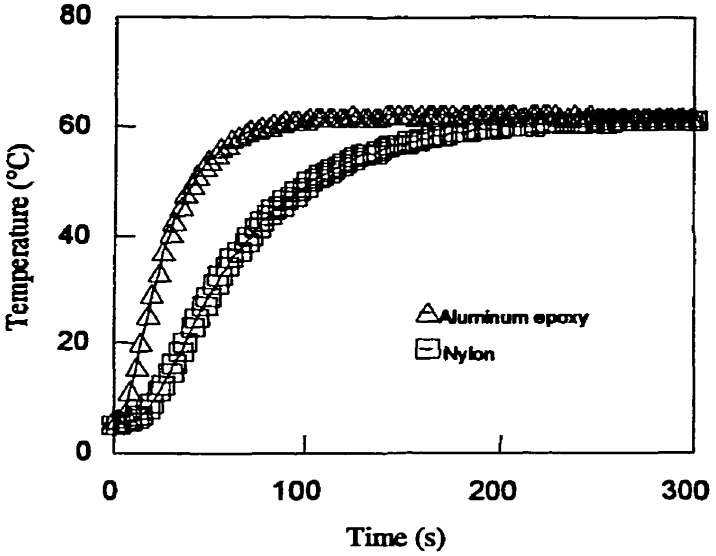

Time-temperature profiles

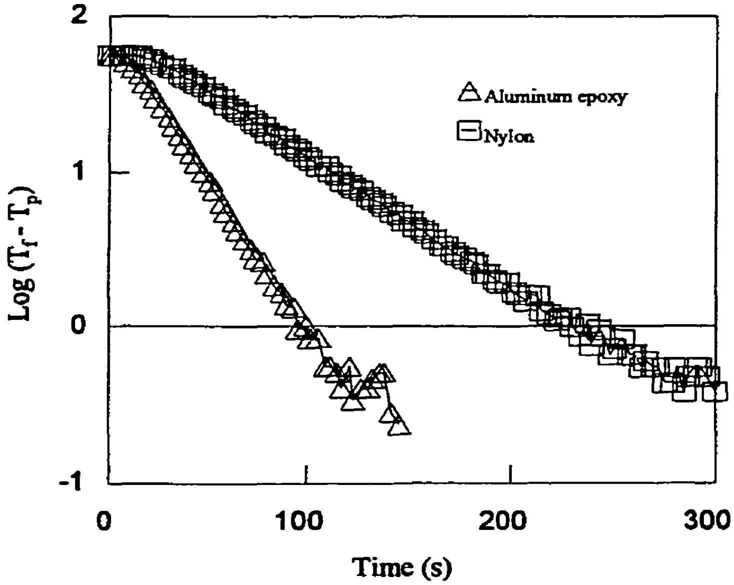

Semi-logarithmic plots of temperature difference versus time

Figure 4. 1. Typical time-temperature and semi-logarithm plots of temperature difference versus time for Nylon and Aluminum epoxy particles of the same size using 1% CMC solution at 60°C as the heating medium.

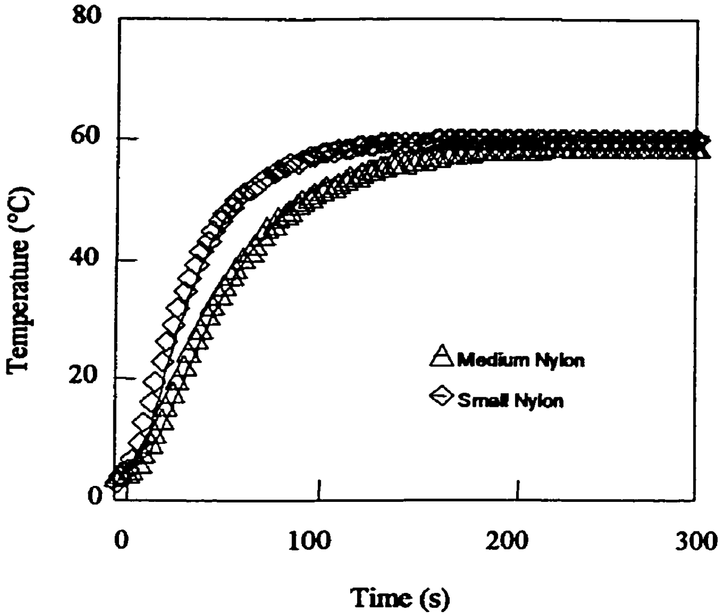

Time-temperature profiles

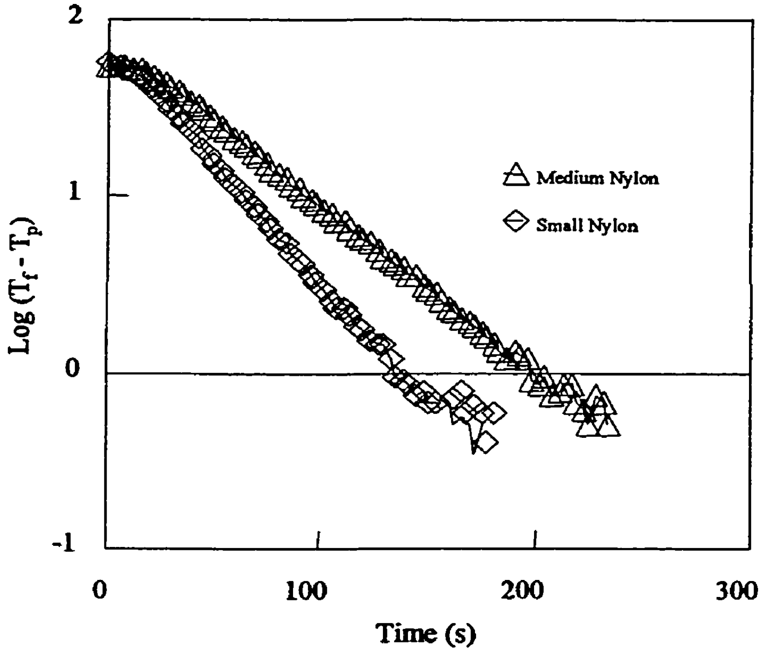

Semi-logarithmic plots of temperature difference versus time

Figure 4. 2. Typical time-temperature and semi-logarithm plots of temperature difference versus time for small and medium Nylon particles using 1% CMC solution at 60°C as the heating medium.

Fluid-to-particle heat transfer coefficient

The means of the fluid-to-particle heat transfer coefficients (h_{fp}) and corresponding coefficients of variation (CV), as influenced by particle velocity, fluid viscosity and temperature, are given in Tables 4.1 and 4.2 for the same size of aluminum epoxy and Nylon particles, respectively. Depending on the experimental condition, values of h_{fp} for the aluminum epoxy particle varied from 530 W/m^{2}K, at the minimum particle velocity (0.1 m/s) with 1% CMC solution at 60^{o}C, to about 2000 W/m^{2}K at maximum particle velocity (0.21 m/s), with water at 60 ^{o}C used as the heating medium. Due to the high range of associated h_{fp} values and high Biot numbers, experiments were not carried out with water at higher temperatures. For the Nylon particle of the same size and same experimental conditions, values of h_{fp} varied from 430 W/m^{2}K to about 1400 W/m^{2}K. Experimental data showed that, in general, values of h_{fp} were higher and CV was slightly lower for the aluminum epoxy particle than for the Nylon particle. Perhaps the surface roughness and not quite perfectly rounded shape of the aluminum epoxy particle are reasons for the associated higher h_{fp} values or they may have resulted from possible inaccuracies in values of thermophysical properties used for these particles.

The analysis of variances (ANOVA) for individual factors (independent factors), particle velocity and material, as well as fluid viscosity and temperature and their interactions on the heat transfer coefficient (dependent variable), are summarized in Table 4.3. The model was highly significant ($p < 0.0001$) with an associated R^2 value greater than 0.97, and CV of less than 11%. Statistical analysis showed that all individual factors and some two way interactions significantly ($p < 0.0001$) influenced h_{fp}, but did not hold for the three way interactions. A T-test grouping, using the least-significant-difference (LSD) procedure, indicated significant differences ($\alpha = 0.05$) among the mean values for the various levels of each factor. The results of the T-test grouping are summarized in Table 4.4 for each factor showing that the values of h_{fp} increased with particle velocity and fluid temperature, and decreased with fluid viscosity. The overall result was about 30% lower for the Nylon particle compared to the aluminum epoxy particle.

Table 4.1. Associated mean values of fluid-to-particle heat transfer coefficient (h_{fp}) and their coefficients of variation (CV) for Aluminum epoxy particle.

V (m/s)	T (°C)	C (%)	P	R	h_{fp} (W/m^{2}K)	CV (%)
0.1	60	0	A	3	1460	11
0.1	60	1	A	4	530	10
0.1	60	0.5	A	4	590	15
0.1	70	1	A	4	650	7
0.1	70	0.5	A	3	750	5
0.1	80	1	A	3	720	10
0.1	80	0.5	A	2	1140	6
0.16	60	0	A	3	1830	11
0.16	60	1	A	4	570	10
0.16	60	0.5	A	3	950	6
0.16	70	1	A	4	730	10
0.16	80	1	A	3	1010	8
0.16	80	0.5	A	2	1290	3
0.21	60	0	A	3	2020	9
0.21	60	1	A	4	630	11
0.21	60	0.5	A	3	1220	9
0.21	70	1	A	4	880	7
0.21	70	0.5	A	3	1360	9
0.21	80	1	A	4	1110	4
0.21	80	0.5	A	3	1380	12

V: Particle velocity; T: Fluid temperature; C: CMC concentration; P: Particle material (A: Aluminum epoxy); R: Replicates; CV: Coefficients of variation

Table 4.2. Associated mean values of fluid-to-particle heat transfer coefficient (h_{fp}) and their coefficient of variations (CV) for Nylon particle.

V (m/s)	T (°C)	C (%)	P	R	h_{fp} (W/m2K)	CV (%)
0.1	60	0	N	3	1120	7
0.1	60	1	N	3	430	17
0.1	60	0.5	N	4	460	15
0.1	70	1	N	4	490	8
0.1	70	0.5	N	3	500	18
0.1	80	1	N	3	500	18
0.1	80	0.5	N	3	640	16
0.16	60	0	N	3	1310	6
0.16	60	1	N	4	520	12
0.16	60	0.5	N	3	620	7
0.16	70	1	N	3	530	18
0.16	80	1	N	3	560	17
0.16	80	0.5	N	3	740	14
0.21	60	0	N	3	1410	6
0.21	60	1	N	4	620	19
0.21	60	0.5	N	4	690	9
0.21	70	1	N	4	660	10
0.21	70	0.5	N	3	730	7
0.21	80	1	N	4	740	8
0.21	80	0.5	N	4	800	4

V: Particle velocity; T: Fluid temperature; C: CMC concentration; P: Particle material (N:Nylon); R: Replicates; CV: Coefficient of variation

Table 4.3. Analysis of variances (ANOVA) for the factorial experiment design of factors influencing the fluid-to-particle heat transfer coefficients using oscillatory method and data associated with particles of different material but the same size.

Source	DF	Type IV SS	Mean Square	F Value	Pr >F
V	2	1681783.18	840891.59	130.28	0.0001
T	2	1082927.77	541463.88	83.89	0.0001
C	1	1050256.41	1050256.41	162.72	0.0001
P	1	2768193.82	2768193.82	428.88	0.0001
V*T	4	11146.32	2786.58	0.43	0.7853
V*C	2	106301.79	53150.90	8.23	0.0006
V*P	2	135034.13	67517.07	10.46	0.0001
T*C	2	13366.25	6683.12	1.04	0.3597
T*P	2	308790.10	154395.05	23.92	0.0001
C*P	1	404804.56	404804.56	62.72	0.0001
V*T*C	3	159221.49	53073.83	8.22	0.0001
V*T*P	4	19345.48	4836.37	0.75	0.5613
V*C*P	2	75991.15	37995.57	5.89	0.0041
T*C*P	2	12180.04	6090.02	0.94	0.3934
V*T*C*P	3	69676.34	23225.45	3.60	0.0169

SAS computing program and general linear procedure (GLM) was used for ANOVA.
V: Particle velocity; T: Fluid temperature; C: CMC concentration; P: Particle material

Table 4.4. T-test grouping using least-significant-difference procedure for the levels of influencing factors on fluid-to-particle heat transfer coefficients using oscillatory method and data associated with particles of different material but same size.

Particle velocity: V (m/s)

Grouping	Mean	N	V
A	876.36	44	0.21
B	720.63	32	0.16
C	590.88	40	0.1

Medium temperature: T (°C)

Grouping	Mean	N	T
A	867.30	37	80
B	720.00	35	70
C	635.57	44	60

CMC concentration (%)

Grouping	Mean	N	C
A	1833.53	17	0
B	830.20	50	0.5
C	662.80	66	1

Particle material: P

Grouping	Mean	N	P
A	873.68	57	A
B	600.93	59	N

A: Aluminum epoxy particle; N: Nylon particle
SAS computing program was used for grouping test.
Means with the same letter are not significantly different at level $\alpha=0.05$.

Likewise, the mean values of h_{fp} and CV for small and medium Nylon particles are given in Tables 4.5 and 4.6. For the small Nylon particle, values of h_{fp} varied from 360 W/m^2K at the minimum particle velocity (0.06 m/s) with and 1% CMC solution at 60 ^oC, to about 1400 W/m^2K for maximum particle velocity (0.12 m/s) with water at 60 ^oC as the heating medium. These values ranged from 350 to 1300 W/m^2K for the medium Nylon particle and the same experimental conditions. Slightly higher values of h_{fp} were observed for the small particle. The statistical analysis of variance (Table 4.7) showed a significant effect ($p < 0.001$) of all the individual factors on h_{fp}, but with regard to their two way or three way interactions. Fluid temperature and particle size were less significant, compared to the fluid viscosity and particle velocity in their effect on h_{fp}. Once again, the model was highly significant ($p < 0.001$) with an associated R^2 value greater than 0.95 and CV less than 12%. The results of the T-test grouping (Table 4.8) showed trends similar to those observed earlier, i.e., h_{fp} increased with particle velocity and fluid temperature, and decreased with fluid viscosity. Overall, the values of h_{fp} were about 15% higher for the small particle when compared to the values for the medium particle.

Factors affecting heat transfer coefficient

A review of studies considering heat transfer coefficient in tube-flow systems, indicates that several factors have been reported to influence h_{fp}. These factors include: particle size and shape, particle and fluid thermophysical properties, particle location, fluid-particle relative velocity, the diameter of the particle in relation to that of the tube, and fluid viscosity and temperature (Maesmans et al., 1992; Stoforos, 1992; Ramaswamy et al., 1997; and Tewari and Jayas 1997).

Table 4.5. Associated mean values of fluid-to-particle heat transfer coefficient (h_{fp}) and their coefficients of variation (CV) for small Nylon particle under different conditions.

V (m/s)	T (°C)	C (%)	P	N	h_{fp} (W/m2K)	CV (%)
0.06	60	0	S	3	1100	11
0.06	60	1	S	4	360	16
0.06	60	0.5	S	3	520	15
0.06	70	1	S	4	490	13
0.06	70	0.5	S	3	530	3
0.06	80	1	S	3	520	7
0.06	80	0.5	S	3	600	18
0.09	60	0	S	3	1250	12
0.09	60	1	S	3	418	11
0.09	60	0.5	S	3	720	15
0.09	70	1	S	3	530	17
0.09	80	1	S	3	518	10
0.09	80	0.5	S	3	790	9
0.12	60	0	S	4	1410	8
0.12	60	1	S	3	570	4
0.12	60	0.5	S	4	748	18
0.12	70	1	S	4	610	12
0.12	70	0.5	S	3	790	12
0.12	80	1	S	4	663	5
0.12	80	0.5	S	4	840	8

V: Particle velocity; T: Fluid temperature; C: CMC concentration; P: Particle size (S: small) ;
N: Replicates

Table 4.6. Associated mean values of fluid-to-particle heat transfer coefficient (h_{fp}) and their coefficient of variations (CV) for medium Nylon particle under different conditions.

V (m/s)	T (°C)	C (%)	P	N	h_{fp} W/m2K)	CV (%)
0.06	60	0	M	3	1070	11
0.06	60	1	M	4	350	14
0.06	60	0.5	M	3	430	10
0.06	70	1	M	4	430	13
0.06	70	0.5	M	3	460	9
0.06	80	1	M	4	470	12
0.06	80	0.5	M	3	520	11
0.09	60	0	M	3	1120	10
0.09	60	1	M	4	440	9
0.09	60	0.5	M	3	580	9
0.09	70	1	M	3	510	4
0.09	80	1	M	3	500	4
0.09	80	0.5	M	3	680	13
0.12	60	0	M	3	1320	8
0.12	60	1	M	3	530	16
0.12	60	0.5	M	3	610	12
0.12	70	1	M	4	580	9
0.12	70	0.5	M	3	640	15
0.12	80	1	M	4	640	10
0.12	80	0.5	M	4	730	9

V: Particle velocity; T: Fluid temperature; C: CMC concentration; P: Particle size (M:medium); N: Replicates

Table 4. 7. Analysis of variances (ANOVA) for the factorial experiment design of factors influencing fluid-to-particle heat transfer coefficients using oscillatory method and data associated with particles of the same material but different sizes.

Source	DF	SS	Mean Square	F Value	Pr > F
V	2	682133.361	341066.681	73.76	0.0001
T	2	189440.846	94720.423	20.48	0.0001
C	1	378720.730	378720.730	81.90	0.0001
P	1	146319.444	146319.444	31.64	0.0001
V*T	4	4531.848	1132.962	0.25	0.9119
V*C	2	42627.830	21313.915	4.61	0.0128
V*P	2	4769.922	23 84.961	0.52	0.5991
T*C	2	3913.678	1956.839	0.42	0.6564
T*P	2	69.926	34.963	0.01	0.9925
C*P	1	27945.523	27945.523	6.04	0.0162
V*T*C	3	6988.339	2329.446	0.50	0.6808
V*T*P	4	3232.369	808.092	0.17	0.9507
V*C*P	2	4201.087	2100.544	0.45	0.6366
T*C*P	2	2350.208	1175.104	0.25	0.7762
V*T*C*P	3	1962.822	654.274	0.14	0.9348

SAS computing program and general linear procedure (GLM) was used for ANOVA.
V: Particle velocity; T: Fluid temperature; C: CMC concentration; P: Particle size

Table 4.8. T-test grouping using least-significant-difference procedure for the levels of influencing factors on fluid-to-particle heat transfer coefficients using oscillatory method and data associated with particles of the same material but different size.

Particle velocity: V (m/s)

Grouping	Mean	N	V
A	666.98	43	0.12
B	577.42	31	0.09
C	464.74	38	0.06

Medium temperature: T (°C)

Grouping	Mean	N	T
A	638.46	39	80
B	553.82	34	70
B			
B	525.90	39	60

CMC concentration: C (%)

Grouping	Mean	N	C
A	1293.53	19	0
B	653.33	48	0.5
C	513.75	64	1

Particle size: P

Grouping	Mean	N	P
A	610.89	56	S
B	536.25	56	M

S: Small Nylon particle; M: Medium Nylon particle
SAS computing program was used for grouping test.
Means with the same letter are not significantly different at level α=0.05.

Effects of particle velocity, particle material and particle size

The mean values of h_{fp}, as influenced by particle velocity, particle material and particle size, are shown in Figures 4.3 through 4.6 for different experimental conditions. The effect of particle velocity on h_{fp} in 1% CMC, at different temperatures, is shown in Figure 4.3 for aluminum epoxy and Nylon particles of the same size. Figure 4.3 indicates that the values of h_{fp}, for both aluminum epoxy and Nylon particles, increased with particle velocity. The same trend was observed at all three temperatures. For the aluminum epoxy particle, increasing the particle velocity by a factor of 2 (from 0.1 to 0.2 m/s) resulted in an almost 50% increase in h_{fp}, with 1% CMC at 80 ^{o}C (from 720 to 1100 W/m^{2}K). However, this increase seemed to have damped to about 20%, at the lower temperature of 60 ^{o}C (from 530 to 630). Within the same temperature margin (60 to 80 ^{o}C), for the Nylon particle, increasing the particle velocity by a factor of 2 resulted in an almost 50% increase in h_{fp}, at different temperatures (Figure 4.3). Overall, the values of h_{fp} for the aluminum epoxy particle were higher than those for the Nylon particles of the same size under the same experimental conditions. Neglecting the effects of other factors but the velocity, the T-test grouping (Table 4.4) indicated that levels of particle velocity were different (α=0.05) from each other with respect to their influence on h_{fp}.

The effect of particle velocity on h_{fp}, for small and medium Nylon particles in 1% CMC solution at different temperatures, is shown in Figure 4.4. Although the range of particle velocity is lower (from 0.06 to 0.13 m/s), the same trend of increasing h_{fp} with particle velocity was observed; there was a 50% increase in h_{fp} when the particle velocity doubled. Once again, regardless of the effects of the other factors but the particle velocity, the T-test grouping showed significant differences (α=0.05) among the mean values of h_{fp}, for the three levels of particle velocity (Table 4.8). In addition, the effects of particle velocity at different concentrations of CMC are shown in Figures 4.4 and 4.5, for particles of different materials and sizes. These will be discussed in the following section. Considering the effect of particle size, slightly higher values of h_{fp} were found to be associated with the smaller particles under the same experimental conditions. Overall mean values of h_{fp} were 610 and 540 W/m^{2}K for small and medium Nylon particles, respectively neglecting the effects of the other factors (Table 4. 8).

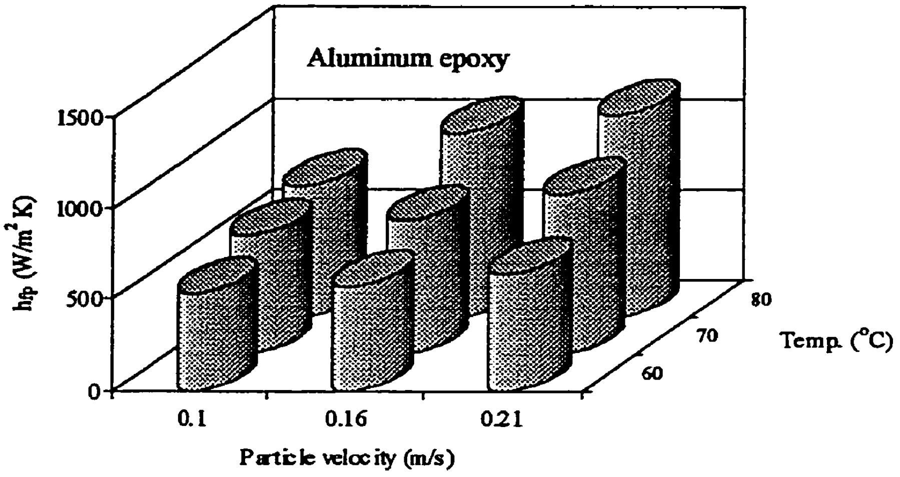

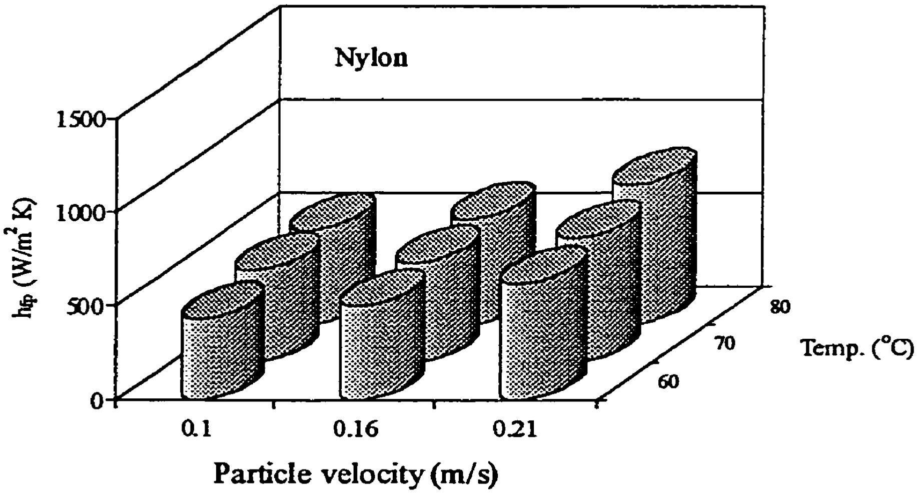

Figure 4.3. Effect of particle velocity on h_{fp} in 1% CMC solution at different temperatures for Aluminum epoxy and Nylon particles.

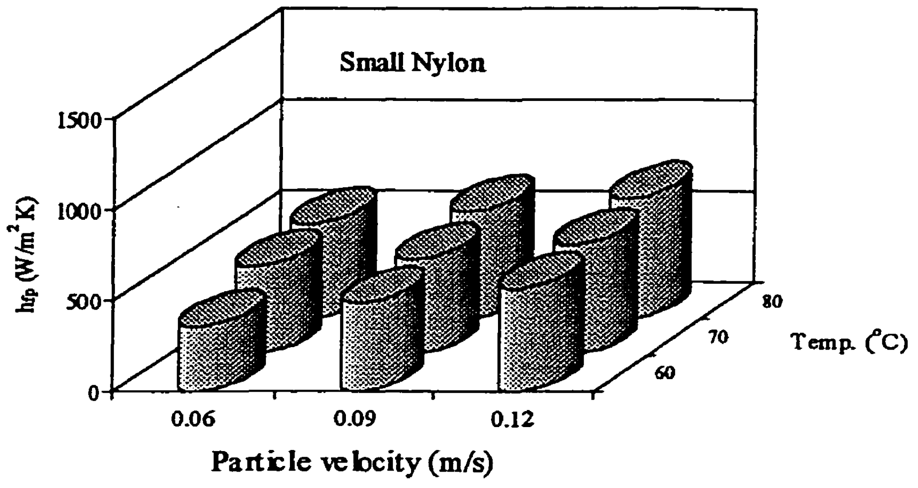

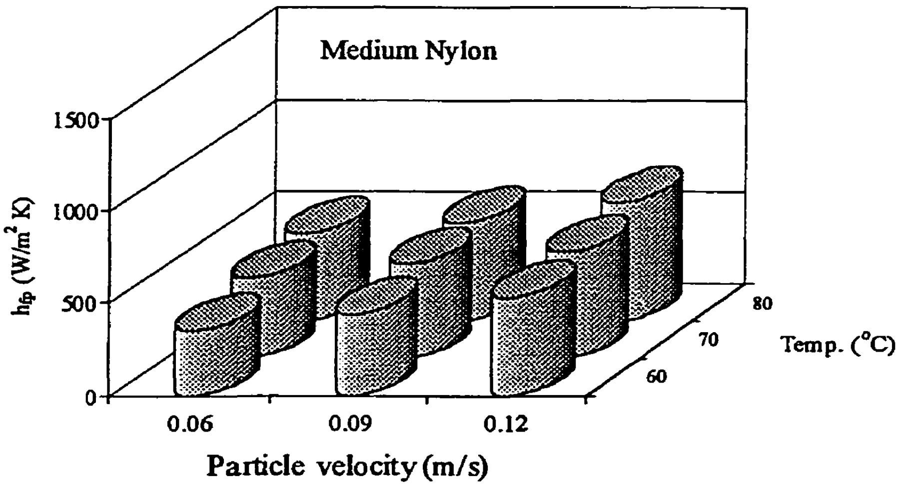

Figure 4.4. Effect of particle velocity on h_{fp} in 1% CMC solution at different temperature for small and medium size of Nylon particles.

The effect of particle size on the heat transfer coefficient in continuous flow systems appears to be non-conclusive (Ramaswamy et al. 1997). Opposite trends have been reported by different authors, regarding the effect of particle size in canning or particle to tube diameter ratio in tube-flow conditions. Lenz and Lund (1978), Deniston *et al.* (1980) found that the heat transfer coefficient increased in the canning process with increasing particle dimension, while Hassan (1984) and Sablani and Ramaswamy (1997) reported a reverse trend. Deniston et al. (1987) reported that potato particle size (2.2 to 3.5 cm in diameter) did not influence h_{fp}. In aseptic processing conditions, Zurtiz et al. (1990), Sastry et al. (1990) and Balasubramaniam and Sastry (1994b) reported an increase in the heat transfer coefficient with increasing spherical particle size, whereas Chandarana et al. (1988), Balasubramaniam and Sastry (1994a), Ramaswamy et al. (1996) found the heat transfer coefficient to decrease with increasing particle size. In this study, the effect of particle size on h_{fp} was also found to decrease with increasing particle size, in agreement with some of the researchers mentioned above. A possible reason for increased h_{fp} could be the differences in the surface area to volume ratios (A/V), with the smaller the particles having higher A/V. The fluid-to-particle heat transfer coefficient is expected to be higher as A/V is increased.

Aside from particle size, in a forced convection situation, the heat transfer coefficient could also be affected by fluid flow rate or particle velocity. The magnitude of the fluid-to-particle heat transfer coefficient depends on the relative fluid-to-particle velocity (Stoforos, 1992). In spite of conflicting trends reported with respect to the effect of particle size, the effect of fluid-to-particle relative velocity on h_{fp} is quite conclusive. Increasing relative velocity has always been reported to increase the associated fluid-to-particle heat transfer coefficient (Chang and Toledo, 1989; Zuritz *et al.*, 1990; Gaze *et al.* 1990; Sablani and Ramaswamy, 1995; Awuah et al. 1996; Chen *et al.*, 1996). The present study concurs with reports in the literature.

With respect to particle properties, Measmans *et al.* (1992) pointed out that such particle properties as density and surface roughness do not necessarily affect particle-fluid motion. In fact, the type of particle material may not influence the magnitude of convective fluid-to-particle heat transfer coefficient. However, Hassan (1984) reported higher values of h_{fp} for potato particles than that for Teflon particles processed in water. Stoforos (1988) also reported different values for aluminum and Teflon spheres under similar experimental conditions. Chandarana *et al.* (1989) reported higher values of h_{fp} from water and starch solutions for food particles such as potato and carrot rather than silicone dices. Astrom and Bark (1994) investigated the effects of influencing factors on h_{fp}, in aseptic processing conditions, and found differences in h_{fp} using spherical particles of different materials. The authors stated that although the convective heat transfer coefficient is primarily a function of fluid properties, it can also be expected that the heat capacity and thermal conductivity of the particle material may also have some influence on h_{fp}. Using potato and Teflon particles processed in water and CMC solution, Awuah *et al.* (1996) observed similar trends in relation to the effect of fluid temperature, concentration and flow rate on h_{fp} for both materials. However, both materials responded somewhat differently in terms of percentage differences between h_{fp} values at different temperature, concentration, and flow rate. In the present study, with respect to the particle material and regardless of the effects of the other factors (velocity, viscosity and temperature), overall, it was found that aluminum epoxy particles exhibited about 30% higher values of h_{fp} than Nylon sphere (Table 4.4). The higher fluid-to-particle heat transfer coefficient associated with aluminum particles (with higher thermal conductivity and thermal diffusivity) may be expected as a result of faster heat conduction within the sphere, thus keeping the particle surface temperature at a level lower than the Nylon sphere. The difference between the fluid temperature around the particle, the boundary layer thickness, and the particle surface temperature could probably alter the interfacial characteristics, which would eventually influence the fluid-to-particle heat transfer coefficient.

Effect of fluid viscosity and temperature on h_{fp}

The average values of h_{fp}, as influenced by the medium viscosity at different particle velocities, are shown in Figures 4.5 and 4.6 for particles of different materials and sizes at a given medium temperature (60 ^{o}C). The mean values of h_{fp}, for aluminum epoxy particle at a constant velocity of 0.1 m/s, varied from 1460 to 530 W/m^2K for

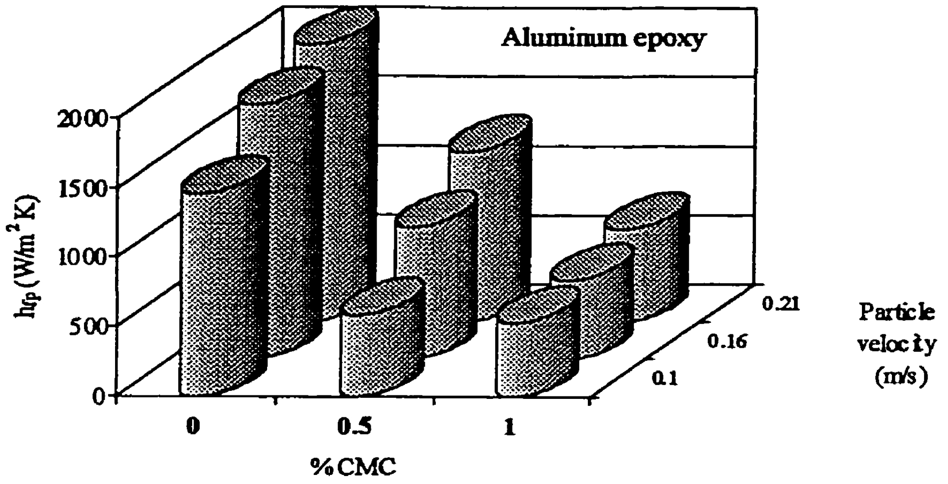

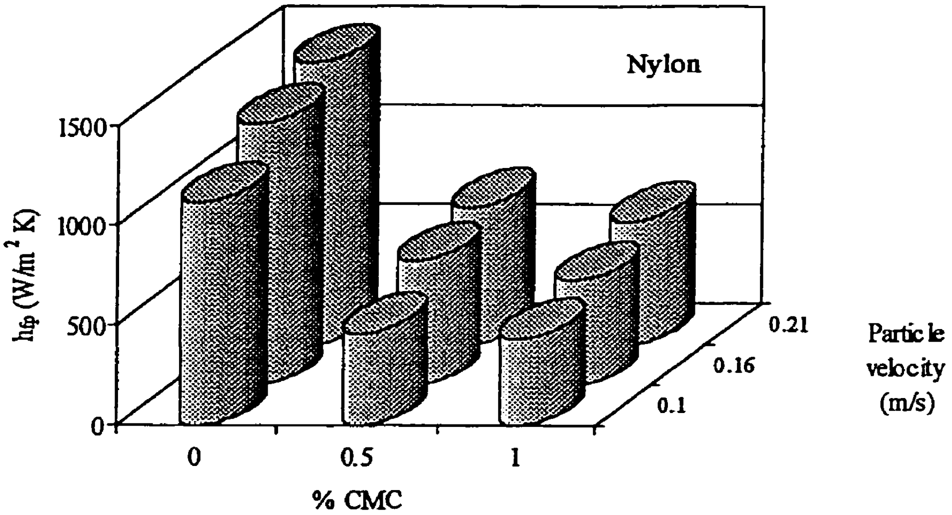

Figure 4.5. Effect of medium viscosity (CMC concentration at a constant temperature, 60 °C) on h_{fp} at different particle velocities for Aluminum epoxy and Nylon particles.

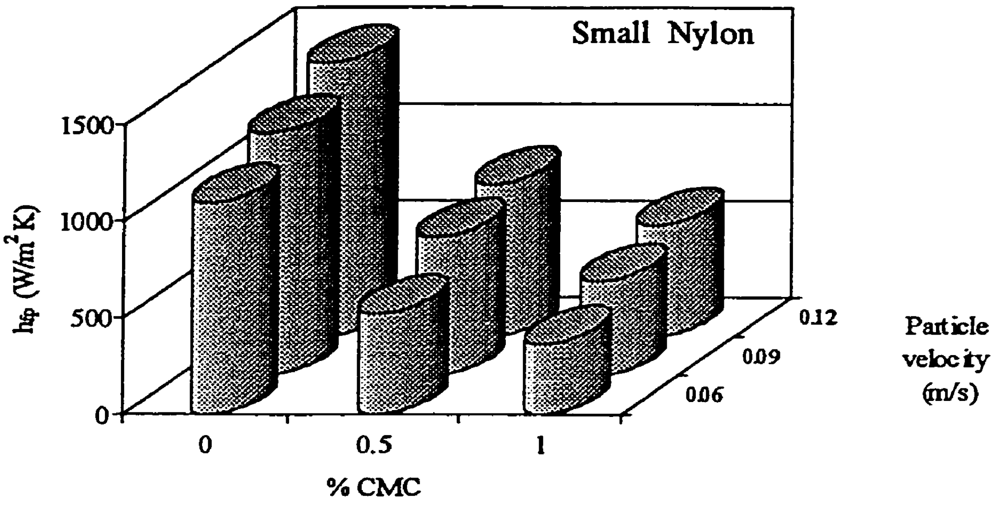

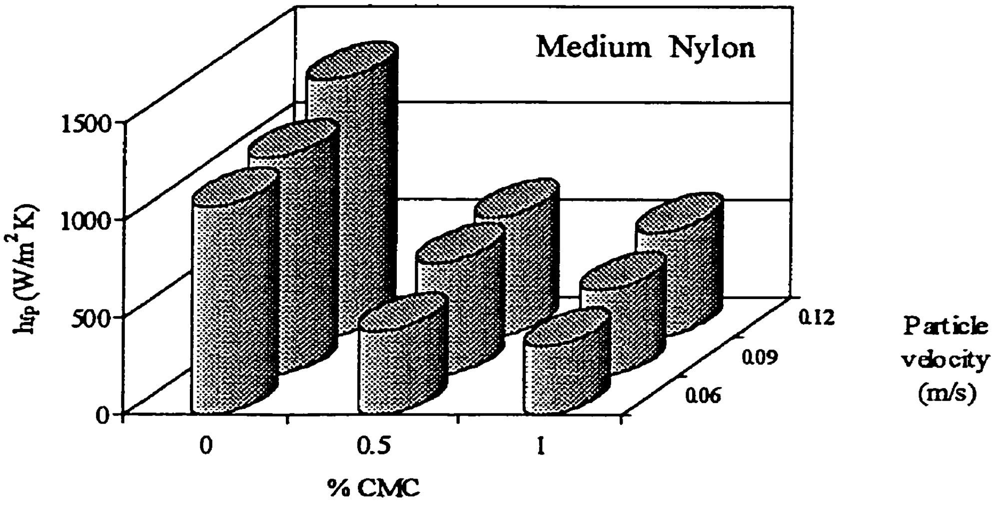

Figure 4.6. Effect of medium viscosity (CMC concentration at a constant temperature, 60 °C) on h_{fp} at different particle velocities for small and medium size of Nylon particles.

water and 1% CMC solution, respectively. An intermediate mean value of 590 W/m^{2}K was obtained for 0.5% CMC solution. The heat transfer coefficient thus decreased with increasing CMC concentration. Consistently, the same trends were observed at the other velocities, and also for the Nylon particles of different sizes.

In addition, the effect of viscosity (CMC concentration), at different temperatures, on the associated heat transfer coefficient is shown in Figure 4.7 for aluminum epoxy and Nylon particles of the same size, at a constant linear particle velocity (0.1 m/s) . A similar plot was also obtained (Figure 4.8) for the small and medium Nylon spheres at a given particle velocity (0.06 m/s). Experiments were carried out, at different temperatures, with 0.5 and 1% concentration of CMC solutions. A general trend of increasing h_{fp} values was observed as the medium temperature increased at a given concentration of CMC. For instance, the values of h_{fp} associated with aluminum epoxy, at a given particle velocity using 0.5% CMC solution as the heating medium, varied from 590 to 1140 W/m^{2}K when the medium temperature changed from 60 to 80 ^{o}C. The higher values of h_{fp} could be due to lower viscosities associated with the heating medium at higher temperature. However, this change seems to be less, from 530 to 720 W/m^{2}K, within the same temperature range and same experimental conditions, with the more viscous 1% CMC solution. Thus, the higher viscosity tends to overshadow the temperature effect which is in agreement with finding by Alhamdan and Sastry (1990) for the evaluation of convection heat transfer coefficient between non-Newtonian fluids and an irregular shaped particle.

Heat transfer to the particulate depends on the rheological characteristics of the heating medium, primely by the fluid apparent viscosity. Higher fluid apparent viscosity of a non-Newtonian fluid retards heat transfer as the decreased turbulence lowers the effective fluid-to-particle relative velocity (Maesmans *et al.*, 1992). Lower values of h_{fp} are associated with a more viscous fluid, resulting from a higher concentration of CMC or lower processing fluid temperature. Thus, the findings in this study are in agreement with several other studies in the literature (Zuritz *et al.* 1987; Chandarana *et al.* 1988; Astrom and Bark, 1994; Awuah *et al.*, 1996; Chen *et al.*, 1997; Chakrabandhu and Singh, 1998).

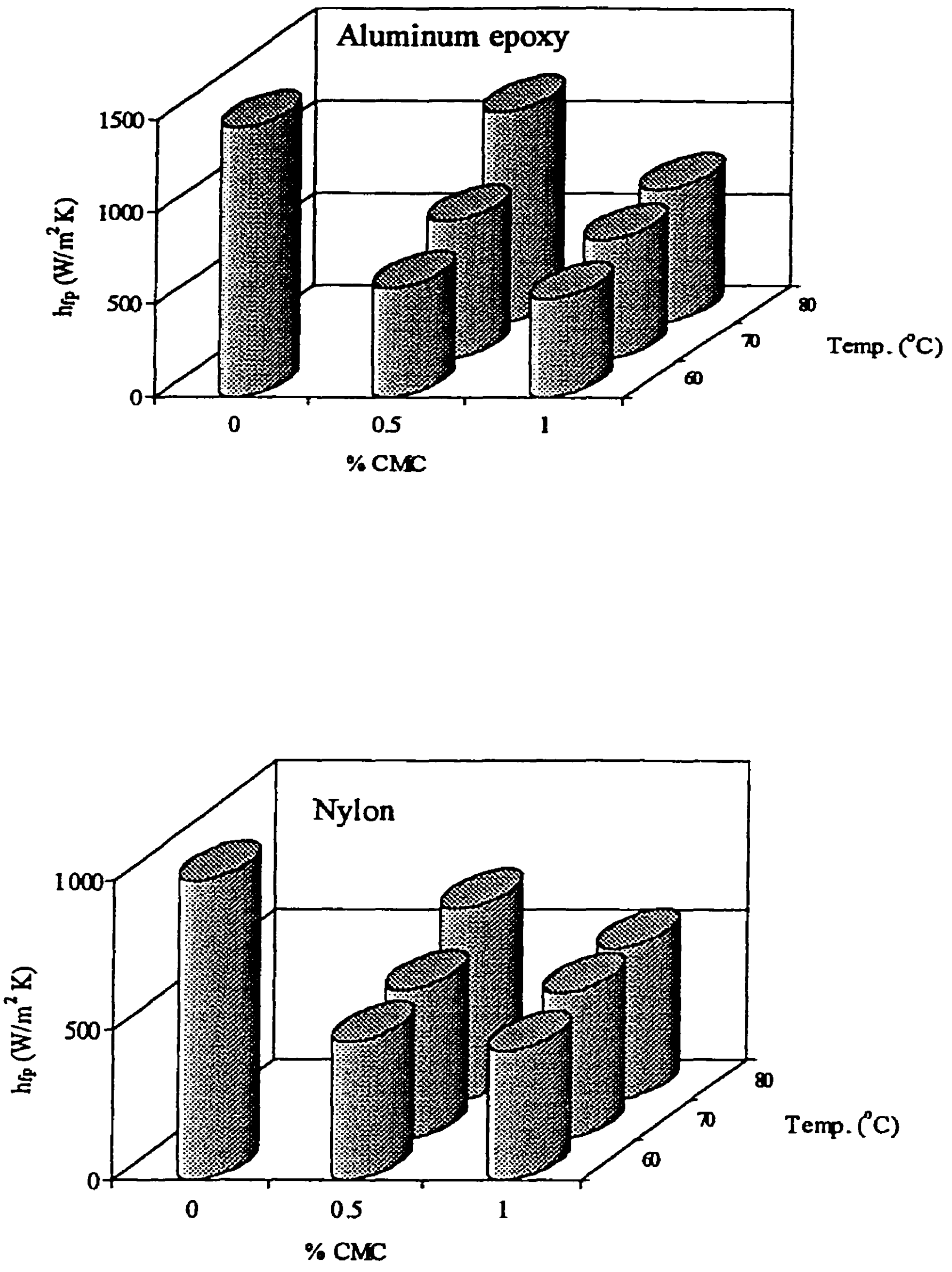

Figure 4.7. Effect of medium viscosity (CMC concentration) and temperature on h_{fp} for Aluminum epoxy and Nylon particle at a given particle velocity (0.1 m/s).

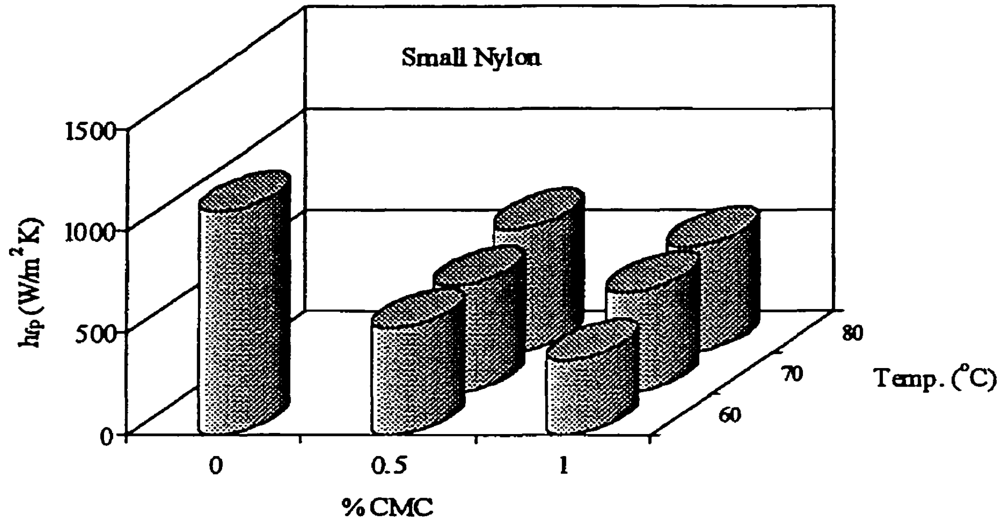

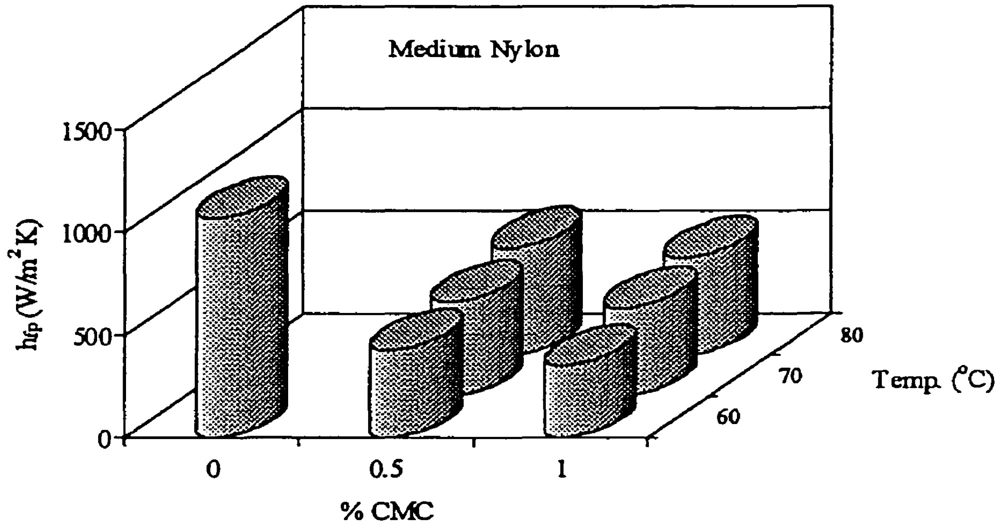

Figure 4.8. Effect of medium viscosity (CMC concentration) and temperature on h_{fp} for small and medium size of Nylon particles at a given particle velocity (0.06 m/s).

CONCLUSIONS

Factors influencing tube-flow fluid-to-particle heat transfer coefficient were investigated using a particle oscillatory motion technique for imparting controlled motion of particles under tube-flow conditions. Experiments were carried out with spherical particles of different sizes and materials in water and various concentration of CMC solution as the heating medium.

Depending on experimental conditions involving different particle materials, particle sizes, particle velocities, fluid viscosities and fluid temperatures, values of h_{fp} varied from 350 to 2000 W/m^2K. Statistical analysis showed significant effects of all the factors on associated h_{fp}. Also, T-test grouping indicated that mean values of h_{fp} were different among the levels of factors. Conventional trends of higher heat transfer coefficient with higher particle velocity and fluid temperature, and lower fluid viscosity were observed. However, with respect to the effect of particle size, a decrease in h_{fp} values was found as the particle size increased.. Some differences were also observed between the h_{fp} values for aluminum epoxy and Nylon particles probably due the effect of particle properties on the boundary layer properties during heating process.

PREFACE TO CHAPTER 5

In the previous section (chapter 3 and 4), a new technique was reported for evaluating h_{fp} under conditions in which the particle could be subjected to a controlled oscillating motion. Although the developed technique was quite useful and effective for evaluating the influence of various factors on h_{fp}, one limitation is that it does not provide "natural movement" of the particle. Hence, other techniques were explored for evaluating h_{fp} when the particle was moving naturally under tube-flow conditions. The thermo-chromic liquid crystal (TLC) technique, which has been widely reported in the literature, was one of the available choices used initially. However, difficulties were experienced with the use of this technique which resulted in too large an experimental variation in evaluated h_{fp}, to be useful in evaluating the influencing factors. The calorimetric technique, detailed in this chapter, was subsequently developed as a suitable alternative.

The calorimetric technique is based on measuring the bulk temperature of a moving particle in tube-flow conditions, for the subsequent evaluation of the fluid-to-particle heat transfer coefficient, using a finite difference model. The advantage of this technique is that the particle is allowed to move "naturally" in a carrier fluid under tube-flow conditions without any interference.

The technique was presented at the Conference of Food Engineering in 1997. A manuscript entitled " A Calorimetric Approach for Evaluation of Fluid-to-Particle Heat Transfer Coefficient Under Tube-Flow Conditions" by M. R. Zareifard, the candidate, and Dr. H. S. Ramaswamy, the supervisor, has been accepted for publication in the Journal of Lebensm.-Wiss. U-Technology. Experimental work and data analysis were carried out by the candidate under the supervision of professor H. S. Ramaswamy. Thus, the second objectives of the thesis will be achieved.

CHAPTER 5

A CALORIMETRIC APPROACH FOR EVALUATION OF FLUID-TO-PARTICLE HEAT TRANSFER COEFFICIENT UNDER TUBE-FLOW CONDITIONS

ABSTRACT

A calorimetric approach was developed to evaluate the bulk temperature of moving particles, from which the associated convective fluid-to-particle heat transfer coefficients (h_{fp}) were evaluated under continuous tube-flow conditions. The technique consisted of introducing a particle at an upstream location into a holding tube, through which a carrier fluid was circulated under pre-stabilized temperature and flow conditions, and retrieving it from a downstream location at a known time interval. The particle was transferred immediately into a specially constructed calorimeter and its bulk temperature was determined upon equilibration. The technique was calibrated using thermocouple equipped particles subjected to various time-temperature treatments. Since the medium temperature, particle initial temperature, exposure time and thermophysical properties were known, the associated h_{fp} could be computed using an iterative numerical technique for the evaluated bulk temperature of the particle. The h_{fp} values, thus obtained from using the calorimetric approach, were comparable with those from traditional techniques involving thermocouple equipped particles. Higher h_{fp} values were associated with moving particles, as compared to stationary particles, particles of larger size and fluid flowing at higher rates.

INTRODUCTION

Determination of the convective fluid-to-particle heat transfer coefficient (h_{fp}), associated with moving particles, poses a unique challenge to investigators because of the difficulty in monitoring the temperature of moving particles without interfering with the particle motion. In basic studies of convection heat transfer, many researchers have developed means and methods by which the convective heat transfer coefficient associated with liquid-solid mixtures can be determined. Such means and methods include: stationary particle, moving thermocouple, liquid crystal, relative velocity, liquid temperature calorimetry, microbiological destruction, melting point and transmitter methods.

Evaluation of h_{fp} for a moving particle in a continuous flow situation is generally difficult because a thermocouple cannot be attached to it without interfering with the flow. Therefore, even for forced convection in a tube-flow situation, some previous studies were limited to simplistic approaches using a fixed particle (Chandarana *et al.*, 1998; Zuritz *et al.*, 1990, Awuah *et al.*, 1995; Kelly *et al.*, 1995; Chen *et al.*, 1997). In these studies h_{fp} was determined by recording the time temperature data of a stationary particle in a moving fluid. These approaches ignore the contribution of particle motion to heat transfer in tube-flow conditions. Some innovative approaches have been used to overcome this problem, for example, Astrom and Bark (1994) determined h_{fp} with a stationary particle which was immersed in a rotating thermos flask containing the carrier fluid. They studied the effect of particle position, with respect to the distance from the rotational center, and relative velocity by rotating the flask. Sastry *et al.* (1989) suggested a moving thermocouple method, in which a thermocouple equipped, spherical particle was pulled at a pre-determined rate in order to simulate the particle motion. Using the same method, Zitoun and Sastry (1994) studied the heat transfer coefficient for cube shaped particles in a continuous tube flow.

The relative velocity approach was used by Balasubramaniam and Sastry (1996) in continuous flow through a horizontal scraped surface heat exchanger in order to estimate the fluid-to-particle heat transfer coefficient from established correlations, like

Ranz and Marshal (1952). The relative velocity was directly determined by videotaping the particle motion and that of the liquid containing a tracer. Sastry *et al.* (1990) compared their experimental values of h_{fp}, using the moving thermocouple technique, with those estimated from the relative velocity method and reported opposing trends. Mankad *et al.* (1997) measured particle-liquid heat transfer using the stationary particle and relative velocity techniques, in systems of varied solid fraction. They concluded that the Ranz and Marshal correlation was acceptable for predicting h_{fp} for single particle data. However, for higher solid fractions the only predictions which were accurate occurred at lower Reynolds number of less than 100.

Recently, thermo-chromic liquid crystals (TLC), which change color with temperature, have been applied to the surface of a particle to get the surface temperature history of a moving particle, in order to evaluate the heat transfer coefficient in continuous tube-flow conditions. Stoforos and Merson (1991) were probably the first to use this technique in food engineering research. Balasubramaniam and Sastry (1994b and 1995) applied the same technique to measure the heat transfer coefficient in continuous tube-flow situations, and observed that the liquid crystal method resulted in higher values of h_{fp}, when compared to the moving thermocouple and relative velocity methods. Meanwhile, Zitoun and Sastry (1994) reported that the relative velocity method yielded higher values of h_{fp} than the liquid crystal method. Balasubramaniam and Sastry (1996a) later compared the three methods (moving thermocouple, liquid crystal, and relative velocity) and concluded that the liquid crystal method yields the highest value because of the freedom of rotation allowed to particle under test conditions. Using TLC material as a temperature indicator, Zareifard et al. (1996) reported up to 40% lower values of h_{fp} under natural convection heat transfer condition when compared to those estimated from the Whitaker (1976) equation. They also reported either under-estimated or over-estimated values of h_{fp} for the laminar flow and turbulent regime, respectively, using the relative velocity method and the Ranz and Marshal (1952) equation. Balasubramaniam and Sastry (1996b) developed a technique for h_{fp} evaluation using a temperature pill in a cylindrical form, with a remote electronic temperature sensor.

In the previous section, a technique involving particle oscillatory motion while being heated in a model holding tube, was detailed for the evaluation of h_{fp}. In this technique, spherical particles, with centrally located thermocouples, were suspended in a curved glass tube to provide lateral movement of the particle as the tube was subjected to an oscillatory motion, while immersed in a prestabilized medium. This technique was subsequently used to evaluate the influence of several factors influencing h_{fp}. While controlled motion of the particle was possible and its effect on h_{fp} could be successfully quantified, the method has one inherent disadvantage. The particle motion is created artificially and, therefore, it lacks the "natural movement". This will impose some restrictions on the particle movement when compared with the motion of a naturally moving particle. Notable among the differences is the lack of a natural "rotational movement" which causes the particle to roll along the tube. Baptista et al. (1997) ascribed a considerable influence to the rotary motion on the associated tube-flow h_{fp}. Hence, the objective of this phase of research was to look at other alternatives for evaluating h_{fp}, which do not restrict the natural movement of the particle. Some preliminary studies were carried out using the thermo-chromic liquid crystal technique for evaluating h_{fp}. The method gave a viable and promising alternative for h_{fp} determination, and concurred with literature (Zitoun and Sastry, 1994; Balasubramaniam and Sastry 1994b, 1995, 1996a). These results were reported in Zareifard et al. (1996). However, when the research was extended to evaluate the influence of factors influencing h_{fp}, associated errors in measurement of transient color changes were found to be very high. The resulting large variability could not be usefully associated with the evaluated h_{fp}. This limited its application as a tool for evaluating the influence of factors affecting h_{fp}.

Attempts to evaluate h_{fp} under tube-flow conditions with natural movement of particles, not attached to a thermocouple, succeeded with the development of the calorimetric approach for h_{fp} evaluation. Therefore, the objective of this research was to use the calorimetric technique to measure the bulk temperature of moving and stationary particles in tube-flow conditions, for the subsequent evaluation of the fluid-to-particle heat transfer coefficient using a finite difference model. The advantage of this technique is that the particle is allowed to move in the tube without any interference. With calibration, the technique could be used for particles of different size and shapes.

THEORETICAL BACKGROUND

The unsteady state heat conduction equation with surface convection, involving an isotropic spherical particle, initially at uniform temperature, when suddenly transferred into a medium at a constant temperature, is given by Carslaw and Jaeger (1959):

$$\frac{\partial U}{\partial t} = \alpha \left(\frac{\partial^2 U}{\partial r^2} + \frac{2}{r} \cdot \frac{\partial U}{\partial r} \right) \qquad (5.1)$$

with the initial and boundary condition as:

$$U(r, 0) = T_i \quad \text{at} \quad t = 0$$

$$\partial U/\partial r = 0 \quad \text{at} \quad r = 0 \ , \quad t > 0$$

$$-K\ A\ \partial T/\partial r = h_{fp}\ A\ (T_f - T_{ps}) \quad \text{at} \quad r = a\ , t > 0$$

Numerical solution

In order to determine h_{fp}, the governing partial differential equation [Eq. (5.1)], with associated initial and boundary conditions, can be solved numerically using a finite difference method. As detailed in many books (Holman, 1990; Chandra and Singh, 1995) the finite difference solutions could involve explicit or implicit schemes or a combination of both. If the thermo-physical properties of an immersed object as well as the initial and boundary conditions are known, these schemes could be used to predict transient temperature distribution at any given location, in the object subjected to a thermal treatment, or alternately could also be used to compute the transient mass average temperature, which is the temperature the object would attain if removed from the system and held in a perfectly insulated surroundings with no heat exchange with the external environment. By a trial and error technique, the same scheme can be used to back calculate the heat transfer coefficient, which would match the experimentally determined transient center or the mass average temperature (bulk temperature) resulting upon equilibration in an adiabatic calorimeter. Alternately, a similar procedure could be used to compute h_{fp} from measured transient surface temperatures (using Thermo-chromic Liquid Crystal technique).

Analytical solution

The analytical solution to Eq. (5.1) is given in chapter 2. The analytical solution, also called the heating rate index, is based on the direct temperature measurement of the particle during heating. By plotting the log of temperature difference versus time, the heating rate index (f_h) can be obtained as the negative reciprocal slope of the straight line portion of the curve. The heating rate index can then be related to particle properties. Therefore, knowing thermo-physical properties of the particle and heating rate index, which can be evaluated from experimental data, Biot number and hence, the heat transfer coefficient (h_{fp}) can be calculated [h_{fp} = Bi (k/a)].

MATERIALS AND METHODS

Preliminary studies using TLC and RV method

To evaluate non-conventional methods for the fluid-to-particle heat transfer coefficient determination, under forced convection heat transfer conditions in a continuous flow system, two methods were considered: I) use of thermo-chromic liquid crystal (TLC) material for obtaining the transiant surface temperature profile of the moving particle in tube-flow, and II) use of Ranz and Marshal (1952) correlation [Eq. 2.18] based on relative velocity of the particle.

Particle preparation

Temperature-insensitive thermo-chromic liquid crystal (TLC) was obtained from Hallcrest Inc. (Glenview, IL). These formulations reflect just a single color below a given transition temperature (called the clearing point) and change to colourless above it. Aluminum spherical particles of 25.4 mm in diameter (Small Part Inc., Miami lakes, FL) were used as model particles. Particle surface was first painted using a water-based black paint and then one hemi-sphere of the particle's surface was coated with TLC (BM/G70C/C11-10) which changes color at 70°C, and the other hemi-sphere was coated with another type of TLC (BM/G80C/C11-10) which changes color at 80°C (nominating temperature). TLC material in the form of liquid was sprayed using an air brush (Badger Air-Brush Co., Franklin Park, IL) at 140 k Pa. Because these chemicals are water-based, a thin layer of water resistant binder (AQB-3) was sprayed on the surface to protect the liquid crystal layer. The coated particle was calibrated for temperature, as a result of the color change, in a transparent water bath with controlled temperature.

Experimental setup and evaluation of h_{fp}

The same experimental setup and numerical procedure for the calorimetric method was used to evaluate h_{fp}; this will be explained in the following section. Experiments were carried out with water as the carrier medium. The total time which the particle spent in the system as well as the time which the particle surface temperature reached 70°C and 80°C (when the corresponding TLC became colourless) were recorded. The velocity of the particle while travelling along the tube was also recorded along with the fluid temperature and fluid flow rate. The particle Re number and Pr number were calculated. Then, the h_{fp} was calculated using the estimated Nu number and the Ranz and Marshall (1952) correlation [Eq. 2.18] .

Calorimetric studies

The challenge continues to evaluate h_{fp} under tube-flow conditions with the natural movement of the particle, using non-conventional methods and following the experienced gained using the TLC method. Attempts have been successful with the calorimetric method with the following procedures involving: calibration, verification and validation of the method against the conventional and reliable direct temperature measurement, using a thermocouple equipped particle.

Particle preparation

Aluminum spherical particles (Small Part Inc., Miami lakes, FL) of three different sizes (19.1, 22.2 and 25.4 mm) were used as test particles and the following thermophysical properties were assumed (Holman, 1990): density (ρ)=2707 kg/m^3, heat capacity (C_p)=896 J/kg.K and thermal conductivity (k)=204 W/m.K ,and thermal diffusivity (α) was calculated as $\alpha=k/\rho\ C_p=8.41\text{x}10^{-5}$ W/m^{2}K .

Selected Aluminum spheres for each size were equipped with a centrally located thermocouple, for calibrating the technique. For this purpose, particles of each size were carefully drilled to the geometric center with a fine drill bit using a high performance electronically equipped lathe (Emco Compact 8, Emco Maier Corporation, Hallein, Austria). A Teflon coated 30 AWG type-T (copper-constantan) thermocouple (Omega Eng. Inc., Stamford, CT), with a welded tip, was introduced to the center of each particle. The gap between the thermocouple wire and the particle was filled and sealed with a 1:1 mixture of epoxy resin and a hardener. The thermocouples were calibrated against an ASTM standard mercury in glass thermometer with a temperature resolution of ± 0.05 ^{o}C.

Calorimetric method: bulk temperature determination

A schematic of the Styrofoam calorimeter is shown in Figure 5.1. A Styrofoam sheet, 10 cm in thickness (Polymos Inc., Terrasse-Vaudreuil, Quebec) was cut into a slab 20 x 20 x 10 cm. Two such slabs were pressed against a preheated stainless steel ball, of the same size as the experimental sphere, and sandwiched between them so as to form two hemispherical cups to hold the test particle for temperature equilibration. A flexible Teflon coated 30 AWG T-type thermocouple (Omega Eng. Inc., Stamford, CT), made with a special flat tip for a better contact with the particle surface, was attached to the bottom of the lower cup, for particle surface temperature measurement. Thus, by placing the test particle in the lower cup of the calorimeter and covering it with the other half, the equilibration of particle temperature could be monitored.

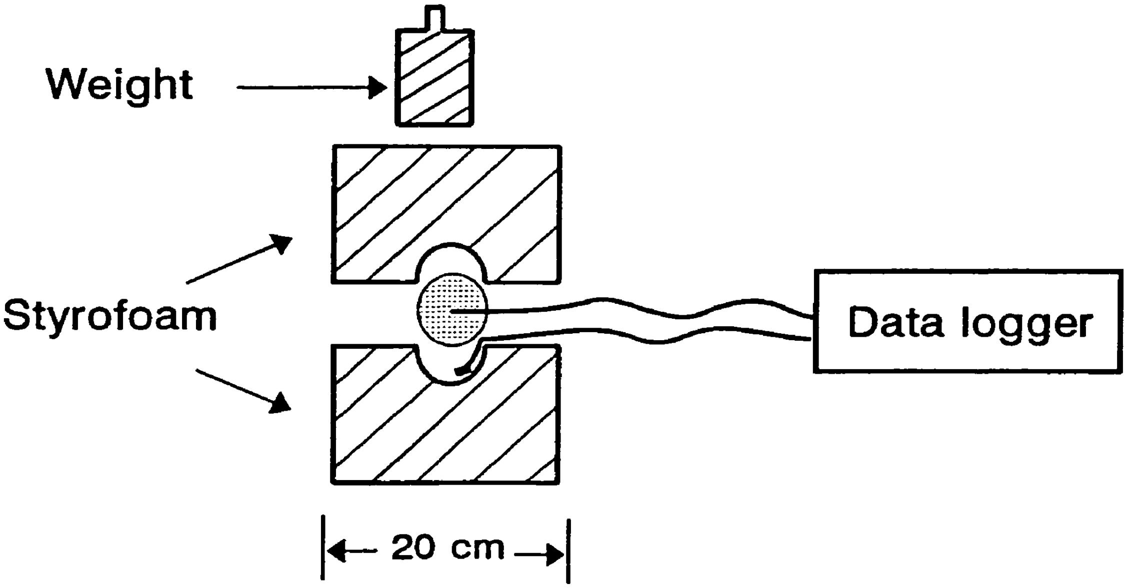

Figure 5.1. Schematic of custom moulded Styrofoam as a calorimeter, with a flat tip thermocouple attached to the bottom of the lower cap to record the particle temperature.

To ensure good contact between the particle and the thermocouple, a small weight was placed on top of the calorimeter after placing the particle inside. The particle surface temperature was thus continuously recorded. When a particle equipped with a center point thermocouple was used, the center temperature was also recorded in addition to the surface temperature.

During equilibration process, some heat loss from the Styrofoam calorimeters to the environment was unavoidable. The calorimeters were therefore calibrated for each particle size at different temperatures in order to arrive at meaningful bulk temperature data. For this purpose, particles were equilibrated to different temperatures in a water bath, and were transferred to the calorimeter. The changes in particle temperature were recorded with respect to time. After an initial quick drop in the particle temperature, as a result of the transfer, there was a slow but steady change in the temperature as a result of heat loss through the calorimeter. By taking the regression of the time-temperature profile over the straight portion, and extrapolating the regression line to time zero, the projected initial temperature of the particle was obtained and compared to the actual initial temperature in order to obtain the correction factors. Since the correction factors were expected to be temperature dependent, calibration data were established for each particle over the entire range of expected temperatures.

Numerical model

A computer program was written in FORTRAN 77 to compute the transient temperature distribution in the spherical particle, for each condition. The numerical procedure involved with the finite difference method has been detailed elsewhere (Sablani and Ramaswamy, 1996). In the above procedure, a Crank-Nicolson scheme for space derivatives and a fully implicit scheme for time derivative were employed for the finite difference solution. A grid with 20 divisions in the spatial direction and a 0.1 second time-step was used in the model. At a given fluid temperature (T_f), the initial particle temperature (T_i), radius (a), thermal conductivity (k) and thermal diffusivity (α) of the particle and an assumed value of h_{fp}, the transient center, surface or mass average (bulk) temperature of the particle was computed as a function of time and compared with the experimental value. The h_{fp} values were then changed sequentially, to reduce the difference between the computed and measured bulk temperature, to less than 0.05 ^{o}C. The flow chart of the procedure is given in Figure 5.2.

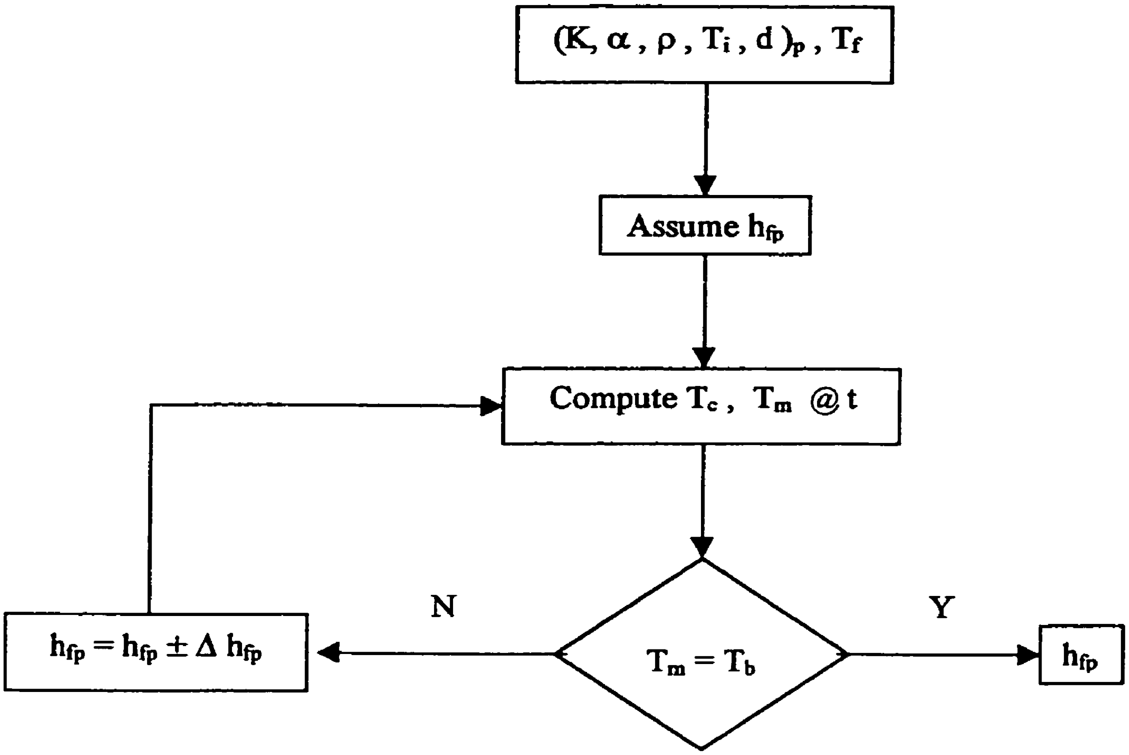

T_b is the bulk temperature of the particle measured experimentally following adiabatic equlibration.
T_m is the mass average (bulk) temperature calculated as $\int T\,dv / V$.

Figure 5.2. Flow chart showing the procedure for mass average (bulk) temperature and h_{fp} calculations using a finite difference computer program.

Validation of the numerical model

The numerical model was validated for this study case. For this purpose, the Aluminum spherical particles with centrally located thermocouples, as described previously, were heated in a water bath and the time-temperature history was recorded at one second time intervals, using a Dash-8 data logger (Metra-Byte Corp. Taunton, MA) connected to a personal computer. From the plot of the logarithm of the particle temperature difference versus time, the heating rate index (f_h) was calculated as the negative reciprocal slope of the linear section of the curve. Equation 2.11 was then used to obtain δ and the Bi number from which the h_{fp} value was calculated (analytical solution). Using the computed value of h_{fp} for the given condition, the time-temperature profile of the particle was then predicted using the finite difference numerical program and compared with the experimental curves.

Some additional experiments were also carried out in the water bath, under different testing conditions, in order to compare the numerical and analytical techniques. In order to achieve mild heating conditions (natural convection), the particle was immersed in a beaker containing preheated water or sucrose solution and placed in a water bath to maintain the temperature. More rapid heating conditions were achieved by heating the particles directly immersed in a well circulated water bath. Experiments were carried out under the following conditions (6 replicates): a) heated under natural convection using water and 50% sucrose solution (g/100 mL), at 75 and 85 ^oC; b) heated under forced circulation using water at 75, 85 and 100 ^oC.

Verification of the calorimetric approach

In order to calculate the fluid to particle heat transfer coefficient by the calorimetric technique, it was necessary to estimate the particle bulk (*i.e.*, mass average) temperature, following known treatment times. For this purpose, experiments were conducted in a water bath at 85 ^oC with particles containing centrally located thermocouples, in order to gather transient center temperature data and the computation of h_{fp}, as described in the previous section. A given particle was heated for known time intervals (10-25 s) and quickly transferred to the calorimeter, after which the equilibrium temperature was estimated by both center and surface temperature data (when there is no thermocouple attached to the particle, the bulk temperature was only estimated using surface thermocouple data). Using the bulk temperature data and the iterative numerical finite difference technique, h_{fp} values were calculated and compared with those obtained from the transient center temperature data (analytical or numerical) obtained during heating. To be meaningful, both these techniques should yield the same value of h_{fp}.

Evaluation of h_{fp} under tube-flow conditions: stationary and moving particle

A schematic of the experimental setup for h_{fp} determination under forced convection heat transfer condition, in a continuous tube-flow system is shown in Figure 5.3.

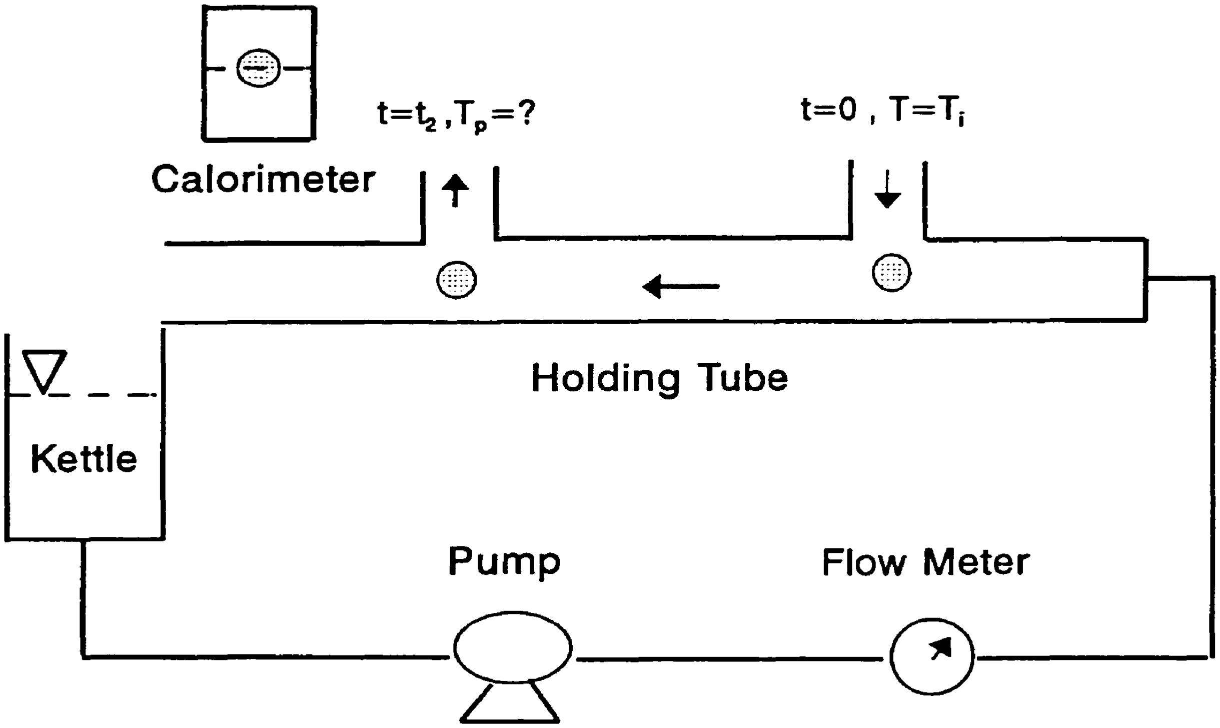

Figure 5.3. Schematic of the experimental setup for h_{fp} determination under tube-flow condition with a moving particle.

A steam jacketed kettle was used to heat the carrier liquid to the desired temperature. The liquid was circulated using a variable-speed pump (Little Giant Pump Co., Oklahama City, OK) through a Pyrex glass tube (0.045 m inside diameter and 1.7 m in length). A flow meter (Model FTB-5005, Omega Eng. Inc, Stamford, CT), installed on line, measured the flow rate. T-joint intersections were installed in order to introduce and retrieve test particles.

To evaluate h_{fp} in a stationary particle position, an aluminum spherical particle of a given size (19.1, 22.2 or 25.4 mm), with a centrally located thermocouple, was introduced into the tube at one of the T-ports, with the carrier fluid prestabilized for temperature and flow conditions. The time-temperature history of the particles was recorded through the data logger. The particle position was fixed at the bottom surface of the tube. For the moving particle situation, the particle without the thermocouple was introduced to the system at the entrance port and retrieved through the second port using a specially perforated plastic scoop, and immediately transferred to the calorimeter for bulk temperature measurement. Total time which the particle spent in the system and the velocity of the particle, while travelling along the tube, were manually recorded and used for h_{fp} computation as well as for calculating the relative velocity.

For tube-flow conditions involving the stationary and moving particles, experiments were carried out with water at 75 ^{o}C and three different particle sizes (19.1, 22.2 and 25.4 mm) and flow rates (13, 16, 19 L/min). All tests were replicated at least six times.

RESULT AND DISCUSSION

h_{fp} evaluated from TLC and RV method

Figure 5.4 shows the plot of h_{fp} for a spherical Aluminum particle versus Re, as evaluated from the TLC method and estimated form the Ranz and Marshall (1952) equation. The values of heat transfer coefficient increased as Re increased.

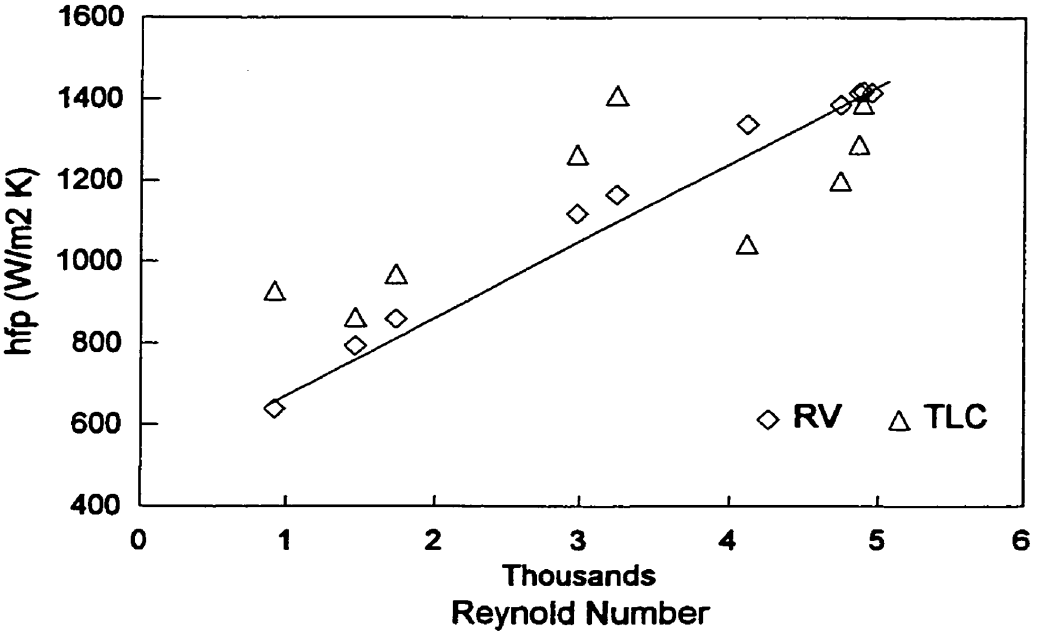

Figure 5.4. Values of h_{fp} for spherical Aluminum particle evaluated from TLC and RV methods, using water as the carrier fluid under tube-flow condition.

Regarding the RV method, it seems that the estimated values of Nu are either under or over-estimatedcompared to the TLC method. The Ranz and Marshall correlation, which was originally developed for a special case of convection heat transfer when the small liquid drops fall freely through the air, is not applicable for estimating h_{fp} under tube-flow processing conditions. The TLC method was found to be promising for h_{fp} evaluation in continuous tube-flow applications, because it provides an estimation of h_{fp} under natural movement of particles in a carrier fluid.

However, this method provides a surface temperature measurement which is very sensitive to variation in h_{fp}. The accuracy of temperature measurements is limited by the range of temperature over which color changes. This method is limited to only the transparent carrier medium and needs to be very carefully calibrated using a high resolution video camera recorder and advanced image analysis computer programs in order to distinguish the transient color change with respect to the temperature. However, these materials are very expensive, the particle preparation is very time consuming and the experiments are not very reproducible. It should be noted that the even thickness of the coated layer is very important. The physical properties of the particle may change due to the several layer of coated material which it is not easily accounted for. In addition, ageing and storage has a significant effect on the quality of the TLC material.

Further, the experimental results are very sensitive to the color and light of the experimental conditions. The experimental error was relatively high, for example, the error associated with a ±2 ^{o}C surface temperature measurement with respect to the transient color change or a ±1 second in time measurement resulted in about 20% variation in h_{fp}. For the worst case scenario of error, associated with both time and temperature (minimum time and maximum temperature) up to a 30% error is possible. Therefore, with such a large error margin and a lack of availability of sophisticated equipment for monitoring color change, it was found that the TLC method is not reliable for further investigative studies of the effects of factors influencing h_{fp}.

h_{fp} evaluated from calorimetric method

Results from the standardization procedure of the calorimetric method, involving calibration, verification and validation of the method against conventional, reliable direct temperature measurement using a thermocouple equipped particle, are given here. The results of the evaluation of h_{fp} under stationary and moving particle conditions also follow.

Calibration of calorimeter for bulk temperature determination

Typical temperature changes in a thermocouple equipped particle equilibrated to 50°C in a water bath when transferred to the calorimeter are shown in Figure 5.5. The figure shows temperature responses from the particle's centrally located thermocouple (center temperature) as well as from the surface temperature thermocouple placed at the bottom of the calorimeter well (surface temperature).

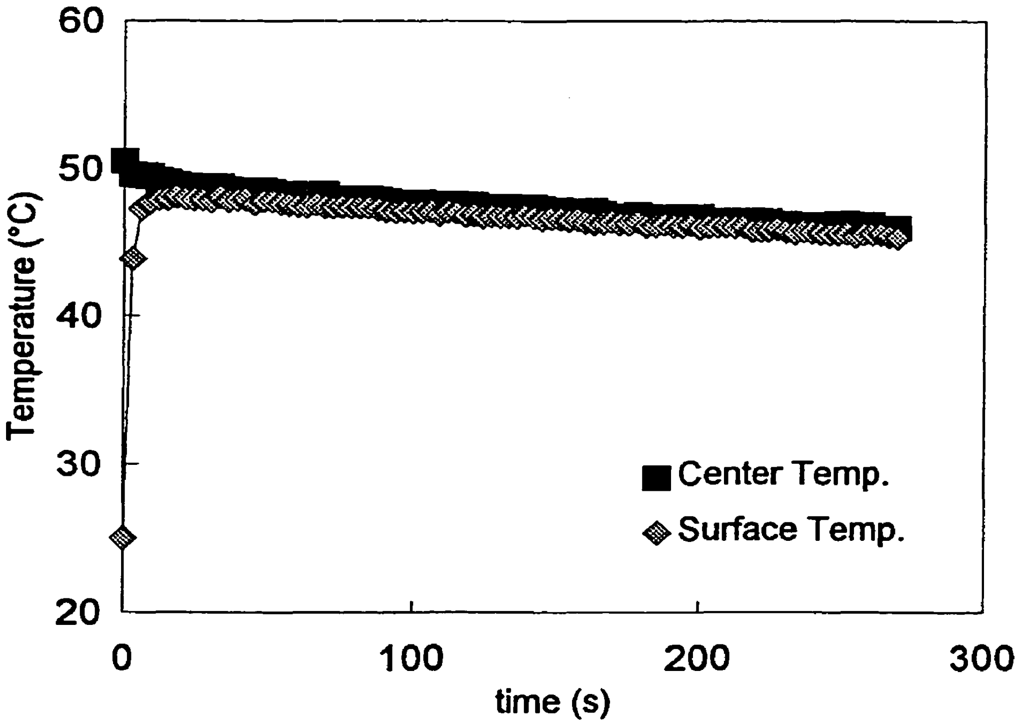

Figure 5.5. A typical temperature drop in the Styrofoam calorimeter for an Aluminum particle (d=25.4 mm) after equilibrium at 50 °C.

The temperature response from the surface thermocouple shows a quick rise as the hot particle comes in contact with the thermocouple placed at the bottom of the calorimeter. The response from the center thermocouple shows an initial drop as the particle exchanges heat within the calorimeter environment. After a relatively short time (about 10 s) the responses from both thermocouples show a similar steady but slow drop in temperature, indicating the gradual loss of heat from the calorimeter. The straight line portions of both center point temperature and surface temperature (which indicate the rate of heat loss) were then extrapolated (by a regression technique) to time zero. For example, the extrapolated values from the center temperature data, for a 25.4 mm aluminium particle equilibrated at 50 ^{o}C, was 49.4 ^{o}C, and that for the surface temperature was 48.3 ^{o}C. Both of them were corrected to 50^{o}C, which was the particle temperature prior to transfer to the calorimeter, thus giving a correction factor of +0.6 for data from the center thermocouple and + 1.7 ^{o}C for data from the surface thermocouple. Similar correction factors were obtained for the entire range of temperatures used with each of the three sizes of particles and the results are summarized in Table 5.1. Calibrated data obtained from the center and surface temperatures and their standard deviation are shown in Figure 5.6. Both techniques showed good reproducibility of results within the temperature range tested.

Table 5.1. Correction factors for centerpoint and surface temperature data.

Temp. (^oC)	Particle size(in)	Centerpoint data	Surface data
50	3/4	0.3 ± 0.1	1.1 ± 0.2
	7/8	0.3 ± 0.1	1.3 ± 0.4
	1	0.6 ± 0.2	1.7 ± 0.5
60	3/4	0.5 ± 0.2	1.4 ± 0.3
	7/8	0.7 ± 0.1	1.8 ± 0.4
	1	0.8 ± 0.3	2.1 ± 0.6
70	3/4	1.0 ± 0.4	2.0 ± 0.4
	7/8	0.7 ± 0.2	2.6 ± 0.6
	1	0.9 ± 0.2	3.2 ± 0.5
80	3/4	1.3 ± 0.3	3.1 ± 0.5
	7/8	1.2 ± 0.2	3.8 ± 0.5
	1	1.5 ± 0.4	4.1 ± 0.6

The correction factors are the mean average of 5 replicates ± the standard deviation.

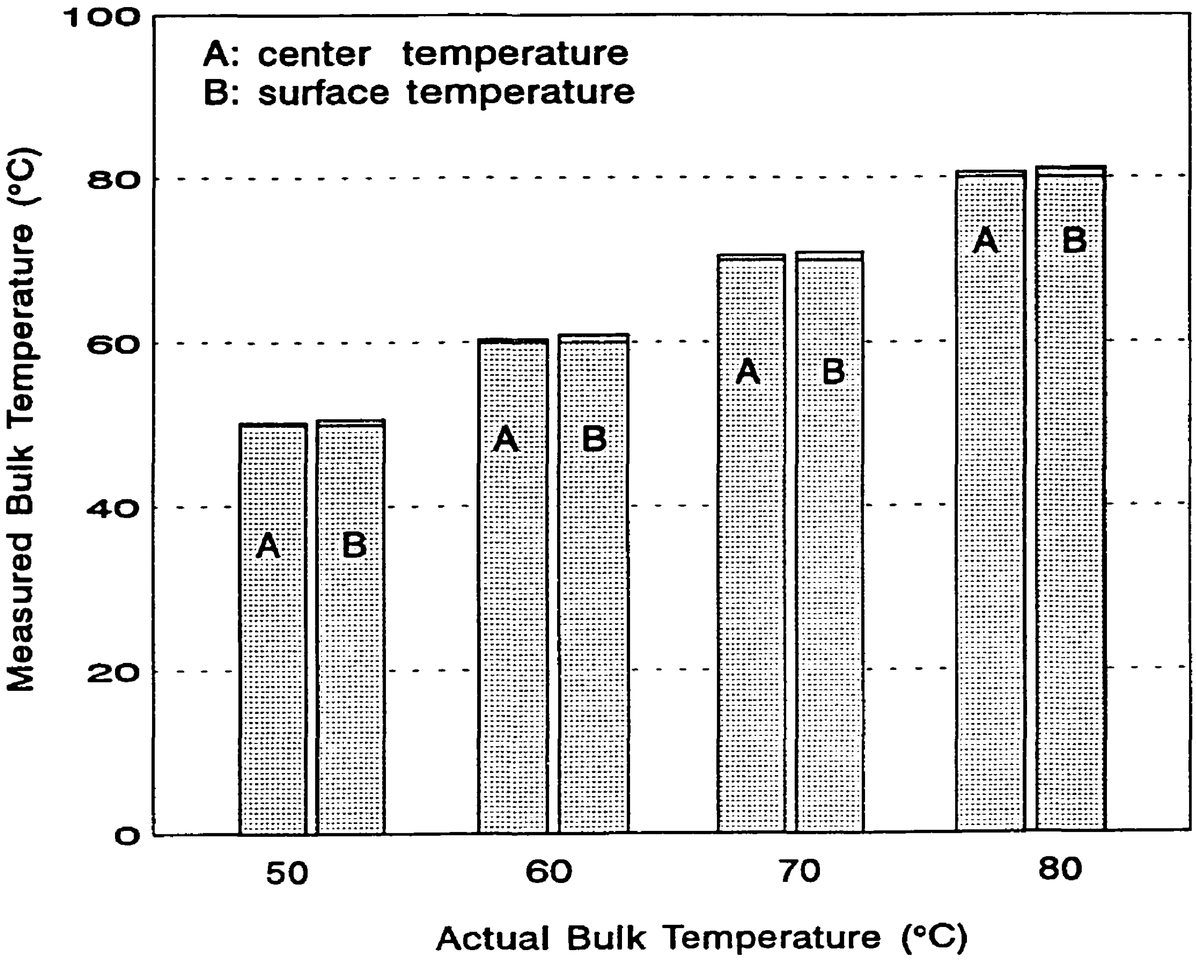

Figure 5.6. Calibrated center and surface temperature data (mean average and standard deviation) for an Aluminum particle in the Styrofoam calorimeter.

Validation of numerical model

A typical temperature profile at the center point of the spherical aluminum particle, (25.4 mm in diameter) heated in the water bath, is shown in Figure 5.7. The initial temperature was 12^{o}C and the fluid temperature was 83 ^{o}C. The fluid-to-particle heat transfer coefficient, calculated analytically, was 845 W/m^{2}K. The center point temperature of the particle, as computed numerically using the above h_{fp}, is also included in the Figure 5.6. Except for some small deviations at the intermediate temperatures, a good match was observed between the experimentally recorded and numerically calculated center point temperatures.

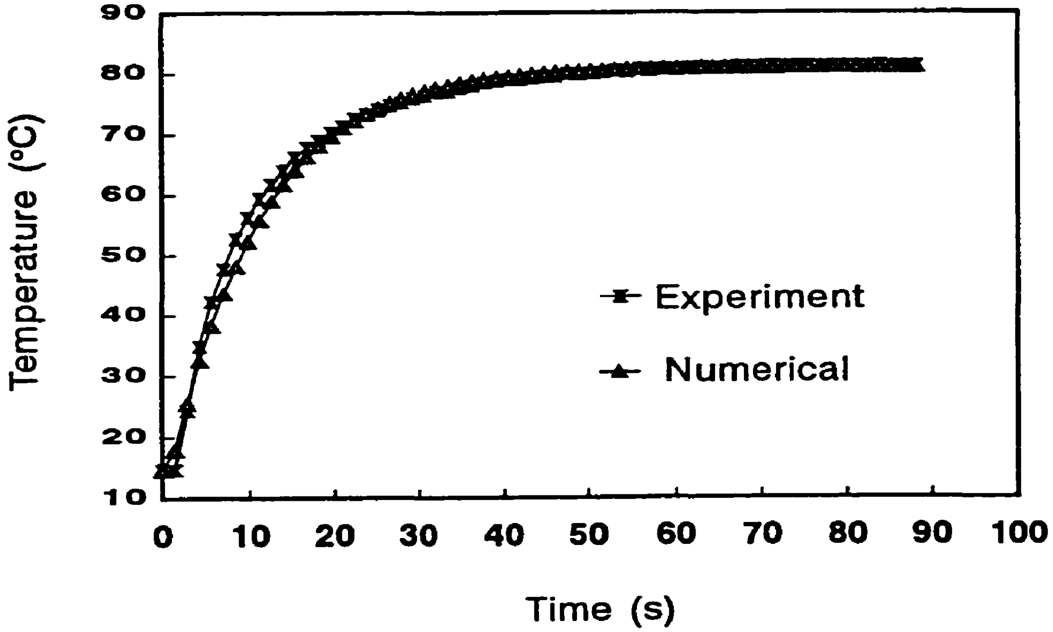

Figure 5.7. Center time-temperature profile for a spherical aluminum particle (d=25.4 mm): experimentally measured and numerically predicted using a finite difference program.

Additional values of h_{fp}, evaluated using both analytical and numerical techniques, are shown in Figure 5.8, for sucrose solution and water at different temperatures and conditions. As expected, h_{fp} values were higher for circulated water compared to still water at the same temperature (from 850 to 1700 W/m^{2}K). Like wise, lower values were obtained with sucrose solutions when compared to water, as a result of an increase of viscosity.

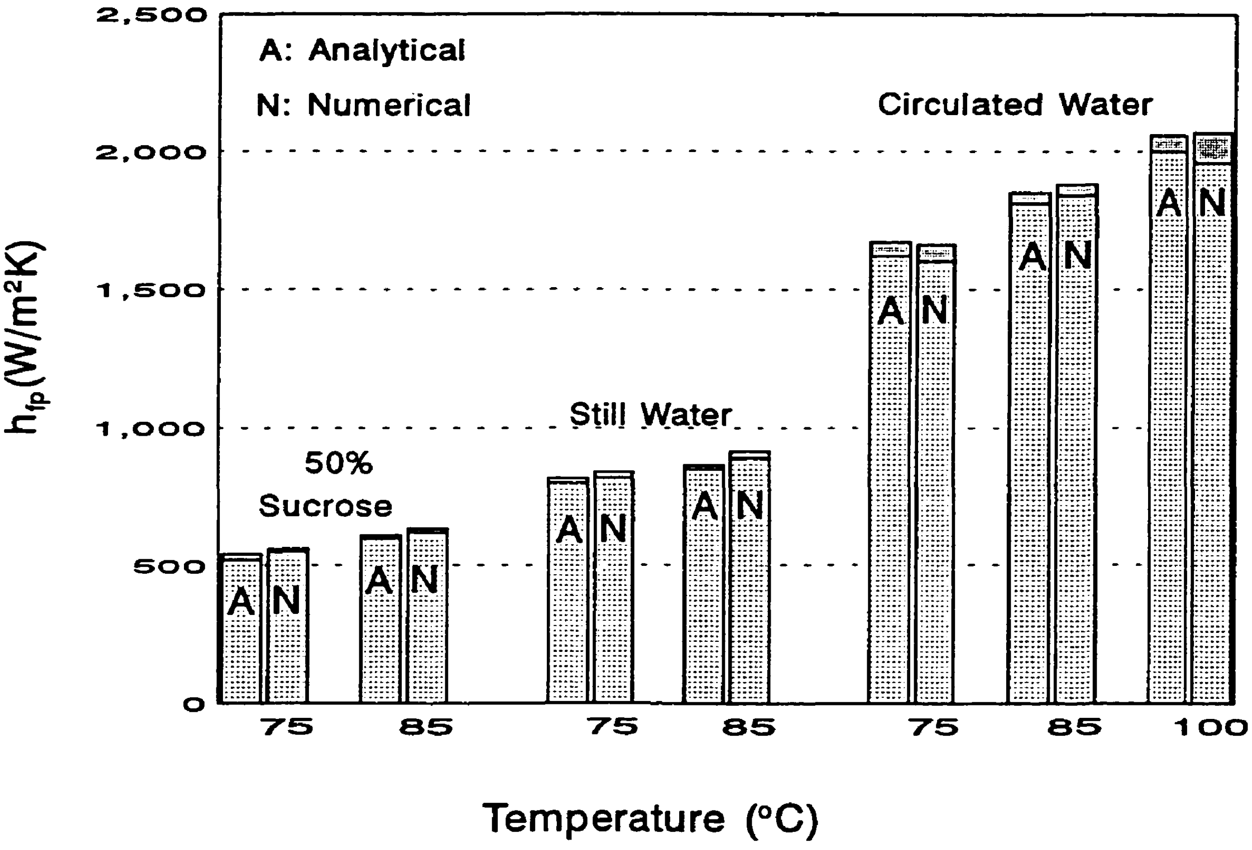

Figure 5.8. Values of h_{fp}, evaluated using analytical and numerical methods, in a water bath condition using still and circulated water as well as a sucrose solution as heating mediums, at different temperatures.

Verification of the calorimetric approach

Verification results for the computation of heat transfer coefficients and particle bulk temperatures using a thermocouple equipped particle and conventional and calorimetric techniques, are summarized in Table 5.2. The heating times refer to the times at which the particle was removed from the water bath and transferred to the calorimeter. Since time-temperature data were continuously recorded, for each treatment condition (*i.e.* heating times 10-25 s), the data could be analyzed to compute the associated f_h from which the h_{fp} values were calculated, using the analytical solution. These are indicated in the second column of Table 5.2. The values in parenthesis indicate the standard deviations in calculated h_{fp} from several replicates (minimum 6). In general, the associated variability was less than 10 %. The third column indicates the h_{fp} values computed from the numerical simulation by a trial and error technique, which resulted in a good match between experimental and predicted center point time-temperature profiles. Once again, there was a good match between the two sets of values, with an average difference of about 5 %, indicating good validity for the numerical approach. While evaluating h_{fp} values from the numerical technique, the mass average temperatures were also calculated for each treatment condition and these are shown as T_m values (forth column), which were then compared to the bulk temperatures (T_b) measured experimentally from the calorimetric technique. Once again, the maximum difference in particle bulk (mass average) temperature was 1.1 ^oC, which again provides good validity for the technique. Finally, the h_{fp} values were computed from the experimental T_b values using the numerical program and these are indicated in the last column. Overall, a less than 10 % variation was observed between the replicates, as well as between those calculated from the center point temperature data and bulk temperature using calorimeter.

The average h_{fp} over the different heating times was about 1000 W/m^2K, except for the very short heating time (10 s) which was just a little higher compared to the rest. This was probably due to a larger temperature gradient at the beginning of the heating, which caused the rapid change of boundary layer around the particle. Immersion of the particle into a fluid and taking it out again after a very short heating time, may generate

Table 5. 2. Comparing the fluid-to-particle heat transfer coefficient (h_{fp}, in W/m^2 K) and associated particle's bulk temperature (°C), numerically computed (T_m) and experimentally measured (T_b) for a 25.4 mm Aluminum particle heated in water at 85°C.

Time (s)	Analytical	Computed		Measured	
	$^{*}h_{fp}$	$^{**}h_{fp}$	T_m	T_b	$^{***}h_{fp}$
10	1180 (100)	1200 (60)	54.9 (0.5)	55.4 (1.7)	1260 (100)
15	980 (60)	920 (30)	57.5 (0.8)	58.1 (1.3)	930 (60)
20	1020 (80)	1000 (40)	64.0 (0.7)	65.1 (0.4)	1070 (30)
25	900 (60)	950 (20)	67.4 (0.7)	68.4 (0.5)	1010 (40)

Values are the average of 6 replicates and the standard deviation is given in the parenthesis.

* h_{fp} analytically calculated based on the real time-temperature data (heating rate index, f_h).

** h_{fp} numerically computed from the FDP to much the real time-temperature data, and then the associated particle's mass average temperature (T_b) was computed.

*** h_{fp} computed from the FDP based on the experimentally measured bulk temperature (T_b).

considerable turbulence around the particle in addition to the normal convection, and hence could result in a higher heat transfer coefficient at the beginning of heating. Aastrom and Bark (1994) also reported that the h_{fp} was not constant during the heating of the test particle in a fluid at rest. They studied the time dependency of the fluid-to-particle heat transfer coefficient and reported up to 2-5 times higher values of convective heat transfer coefficients at the initial phase of the heating.

h_{fp} under tube-flow condition: stationary and moving particle

The fluid-to-particle heat transfer coefficients, evaluated for the stationary particle placed at the bottom surface in the tube (thermocouple approach) as well as the moving particle (calorimetric approach) in tube-flow conditions, are shown in Figures 5.9 and 5.10. Experiments were repeated six times for each particle size and flow rate. Both averages of h_{fp} and the standard deviations for each particle size and flow rate are shown in Figures 5.9 and 5.10. Overall, the coefficients of variation were low, at less than 5%.

For the stationary particle, h_{fp} varied from 1200±30 W/m^2K for the small particle (19.1 mm in diameter) at the lowest flow rate (13 L/min) to 2100±50 W/m^2K for the largest particle (25.4 mm in diameter) at the maximum flow rate (19 L/min). The values of h_{fp} increased as particle size increased, at any given flow rate. This can be explained by the fact that the opening cross section area, also called the "projected area" for the flow, decreases as particle size increases since the tube diameter is constant. For any given flow rate, this could result in an increase in the relative velocity of fluid around the larger particle and hence an increase in h_{fp}. The same trend was observed for all cases involving different flow rates, under both stationary and moving particle conditions.

For the moving particle situation, involving similar experimental conditions, h_{fp} ranged from 1450±50 W/m^2K for the small particle size at the lowest flow rate to 2520±70 W/m^2K for the largest particle size at the maximum flow rate. Thus, slightly higher values of h_{fp}, at about 10-20%, were observed with the moving particle when compared to those associated with the stationary particle.

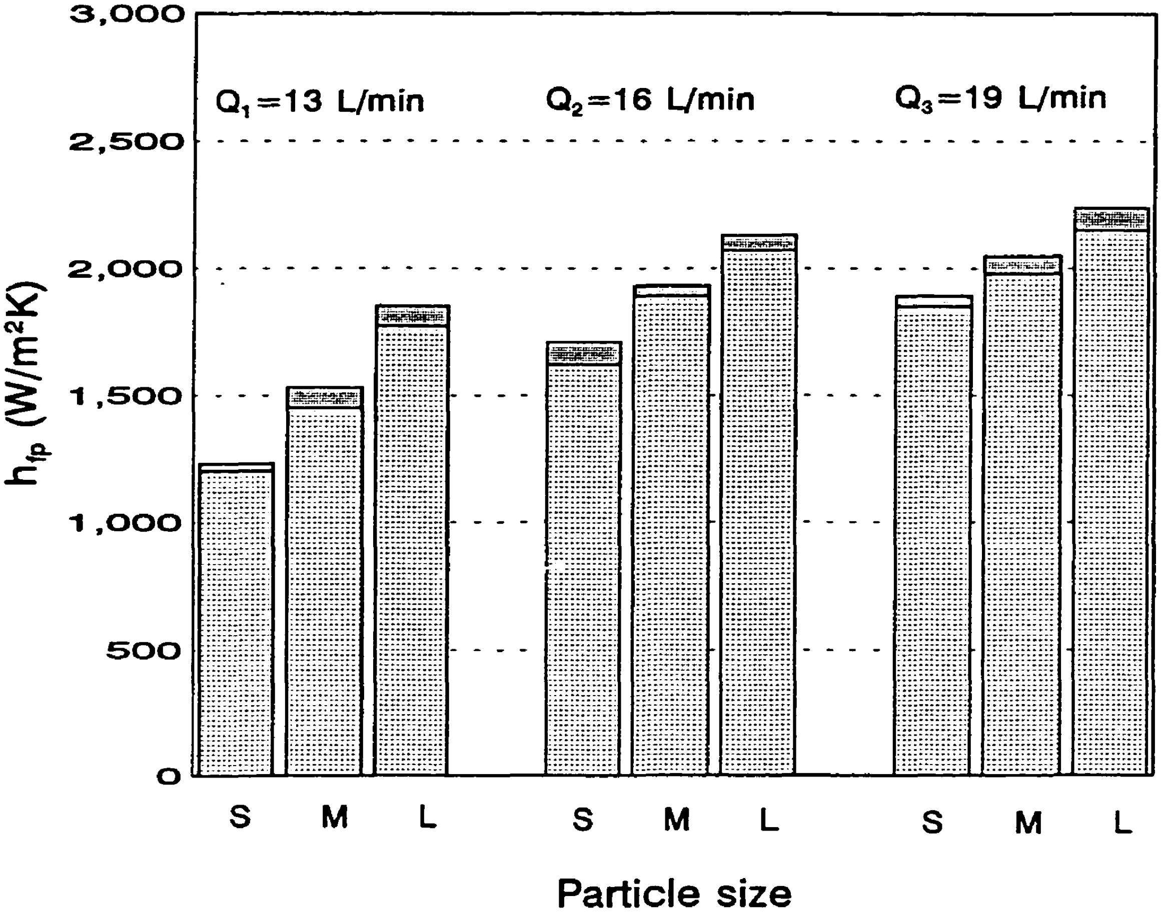

Figure 5.9. Values of h_{fp} for stationary particles of different sizes in tube-flow conditions at different flow rates (S: small, M: medium, L: large particles).

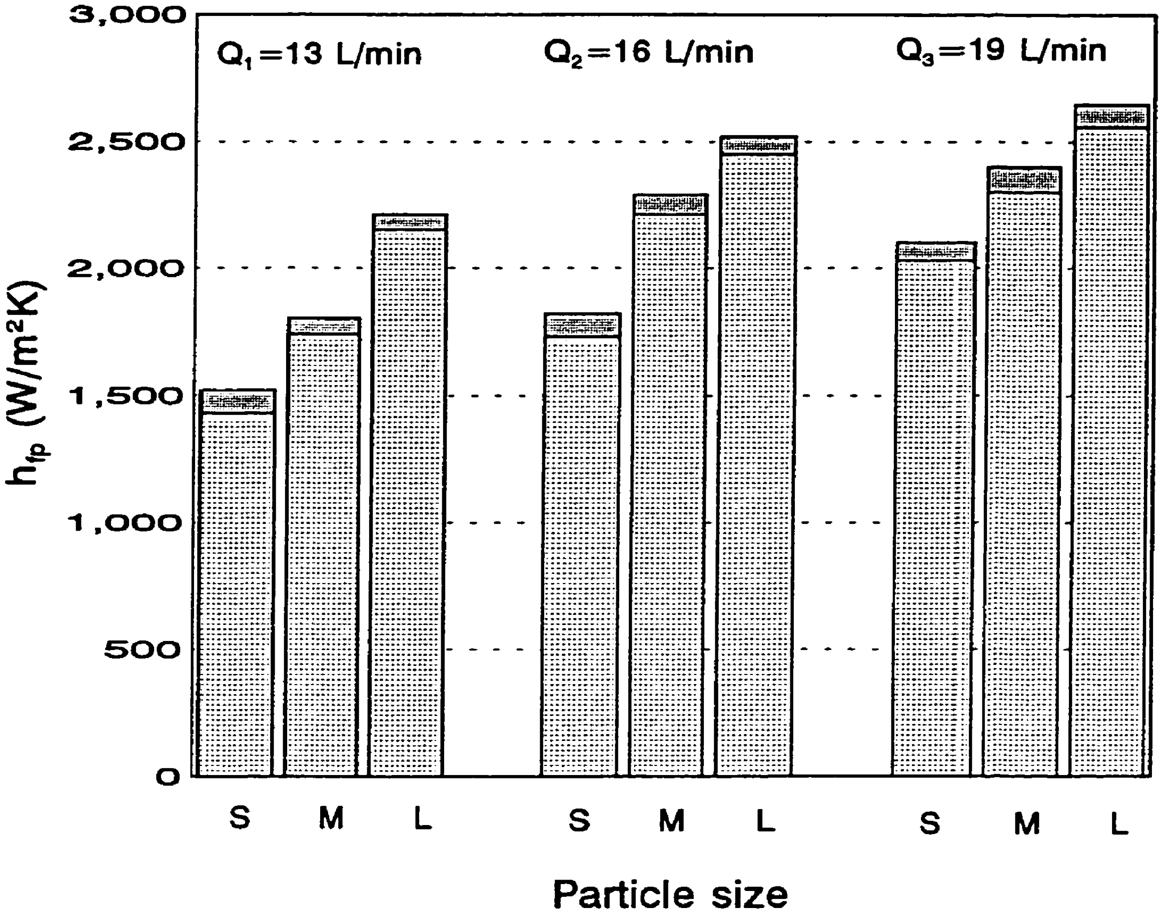

Figure 5.10. Values of h_{fp} for moving particles of different sizes in tube-flow condition at different flow rates (S: small, M: medium, L: large particles).

Higher values of h_{fp} in the moving particle condition were expected, due to the important effect of the particle rolling along the tube wall which affects the boundary layer surrounding the particle.

The results of this study are in agreement with what those reported by Sastry *et al.* (1990) and Zuritz *et al* (1990), who studied the effects of particle size and flow rate on h_{fp} using a moving thermocouple method. The authors reported that the values of h_{fp} increased with particle size and flow rate. However, Chandrana *et al.* (1988) and Ramaswamy *et al.* (1996), found h_{fp} increased with decreasing cube or cylinder size, while using the stationary particle technique. Also, Baptista *et al.* (1997) showed that both the relative fluid-to-particle velocity and the particle rotational velocity influenced the heat transfer coefficient, although it was not possible to individualize their single effect.

CONCLUSIONS

Preliminary studies indicated a good potential for Thermo-chromic Liquid Crystal (TLC) and relative velocity (RV) techniques for the evaluation of the fluid-to-particle heat transfer coefficient (h_{fp}) under tube flow conditions. However, the associated large variability in measurements has limited the scope of these techniques as reliable tools for evaluating the influence of factors affecting h_{fp}. A calorimetric technique was developed for evaluating h_{fp} under tube flow conditions. The technique gave h_{fp} values comparable to those from the more conventional methods and indicated trends of association with higher h_{fp} values at higher medium flow rates, lower viscosity and higher particle size. Values of h_{fp} for moving particles were found to be about 10-20% higher than those for the stationary particle under the same experimental conditions. The calorimetric method shows good potential for evaluating h_{fp} in continuous tube-flow applications because it permits the evaluation of h_{fp} under natural movement of particles in a carrier fluid.

PREFACE TO CHAPTER 6

In chapter 4, influencing factors associated with fluid-to-particle heat transfer coefficient (h_{fp}) was evaluated under different experimental conditions using the particle oscillatory motion technique involving direct temperature measurement. A calorimetric method, detailed in the previous chapter involving with bulk temperature measurement of a free particle, was subsequently developed to evaluate h_{fp} with particle undergoing more natural movement under tube-flow conditions.

There is a need for more data for the purpose of modeling. Factors influencing h_{fp} under tube-flow conditions were investigated in this chapter using the previously developed calorimetric technique. Such factors included: the flow rate of the carrier fluid, fluid viscosity and fluid temperature as well as the particle size

The results of this study were presented partially in the annual meeting of the Institute of Food Technologists (IFT) in 1998. A manuscript entitled "Evaluation of factors influencing tube-flow fluid-to-particle heat transfer coefficient using a calorimetric technique" was submitted for publication in the Journal of Food Engineering (Zareifard and Ramaswamy, 1999).

Experimental work and data analysis were carried out by the candidate, under the supervision of professor Ramaswamy. This will fulfil the third objective of the thesis and a modified version of the paper is presented here as the sixth chapter of the thesis.

CHAPTER 6

EVALUATION OF FACTORS INFLUENCING TUBE-FLOW FLUID-TO-PARTICLE HEAT TRANSFER COEFFICIENT USING A CALORIMETRIC TECHNIQUE

ABSTRACT

A previously developed calorimetric technique involving bulk or mass average temperature measurement of a moving particle without interfering its motion was used to evaluate the effect of fluid flow rate, viscosity and temperature as well as particle size on the associated fluid-to-particle heat transfer coefficient (h_{fp}) under tube-flow condition. Experiments were carried out for different flow rates (9 to 19 L/min), concentrations of carboxymethyl cellulose solution (CMC) in the carrier fluid (0 to 1 % CMC solution) and fluid temperature (50 to 70^{o}C) as well as Aluminum spherical particles of different sizes (19 to 25.4 mm). The results of over 300 experiments indicated that the h_{fp} values, which ranged from 650 to 2660 W/m^{2}K depending on the experimental conditions, increased significantly with an increase in fluid flow rate and particle size, and decreased with CMC concentration and temperature.

INTRODUCTION

Two of the important parameters influencing the process design for continuous tube-flow of liquid and particle mixture are the convective fluid-to-particle heat transfer coefficient (h_{fp}) and the residence time distribution (RTD). When a solid particle is introduced in to a moving fluid, the flow phenomenon and therefore the rate of heat penetration in to the suspended particle, becomes a function of the boundary layer surrounding the particle resulting in a thermal lag between the fluid and the particle surface. The thicker the boundary layer, the lower the rate of heat transfer. Information available in literature on h_{fp} associated with continuous flow systems is generally scarce, and often inconsistent or even contradictory, which has limited the commercial modeling of aseptic processing of particulate fluids (Larkin 1989, Chandarana and Gavin 1989, Lee and Singh 1990, Balasubramaniam and Sastry 1996; Ramaswamy *et al.* 1997). Literature data on heat transfer in continuous flow systems containing particulate indicate that h_{fp} is likely to be influenced by particle size and shape, particle and fluid thermo-physical properties, particle location, fluid-to-particle relative velocity, particle-to-tube diameter ratio, fluid viscosity and temperature (Ramaswamy *et al.*, 1997).

Researchers have tried to investigate the effect of some of the above mentioned parameters on the fluid-to-particle heat transfer coefficient using different means and methods. These methods partially simulated aseptic processing condition of particulate food. The available information with respect to evaluation of various factors influencing h_{fp} has been detailed in the literature review of the thesis (chapter 2) as well as chapter 4, and hence will not reproduced here.

The objective of this study was to apply a previously developed calorimetric technique (not used in any of the detailed studies reported so far) for evaluating the effect of different factors such as fluid flow rate, CMC concentration, temperature and particle size on the associated tube-flow fluid-to-particle heat transfer coefficient (h_{fp}). The particle is allowed to move in the tube without any interference using calorimetric technique. This technique shows good potential for evaluating h_{fp} under tube-flow applications permitting more natural movement of particles in a carrier fluid.

MATERIALS AND METHODS

The calorimetric method developed for the evaluation of fluid-to-particle heat transfer coefficient is detailed in chapter 5. Briefly, the technique consists of introducing a particle at an upstream location into a holding tube, in which a carrier fluid under pre-stabilized temperature and flow conditions is circulated, and retrieving it from a downstream location after a known time interval. The particle is transferred immediately into a specially constructed calorimeter and its bulk temperature is determined upon equilibration. Knowing the medium temperature, particle initial temperature, exposure time (residence time) and thermo-physical properties, the associated h_{fp} can be computed from the evaluated bulk temperature of the particle using an iterative numerical technique. The procedure involves numerical computation of bulk temperature (also known as mass average temperature) for a given heating time (residence time) using the available property data and an assumed h_{fp} value, and comparing it with the experimental value. Depending on whether the computed bulk temperature value is lower or higher than the experimental value, the assumed h_{fp} value is increased or decreased, and a new bulk temperature is computed. By trial and error this procedure is continued until the difference between the computed and experimentally measured bulk temperature is less than $0.05^{o}C$ and the converged value of h_{fp} so calculated is taken as h_{fp} for the test run. In order to be useful, it is necessary to carefully calibrate the calorimeter for the bulk temperature measurement and compare h_{fp} values with thermocouple equipped particles subjected to various time-temperature treatments.

Experimental setup

Figure 6.1 shows a schematic of the experimental setup used for the h_{fp} determination under continuous flow conditions. A steam-jacketed kettle was used to heat the carrier liquid to the desired temperature. The liquid was pumped using a variable-speed pump (Little Giant Pump Company, Oklahama City, OK) through a Pyrex glass tube (0.045 m inside diameter and 1.7 m in length) and recycled to the kettle.

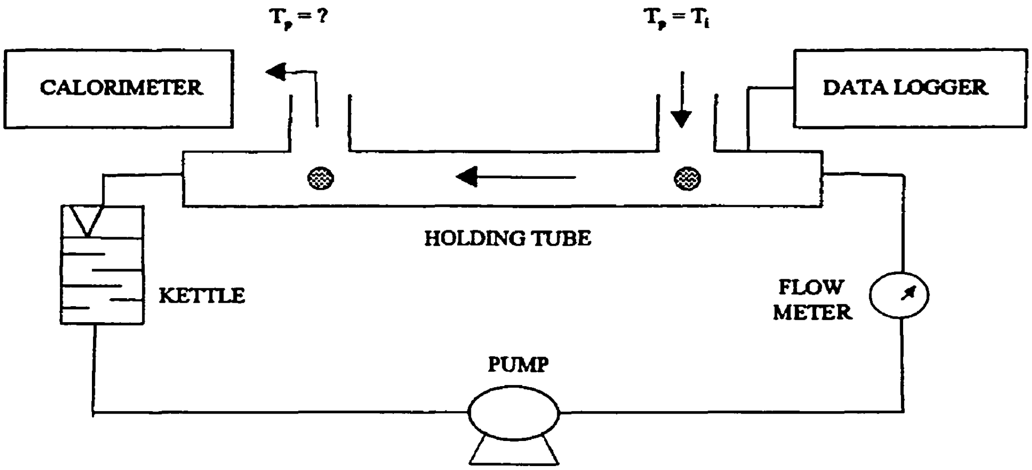

a) Experimental set up

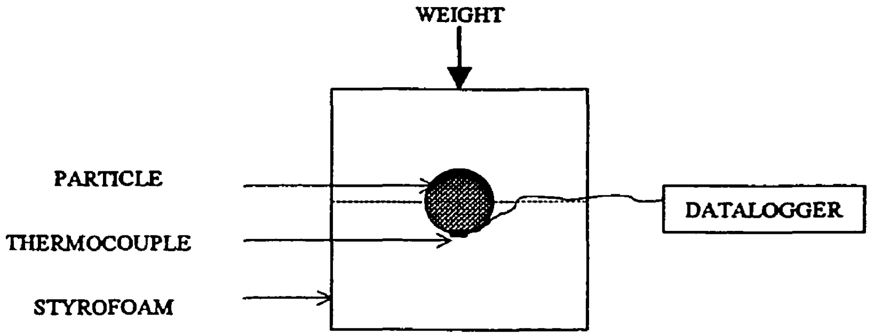

b) Styrofoam Calorimeter

Figure 6.1. Experimental set-up (a) and the calorimeter (b) for h_{fp} evaluation under tube-flow condition using calorimetric approach involving particle bulk or mass average temperature measurement.

T-joint intersections were installed on line to permit introduction and retrieval of the test particle through the system. A flow meter (Model FTB-5005, Omega Eng. Inc, Stamford, CT) installed on line measured the flow rate.

A single particle, at a uniform initial temperature, was introduced in to the system through the entrance port of the holding tube and the time was noted. When the particle reached the second port, it was retrieved quickly using a special perforated plastic scoop and immediately transferred to a custom moulded Styrofoam calorimeter for the measurement of particle bulk temperature. The time at which the particle was transferred was noted as well as the time interval to pass a preset distance between the entry and exit ports to determine the particle residence time and particle velocity.

Test particles and CMC preparation

Aluminum spherical particles (Small Parts Inc., Miami lakes, FL) of three sizes (19.05, 22.22 and 25.4 mm in diameter named, respectively, as small, medium and large particle) were used as test particles in a Pyrex glass holding tube of 45 mm inside diameter. Thermo-physical properties of test particles were: density (ρ)=2707 kg/m^3, heat capacity (C_p)=896 J/kg K, thermal conductivity (k)=204 W/m K (Holman, 1990), and thermal diffusivity calculated as $\alpha = k/\rho\ C_p = 8.42\text{x}10^{-5}$ W/m^{2}K. Water and commercial carboxymethyl cellulose (CMC, Sigma Chemicals, St. Louis, MO) of three concentrations (0.25, 0.5 and 1 % w/w) were used as carrier fluids. CMC solutions were prepared by slowly adding the known amount of CMC powder to distilled water while continuously mixing using an electrically operated portable hand mixer. The solution was then thoroughly mixed using a variable speed mixer (Hobert Model D-300, Hobert Canada Inc., Mississauga, ON) to complete the dissolution of CMC. The solution was left for 24 hours to release air bobbles and also to ensure total dispersion of the powder.

Rheological and thermal properties of carrier fluid

Rheological data were obtained using a rotational viscometer Model RV20 (Haake Mess-Technik, Karlsruhe, Germany) coupled to an M-S OSC measuring head and a D100/300 sensor system assembly interfaced to a microcomputer for control and data acquisition as detailed in Abdelrahim and Ramaswamy (1995). The rheograms were characterized using the classical power law model. By plotting the logarithmic values of shear stress (τ in Pa) versus shear rate ($\dot{\gamma}$ in s^{-1}) and taking the regression over the straight portion of the plot, the power law parameters, consistency coefficient (m in Pa.s^n) and flow behavior index (n, dimensionless) were evaluated:

$$\tau = m \ \dot{\gamma}^{n}$$

The maximum duration of a set of experiments was about 3 hours. During this period, the prepared solution of CMC was continuously circulated through the system stabilizing it for testing at a constant temperature and a constant flow rate. Samples of CMC solutions taken after every each hour of processing were also evaluated for rheological characteristics to make sure the computed m and n values did not change more than 5% during testing.

Thermal conductivity (k_f) and specific heat (C_p) of the solution were estimated using the correlation proposed by Singh and Heldman (1993):

$$k_f = (326.575 + 1.0412\ T_f - 0.00337\ T_f^{\ 2})(\ 0.796 + 0.00934\ \%W)10^3$$

$$C_p = 1.675 + 0.025\ (\ M\%)$$

where T_f is the temperature (^oC) and %W is the percentage moisture content of the fluid.

Test conditions

To study the effect of influencing factors on h_{fp}, a set of experiments was first carried out with water as the carrier fluid at a constant temperature (70^{o}C). In this set of experiments, three flow rates (2.17, 2.67 and 3.17 x10^{-4} m^3/s or 13, 16, 19 L/min) and three particle sizes (19.05, 22.22 and 25.4 mm) were employed. The distance between the entry and exit ports was set to make sure the particle temperature after exit point would be sufficiently below the fluid temperature for accurate data interpretation. Additional tube lengths were provided before and after the test section to minimize fluid disturbance. A minimum flow rate was selected in a way that even the smallest particle would move smoothly in the tube during experiment. Experiments were repeated at least four times for each treatment.

Experiments were also carried out using a non-Newtonian fluid (carboxymethyl cellulose solution, CMC) at different concentrations and temperatures as carrier medium. For this fluid, another set of experiments was carried out with four factors: flow rate, CMC concentration and temperature as well as particle size (flow rate: 1.50, 1.83, 2.17, 2.67 $\times 10^{-4}$ m^3/s corresponding to 9, 11, 13, 16 L/min; CMC concentration: 0.25, 0.5 and 1 %; fluid temperature: 50, 60 and 70°C; and particle sizes: 19.05, 22.22 and 25.4 mm in diameter). Experiments were again repeated at least four times. Due to the difficulties in achieving desired particle motion, the highest flow rate was used only for the lowest concentration and the lowest flow rate for the highest concentration. The intermediate flow rates were used for all concentrations. In all, over 300 experiments were carried out with water and different concentrations of CMC solutions as the carrier fluid.

Statistical analysis

SAS computer program (SAS Institute Inc. 1997) and generalized linear modeling (GLM) procedure were used to study the effects of individual factors (flow rate, particle size, fluid concentration and temperature) and their interaction on the associated fluid-to-particle heat transfer coefficient by analysis of variance (ANOVA). Also, using the same statistical program, least-significant-difference (LSD) grouping tests were performed to see if, statistically, there were significant differences among the means of the variables under investigation.

RESULTS AND DISCUSSION

Rheological properties of carrier fluids

Rheological properties of the CMC solutions were determined using a rotational viscometer for each set of experiments. A typical rheogram (shear stress versus shear rate) involving a programmed shear rate from 0-500 s^{-1} in 10 min (upward curve) followed by a steady shear at 500 s^{-1} for 20 min (stress decay curve) and by a programmed downward shear from 500-0 s^{-1} for 10 min (downward curve) is shown in Figure 6.2 for 1% CMC solution at different temperature. Mean computed values and standard deviations of consistency coefficients (m) and flow behavior indices (n) for different CMC solutions of different concentrations at different temperature are summarized in Table 6.1. The consistency coefficient increased with CMC concentration and decreased with temperature. The flow behavior index showed the opposite trend.

Rheological properties of CMC solutions were also determined after every hour of processing to see whether significant changes took place during a given run. Typical mean values and standard deviations for three replicates of consistency coefficient (m in $Pa.s^n$) and flow behavior index (n) are given in Table 6.2 after 1, 2 and 3 hours of processing of the solution. No significant differences ($p>0.05$) were observed for the rheological parameters for the duration of the experiment. The stress decay behavior shown in Figure 6.2 (middle part) also confirms that during steady shear, the CMC solution viscosity was relatively stable.

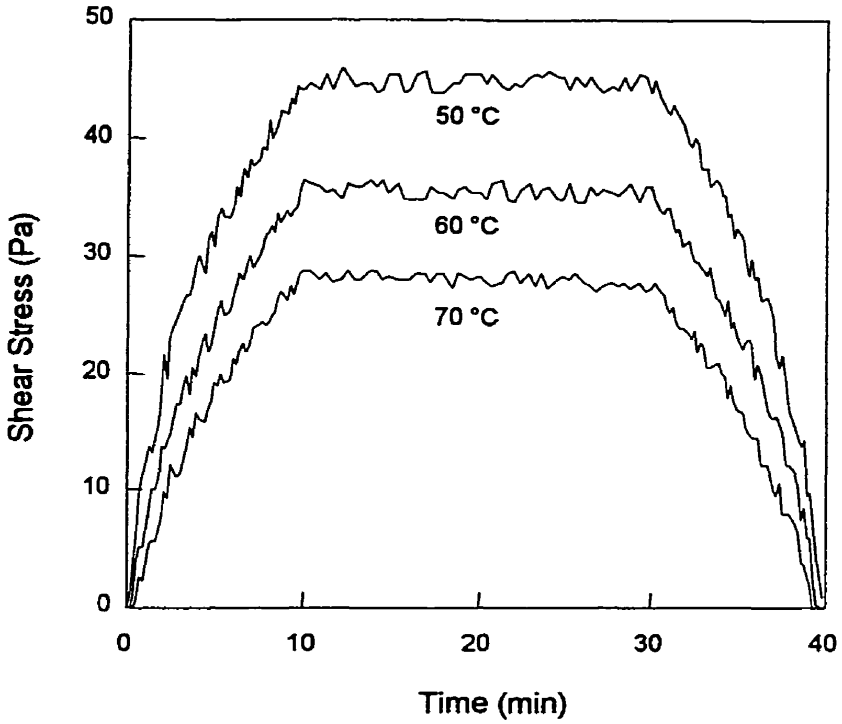

Figure 6.2. Typical shear stress versus time curves for 1% CMC solution at different temperatures under a programmed shear linearly increasing from 0 to 500 s^{-1} for 10 min followed by a steady shear at 500 s^{-1} for 20 min and a subsequent downward shear from 500 to 0 s^{-1} in the final 10 min.

Table 6.1. Power law model parameters of CMC solutions for different concentration and temperature were determined using a rotational viscometer.

CMC %	Temp °C	m Pa.s^n	n
0.25	50	0.150 ± 0.031	0.785 ± 0.030
0.25	60	0.052 ± 0.018	0.821 ± 0.015
0.25	70	0.011 ± 0.028	0.976 ± 0.021
0.50	50	0.510 ± 0.020	0.590 ± 0.011
0.50	60	0.252 ± 0.033	0.681 ± 0.026
0.50	70	0.115 ± 0.045	0.754 ± 0.017
1	50	1.715 ± 0.151	0.560 ± 0.019
1	60	1.191 ± 0.101	0.510 ± 0.029
1	70	0.778 ± 0.082	0.583 ± 0.031

Results are means ± standard deviations of three replicates ($\tau = m \dot{\gamma}^n$; m: consistency coefficient and n: flow behavior index).

Table 6.2. Power law rheological parameters of 1% CMC solution at 50 °C for different duration of experiments.

Duration of Experiment	Temp. °C	m (Pa.s^n)	n
1 hr	50	1.714±0.103 ^{a}	0.566±0.011 ^{b}
2 hr	50	1.729±0.151 ^{a}	0.570±0.019 ^{b}
3 hr	50	1.703±0.016 ^{a}	0.563±0.017 ^{b}

Results are means ± standard deviations of 3 replicates ($\sigma = m \dot{\gamma}^n$; m: consistency coefficient and n: flow behavior index). Means within a column showing the same letter superscription are not significantly different from each other ($\rho > 0.05$).

Fluid-to-particle heat transfer coefficient

Means and standard deviations of fluid-to-particle heat transfer coefficient, h_{fp}, as influenced by flow rate, particle size, CMC concentration and temperature are given in Tables 6.3 to 6.6. Depending on the experimental condition, values of h_{fp} varied from 1400 to 2600 W/m^2 K for water as the carrier medium and from 600 to 1400 W/m^2K for different concentration of CMC solutions. In general, results were very consistent and variations among the mean were less than 5%. The analysis of variances (ANOVA) results for individual factors (independent variables) - fluid flow rate, CMC concentration, temperature and particle size as well as their interactions, on the heat transfer coefficient (dependent variable) are summarized in Table 6.7. The model was significant ($p<0.05$) with an associated R^2 value greater than 0.99. Statistical analysis indicated that all individual factors and their two way interactions significantly ($p<0.05$) influenced the h_{fp}, but not the three way interactions. T-test grouping using least-significant-difference (LSD) procedure indicated significant differences ($p<0.05$) among the means and the mean values of h_{fp} increased with increasing flow rate and particle size, and decreased with increasing CMC concentration and temperature (Table 6.8).

Influence of flow rate and particle size on h_{fp}

There were some difficulties with respect to achieving the desired particle motion in the tube. At the lower viscosity (0 % CMC, *i.e.*, water) a higher flow rate was required to let the particle move in the holding tube. Therefore, the fluid flow rate was a limiting factor with respect to the smallest particle with water as the carrier medium. The flow rate could be decreased at high levels of CMC concentration. The higher drag force associated with the higher viscosity perhaps facilitated moving of the particle even at lower fluid flow rates. For the above reasons, it was not possible to run the experiments while using water as the carrier medium at flow rates less than 13 L/min. The maximum flow rate was 19 L/min with water, which was too high for CMC solution. The minimum flow rate was 9 L/min and maximum 16 L/min with 1% CMC solution. Experiments were carried out for three particle sizes (small, medium and large; 19.05, 22.22 and 25.4 mm respectively) at each flow rate.

Table 6.3. Values of h_{fp} (W/m ^{2} K) associated with different spherical particles at various fluid flow rates and CMC concentrations at 70 °C.

Flow Rate (l/min)	Particle size	% of CMC concentration 0	0.25	1
19	s	2030±70		
	m	2300±60		
	l	2660±90		
16	s	1730±90	1240±40	
	m	2150±80	1320±20	
	l	2550±60	1350±30	
13	s	1430±50	1000±10	740±20
	m	1730±60	1070±40	810±10
	l	2200±60	1140±40	890±20
11	s		880±20	680±10
	m		930±20	720±10
	l		980±10	840±10
9	s			650±10
	m			700±10
	l			750±10

Values are the means of four replicates ± standard deviation.
s: small; m: medium; l: large

Table 6.4. Values of h_{fp} ($W/m^2 K$) associated with different particle size, fluid concentration and temperature at a constant flow rate.

Flow Rate l/min	Particle size	Temp. °C	% CMC Concentration		
			0.25	0.5	1
11	s	50	920 ± 20	790 ± 20	750 ± 30
	m		960 ± 10	880 ± 10	860 ± 10
	l		980 ± 10	950 ± 10	900 ± 10
	s	60	890 ± 20	770 ± 10	710 ± 10
	m		990 ± 20	830 ± 10	780 ± 10
	l		1020 ± 10	930 ± 10	870 ± 10
	s	70	880 ± 20	750 ± 10	680 ± 10
	m		930 ± 20	810 ± 20	720 ± 10
	l		980 ± 10	900 ± 10	840 ± 10

Values are the means of four replicates ± standard deviations. s: small ; m: medium; l: large.

Table 6.5. Values of h_{fp} ($W/m^2 K$) associated with different fluid flow rates and particle sizes at 0.25 % CMC concentration but different temperatures.

CMC %	Particle size	Temp. °C	Fluid flow rate (l/min)		
			11	13	16
0.25	s	50	920 ± 20	1090 ± 20	1310 ± 20
	m		960 ± 10	1100 ± 20	1420 ± 50
	l		980 ± 10	1190 ± 10	1490 ± 60
	s	60	890 ± 20	1070 ± 10	1260 ± 20
	m		990 ± 20	1120 ± 40	1310 ± 20
	l		1020 ±10	1180 ± 30	1390 ± 30
	s	70	880 ± 20	1000 ± 10	1240 ± 40
	m		930 ± 20	1070 ± 40	1320 ± 20
	l		980 ± 10	1140 ± 40	1350 ± 30

Values are the means of four replicates ± standard deviations. s: small ; m: medium; l: large

Table 6.6. Values of h_{fp} (W/m^2 K) associated with different fluid flow rates and particle sizes at 1% CMC concentration but different temperatures.

CMC %	Particle size	Temp. °C	Fluid flow rate (l/min)		
			9	11	13
1	S	50	740 ± 20	750 ± 30	890 ± 20
	M		800 ± 20	860 ± 10	910 ± 20
	L		870 ± 20	900 ± 10	1020 ± 30
	S	60	680 ± 10	710 ± 10	820 ± 10
	M		730 ± 10	780 ± 10	870 ± 10
	L		800 ± 10	870 ± 10	970 ± 10
	S	70	650 ± 10	680 ± 10	740 ± 20
	M		700 ± 10	720 ± 10	810 ± 10
	L		750 ± 10	840 ± 10	890 ± 20

Values are the means of four replicates ± standard deviations. .s: small ; m: medium; l: large.

Table 6.7. Analysis of variances (ANOVA) of factors influencing the fluid-to-particle heat transfer coefficient, h_{fp}.

Source	DF	SS	Mean Square	F Value	Pr > F
F	4	2010807.808	502701.952	414.20	0.0001
C	3	9621009.621	3207003.207	2642.43	0.0001
S	2	2116575.694	1058287.847	871.98	0.0001
T	2	387916.667	193958.333	159.81	0.0001
F*C	2	83167.376	41583.688	34.26	0.0001
F*S	8	47644.444	5955.556	4.91	0.0001
F*T	6	36682.037	6113.673	5.04	0.0001
C*S	6	992485.298	165414.216	136.29	0.0001
T*C	4	30286.508	7571.627	6.24	0.0001
T*S	4	2733.333	683.333	0.56	0.6897
F*C*S	4	873.050	218.262	0.18	0.9487
F*T*S	12	25596.296	2133.025	1.76	0.0568
T*C*S	8	7544.444	943.056	0.78	0.6234
F*T*C*S	6	8537.500	1422.917	1.17	0.3221

F: Flow Rate; C: CMC Concentration; S: Particle Size; T: Temperature.

Table 6.8. T-test grouping for the levels of influencing factors on mean values of fluid-to-particle heat transfer coefficient (h_{fp}.in W/m^2 K).

F: Flow Rate (L/min)

T Grouping	Mean	F
A	2327.500	19
B	1546.250	16
C	1106.786	13
D	870.185	11
E	747.222	9

Least Significant Difference = 17.155

S: Particle Size (mm)

T Grouping	Mean	S
A	1205.313	25.4
B	1090.729	22.2
C	995.625	19.1

Least Significant Difference = 10.005

C: CMC Concentration (%)

T Grouping	Mean	C
A	2080.278	0
B	1139.259	0.25
C	853.889	0.5
D	808.611	1

Least Significant Difference = 13.34

T: Temperature (°C)

T Grouping	Mean	T
A	1005.952	50
B	952.976	60
C	913.095	70

Least Significant Difference = 10.147

Means (h_{fp} in W/m^2 K) with the same letter are not significantly different at level α=0.05.

The mean values and standard deviations of h_{fp} for different flow rates, fluid concentrations and particle sizes are given in Table 6.3. In general, values of h_{fp} varied from 650 W/m^2K for the small particle in 1% CMC solution to 2660 W/m^2K for the large particle in water. The effect of particle size and flow rate on h_{fp} are shown in Figure 6.3a for water, Figure 6.3b for 0.25 % CMC and Figure 6.3c for 1% CMC solution as the carrier fluid. h_{fp} values increased with particle size and flow rate with each carrier fluid. The values varied from 1430 to 2660 W/m^2K for water, 860 to 1350 W/m^2K for 0.25% CMC and 650 to 890 W/m^2K for 1% CMC solution, thus showing a decreasing trend in h_{fp} with increasing viscosity. This can be explained by the fact that as the particle size increases, the cross sectional area available for the fluid flow decreases resulting in a local increase in the fluid velocity around the particle. This will result in an enhanced heat transfer coefficient since the thermal boundary layer thickness around the particle surface effectively decreases at higher flow rates. However, this increase seems to be somewhat dampened at higher viscosity levels, *i.e.* at high CMC concentration, providing an interaction effect between the particle size and CMC concentration. For example while using water at 70^oC as the carrier fluid at 13 L/min flow rate, h_{fp} increased by about 30% as particle size increased from small to large, for the same flow rate and same fluid temperature, h_{fp} increased just by 17% with 1% CMC solution (Table 6.3).

With respect to the flow rate, as expected the heat transfer coefficient increased significantly as flow rate increased. Figure 6.4 shows the effect of flow rate at different levels of CMC concentration with a constant particle size (large particle d=25.4 mm). As can be expected, an increase in fluid flow rate results in an increase in particle velocity and enhances the heat transfer coefficient. With 1% CMC solution as the carrier fluid and a large particle, the particle linear velocity (v_p=distance/time) increased from 0.06 to 0.09 m/s as the flow rate increased from 9 to 13 L/min. The higher particle linear velocity also tend to increase the particle angular velocity (number of rotation per unit time, $\omega=v/r$) which contributes to further enhance the heat transfer coefficient (Baptista et al., 1997, Chakrabandhu and Singh 1998).

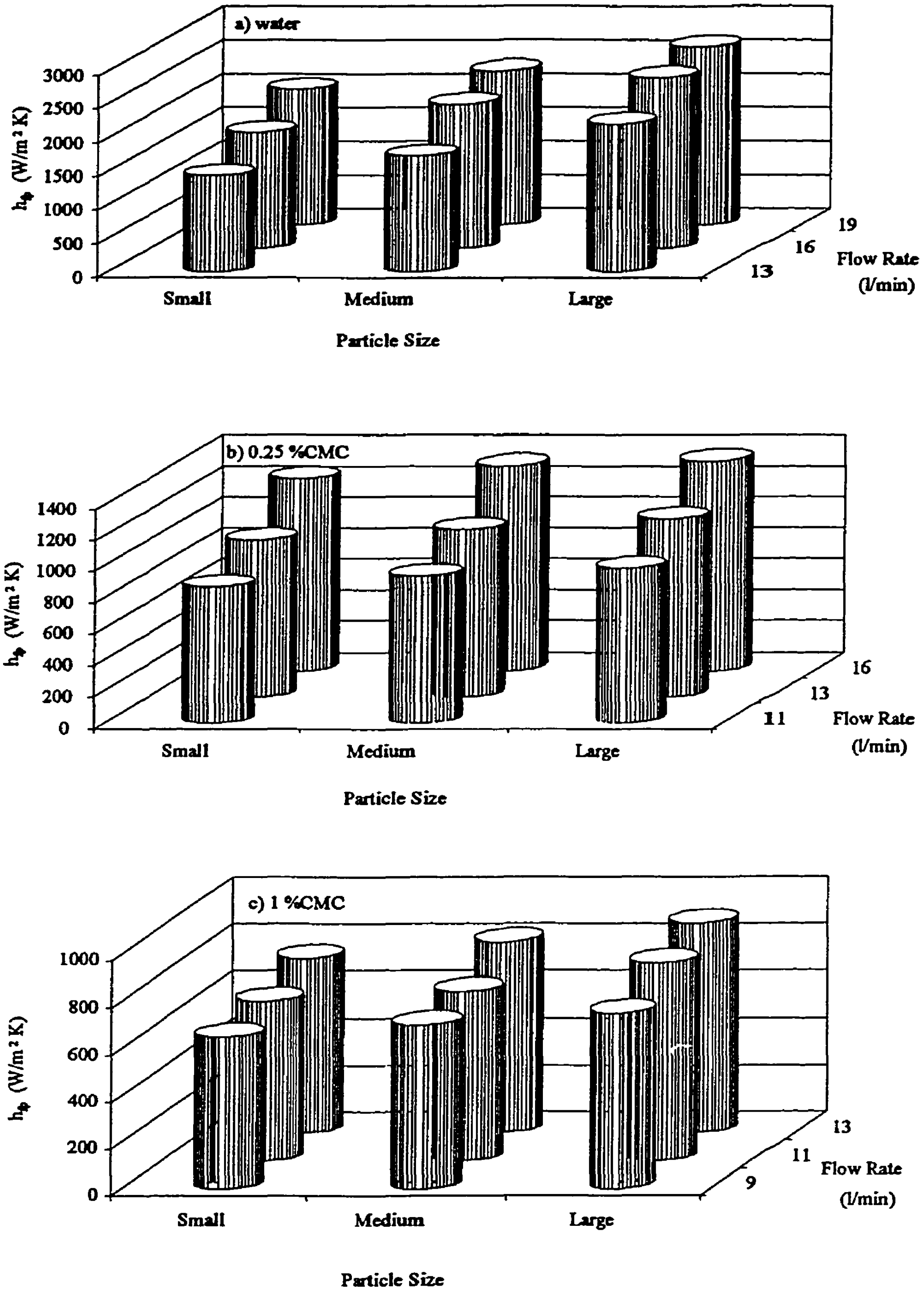

Figure 6.3. Effect of flow rate and particle size on fluid-to-particle heat transfer coefficient using different media as carrier fluid: a) water, b) 0.25% CMC, c) 1% CMC solution at 70°C.

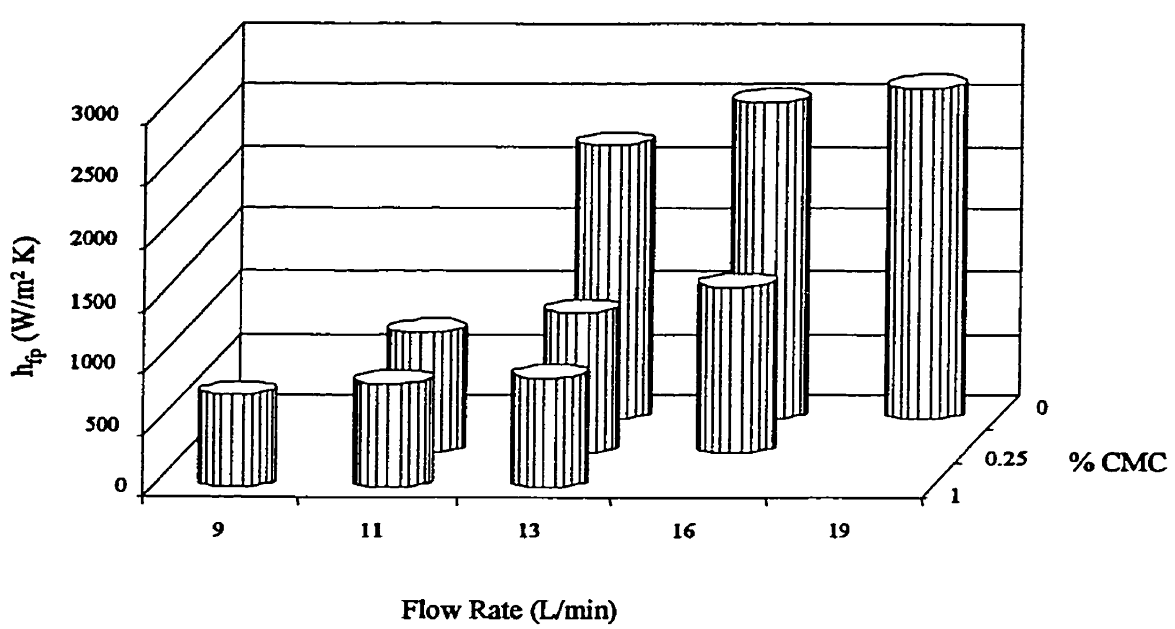

Figure 6.4. Effect of flow rate and carrier fluid viscosity (% CMC concentration) on fluid-to-particle heat transfer coefficient (h_{fp}) for a given particle size (d= 25.4 mm).

This trend was observed clearly under all concentrations of CMC solution. The effect of flow rate on h_{fp} is consistent in the literature, no mater which technique or what carrier fluids have been used: higher the fluid flow rate, higher the h_{fp}.

However, with regard to the particle size or particle to tube diameter ratio (d/D), there are some contradictory reports (Ramaswamy *et al.*, 1997). The results of the present study are in agreement with Sastry *et al.* (1990) who reported, using a moving thermocouple method for spherical particles, that h_{fp} increased with increasing particle size. Sastry *et al.* (1990) pointed out that as the particle size increases, the presence of the wall becomes a contributing factor because part of the particle comes into contact with the slow-moving fluid within the laminar sub-layer whereas other portions stay with the faster-moving fluid. However, the present findings are in contrast to the result of Zitoun and Sastry (1994b) who, using the same technique but cubical particles, reported the opposite trend and assigned it to differences in flow regime and particle shape. Balasubramaniam and Sastry (1994b) reported an increase in h_{fp} with increasing particle size, using a liquid crystal technique, but reported that particle size effects were not so clear cut while using the moving thermocouple method due to the lack of control over the radial location. Zuritz *et al.* (1990) also reported an increase in heat transfer coefficient with an increasing spherical particle size, where as Chandarana *et al.* (1988) found the heat transfer coefficient to decrease with increasing cube size. Using finite cylinders (diameter ranging from 15.9 to 25.4 mm and 25.4 mm length) in two holding tube of diameters 50.8 and 76.2 mm, Ramaswamy *et al.* (1996) found no clear-cut effect of particle-to-tube diameter; however, the heat transfer coefficient was found to increase with decreasing particle size. Awuah *et al.* (1996) reported slightly higher values of h_{fp} for potato particles as compared with Teflon particles while both followed the same conventional trend with respect to the effect of flow rate and fluid viscosity; h_{fp} values increased as flow rate increased or viscosity decreased. Also, in a study comparing h_{fp} evaluation based on two analytical methods (rate and ratio methods) using transient time-temperature data obtained from regular objects, Awuah *et al.* (1995) reported different values of h_{fp} for particles of different shapes and material, but of the same size.

Effect of CMC concentration and temperature

CMC concentration is another important factor, besides the flow rate, which can affect the fluid viscosity, particle velocity and hence the associated convective heat transfer coefficient in continuous flow system containing particulate. Higher viscosity, associated with carrier fluid at higher CMC concentration, is expected to retard the rate of heat transfer. The effect of fluid viscosity on h_{fp} for forced convection has been reported in several studies (Chnadarana *et al.* 1988; Zuritz *et al.*, 1990; Kelly *et al.* 1995; Balasubramaniam and Sastry, 1996; Bhamidipati and Singh 1995; Ramaswamy *et al.* 1996; Zareifard and Ramaswamy 1997; Baptista *et al.*, 1997 and Mankad *et al.* 1997). The higher viscosity of the fluid, in which a particle is immersed, hampers heat transfer, at least when the low turbulence decreases the effective relative particle-to-fluid velocity at the interface (Maesmans *et al.* 1992). The means and standard deviations values of h_{fp} associated with different particle sizes at a constant flow rate are given in Table 6.4 for different levels of CMC concentrations and different fluid temperatures. The values of h_{fp} varied from 680 W/m^2K for the small particle and 1% CMC to 1020 W/m^2K for the large particle and 0.25% CMC. The effect of particle size and levels of CMC concentration are shown in Figure 6.5a, and Figure 6.5b for flow rates of 11 and 13 L/min, respectively.

As can be see, the effects are clear - the heat transfer coefficient decreases as fluid viscosity (% CMC) increases or particle size decreases. This is in agreement with several other studies which confirm lower heat transfer coefficient with more viscous carrier fluids (Zuritz *et al.* 1990; Gaze *et al.* 1990; Balasubramaniam and Sastry 1994a,b; Kelly *et al.*, 1995, Chen *et al.* 1996; Awuah *et al.* 1995).

With respect to the temperature effect, it is generally recognized that viscosity decreases as the fluid temperature increases which should be expected to result in an enhanced convective heat transfer coefficient. Some data on temperature effect under different conditions are given in Table 6.4. Additional data on h_{fp} associated with different particle sizes and fluid flow rate as influenced by temperature is given in Table 6.5 for 0.25% CMC and in Table 6.6 for 1% CMC solution.

The analysis of variance results for the pooled data (Table 6.8) indicates that h_{fp} values decrease at higher temperatures, contrary to common expectations. Since viscosity decreases at higher temperature, it should be apparent that there is direct relationship between h_{fp} and viscosity, with higher values associated with higher viscosity. However, it should also be recognized that there may be other factors or interactions (fluid velocity, particle size, CMC concentration) which may counter-balance the temperature effect on h_{fp}. In addition, the particle velocity and/or particle-to-fluid relative velocity also influence h_{fp}. Higher particle velocities and higher particle-to-fluid relative velocities will result in higher value of h_{fp}.

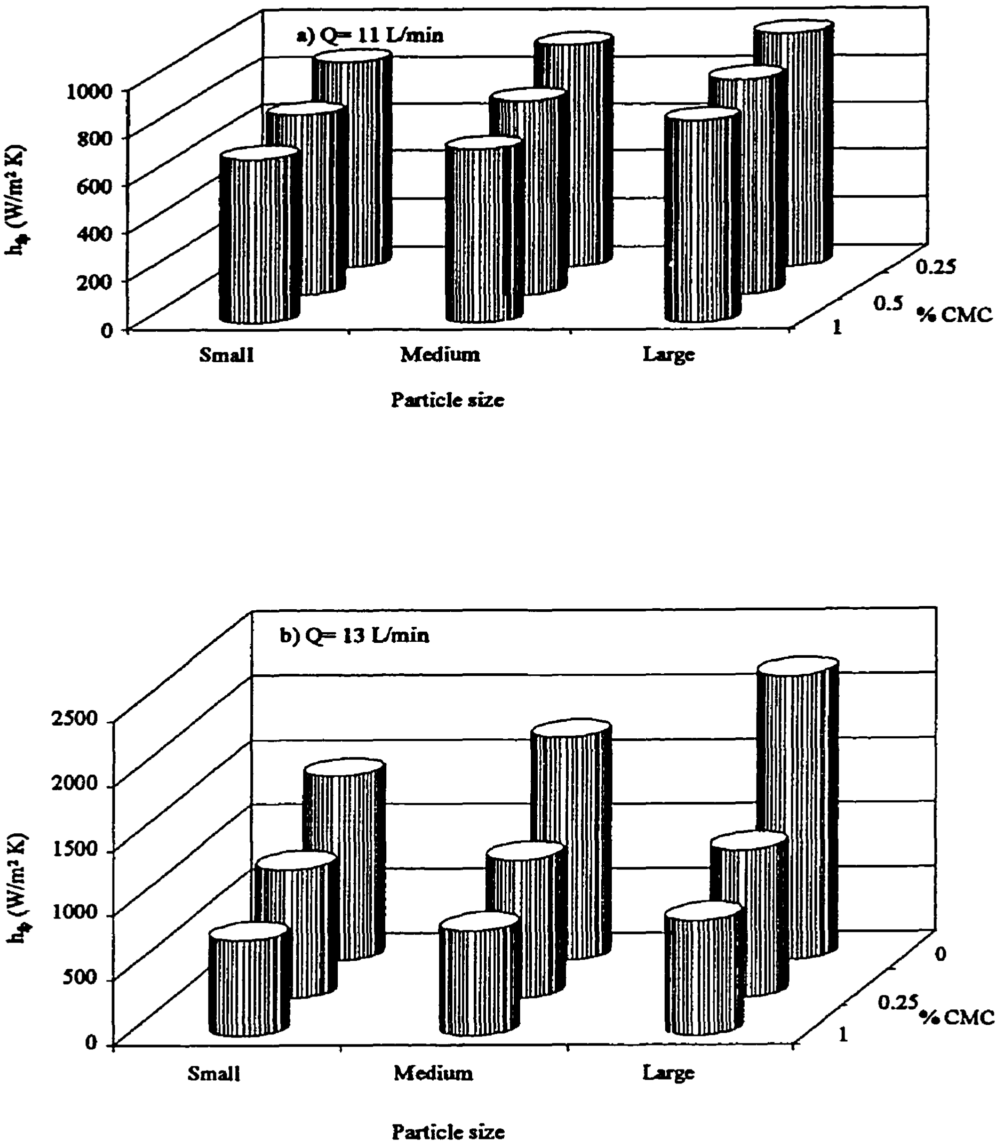

Figure 6.5. Effect of particle size and carrier fluid viscosity (% CMC concentration) on fluid-to-particle heat transfer coefficient at two fluid flow rates: a) Q=11 L/min; b) Q=13 L/min.

In the experimental set-up, the fluid velocity, CMC concentration, temperature and particle size could be set at appropriate set levels, but the particle velocity was somewhat variable and not well controlled. The particle velocity increased with particle size, fluid flow rate and CMC concentration, but decreased as the temperature increased (due to lowering of viscosity) – a trend also observed with h_{fp}. The temperature effect on particle velocity also depended on CMC concentration (or initial viscosity level). Results indicated that changing fluid temperatures affected h_{fp} values more so at higher CMC concentration, but this effect seemed to be tapering off at lower CMC concentration (Table 6.4).

The simple explanation to this unusual behave could be the particle velocity. At the lower temperature, the increased viscosity of the fluid results in a higher drag force and hence results in a higher particle velocity. For example with 1% CMC (fluid flow rate 13 L/min) the velocity of the large particle decreased from 0.092 m/s at 50°C to 0.086 at 60°C and to 0.079 at 70°C. Decreasing the particle velocity by about 20% caused a 10% reduction in h_{fp}. It seems that temperature effect on lowering of particle velocity was more dominant than other factors, which affected the h_{fp}. These results are in agreement with those of Dutta and Sastry (1990) who suggested that the most critical factor affecting particle velocity and, hence h_{fp}, is the fluid viscosity. Chakrabandha and Singh (1998) also reported that rotational velocity of particle significantly decreased as the fluid temperature increased. Other factors, like particle size, shape, fluid and particle density also affect particle velocity.

Studying the effect of temperature and viscosity together is somehow confusing and more complicated. Particle velocity is viscosity dependent and viscosity is temperature dependent. The more viscous the fluid, the higher the particle velocity. And higher the temperature, lower is the viscosity. Hence, at higher temperature h_{fp} is expected to be decrease as a result of lower particle velocity while at the same time it is expected increase due to lower viscosity. Most work in the literature concerning h_{fp} evaluation have been carried out at a constant fluid temperature with the exception of few. Alhamdan and Sastry (1990) studied the effect of fluid temperature in natural convection (no particle motion), Awuah *et al.* (1996) studied the temperature effect with a stationary particle (hence no particle velocity involved), and Bhmidipati and Singh (1995) studied the effect at very low values of h_{fp}(108-195 W/m^{2}K). Alhamdan and Sastry (1990) reported that the h_{fp} values increased with fluid temperature with the lower viscosity fluids but not so much with the higher viscosity fluid and pointed that the higher viscosity tends to overshadow influence of temperature, something similar to what has been found in this study.

CONCLUSIONS

Convective fluid-to-particle heat transfer coefficient was evaluated, using a previously developed calorimetric technique, under tube-flow conditions without interfering the particle motion. Factors influencing h_{fp} such as fluid flow rate, h_{fp} concentration and temperature as well as the particle size were investigated using spherical aluminum particles. Values of h_{fp} varied from 650 to 2660 W/m^{2}K for different experimental conditions and followed the conventional trends of increasing with increasing fluid flow rates or decreasing CMC concentration. However, contrary to common expectations, h_{fp} decreased as the temperature increased. In fact, it was found that the particle velocity decreased at higher fluid temperature or lower viscosity due to the diminishing drag force. Particle velocity is one of the influencing factors associated with h_{fp} under tube-flow conditions with freely moving particle. It was also found that the values of h_{fp} increased with particle size in agreement with some studies in the literature.

PREFACE TO CHAPTER 7

Knowledge of fluid-to-particle heat transfer coefficient (h_{fp}) is important for the process design of particulate food in continuous flow system. However, experimental determination of h_{fp} is a difficult task. Therefore, several attempts have made to develope models in order to predict values of h_{fp} under tube-flow conditions.

In the previous chapters h_{fp} evaluated under various experimental conditions using two different developed techniques: particle oscillatory motion and calorimetric approach. Several parameters affecting h_{fp} associated with spherical particles and both Newtonian and non-Newtonian carrier fluid under tube-flow conditions were investigated.

In the following chapter, data obtained from both method will be analyzed to develop dimensionless correlations based on the two approaches: 1) immersing a particle in a stagnant fluid with the existence of a relative velocity and, 2) a free particle rotating and moving simultaneously in a moving fluid.

The result of this study were presented partially in food engineering section of two scientific conferences: Institute of Food Technologist (IFT), 1998 and Canadian Institute of Food Technologist (CIFT), 1999. All the experimental work and data analysis were carried out by the candidate under the supervison of professor H. S. Ramaswamy. This, will fulfill the last objectives of the thesis. A manuscript entitled: "Dimensionless correlations for forced convection heat transfer to spherical particles under tube-flow conditions" has been prepared for publication by M. R. Zareifard and H. S. Ramaswamy which is presented in the following chapter.

CHAPTER 7

DIMENSIONLESS CORRELATIONS FOR FORCED CONVECTION HEAT TRANSFER TO SPHERICAL PARTICLES UNDER TUBE-FLOW CONDITIONS

ABSTRACT

Dimensionless correlations for estimating heat transfer coefficients for spherical particles under forced convection heat transfer regimes and tube-flow conditions were investigated using multiple regression and backward elimination procedures on statistically significant dimensionless groups. Two different previously developed techniques: 1) particle oscillatory motion and 2) a calorimetric approach were employed to evaluate convection fluid-to-particle heat transfer coefficient (h_{fp}) under tube-flow conditions. About 600 experiments were carried out with spherical particles of different materials (Nylon and Aluminium) and sizes (12.7-25.4 mm). Model particles were subjected to heat transfer under different experimental conditions (carrier fluid: 0-1% of carboxymethyl cellulose solution, w/w basis; fluid temperature: 50-90 ^{o}C; particle linear velocity of 0.06-0.21 m/s using the particle oscillatory motion method and fluid flow rate at 9-19 L/min using the calorimetric method). The material properties, particle size and velocity were found to have significant effects on the heat transfer coefficient and hence Nusselt number. A series of correlations were developed in the form of Nusselt number as a function of other influencing dimensionless numbers such as Reynolds and Prandtl numbers. Introducing some non-conventional ratios such as: the diffusivity ratio defined as the ratio of fluid to particle thermal diffusivity, particle-to-tube diameter ratio (d/D), and particle-to-fluid velocity ratio (V_p/V_f) were found to improve the model prediction. Coefficient of determination (R^2) ranging from 0.88 to 0.99 were obtained for different correlations between the Nusselt number and other dimensionless group numbers.

INTRODUCTION

One of the potential advantages of aseptic processing of particulate foods is the minimum loss of nutrients and overall quality due to the use of high temperature and short time processing technique. However, having a safe processed food requires achievement of adequate lethality. Processing time and heating rate are important parameters to be considered for any thermal processing procedure which are well defined in conventional canning process. In aseptic processing of particulate food, both the residence time and the heating rate of particles are still topics of controversial discussion, and have been dealt with academic, regulatory as well as industry sectors.

To design a process that ensures the commercial sterility of continuously processed foods containing particulates, thermal process calculations require accurate time-temperature data. Due to difficulties in measuring the temperature of a particle as it moves through the sections of an aseptic processing system, the particle centre temperatures are predicted by mathematically modelling the heat transfer to the particle.

Experimental determination of fluid-to-particle heat transfer coefficient (h_{fp}) in a continuous flow system is a very difficult task due to difficulties in time-temperature data acquisition of a moving particle. Therefore, a conservative approach based on a stationary condition has been suggested (Dignan et al., 1989). Some researchers have simulated flow conditions pertaining to the existence of relative linear velocities by maintaining a particle fixed and immersed in a moving fluid inside a tube. In this case, the particle's motion is restricted and the particle does not rotate. In fact, the particle and fluid often move at different velocities (Palmier et al., 1992; Dutta and Sastry 1990a,b; Ramaswamy et al., 1992; Grabowski and Ramaswamy, 1995). In addition, the free particle may show a rotational movement affecting the boundary layer and probably increasing the heat transfer coefficient (Sastry and Zuritz, 1987; Baptista et al., 1997a; Chakrabandhu and Singh, 1998; Ramaswamy and Zareifard 1999). Some other researchers have reported values of h_{fp} in tube-flow conditions which clearly shows that stationary approach is too conservative (Zuritz et al., 1990; Balasubramaiam, 1993; Mwangi et al., 1992; Zitoun and Sastry, 1994a, 1994b; Zareifard and Ramaswamy 1997).

Dimensional analysis is a useful technique for generalisation of data as it reduces the number of variables that must be studied and permits the grouping of physical variables that affect the process of heat transfer. In the dimensional analysis of convection heat transfer, the Nusselt number (Nu) a dimensionless measure of convective heat transfer coefficient, is correlated with other dimensionless numbers such as: Reynolds number (Re), Prandtl number (Pr) and Grashof number (Gr).

Kramers (1946), Ranz and Marshall (1952), and Whitaker (1972) probably were the firsts who presented empirical equations to correlate the dependence between heat transfer and thermophysical properties of the particle and fluid as well as flow conditions. During the last decade researchers have been interested in the subject and have tried to develop different forms of models to predict fluid-to-particle heat transfer coefficient for processing of particulate food under tube-flow conditions (Chandarana et al., 1988 and 1990; Zuritz et al., 1990; Mwangi et al., 1992; Zitoun and Sastry, 1994; Awuah and Ramaswamy, 1996; Sablani et al., 1997; Chakrabandhu and Singh, 1998).

Established dimensionless correlations from the published literature is summarized in Table 7.1. There are very few studies dealing with rotating particles. Astrom and Bark (1994) developed correlations for still particles immersed in a thermo-flask rotating at different rotational speed when the test particle was positioned at different distances from the rotational centre. Baptista et al. 1997, developed a correlation considering generalised Re and Pr for rotational velocity using hollow spherical particles coated with liquid crystal material at very low temperature and Bi<0.1 conditions. Recently, Chakrabandhu and Singh (1998) developed correlations for a single particle fixed at a stationary position for two cases: the particle is at rest and when it can rotate around a rod passing through, when a sufficient velocity gradient existed. However, in both cases there was no transitional velocity involved.

In the previous four chapters, h_{fp} values were evaluated under conditions in which a controlled motion of the particle was achieved using the oscillatory technique or under conditions in which the particle was moving freely in a liquid under tube-flow conditions.

Table 7.1. Some of the published dimensionless correlations for estimating Nusselt number forced convection heat transfer conditions.

Reference	Fluid	Particle	Equation (Nu=.....)	R^2
Kramers (1946)	air, oil, water	sphere (steel)	$2+1.3\ Pr^{0.15}+0.66Re^{0.5}\ Pr^{0.31}$	--
Ranz & Marshal (1952)	air	sphere	$2+0.6Re^{0.5}\ Pr^{0.33}$	--
Whitaker (1972)	air, oil, water	sphere	$2+(0.4Re^{0.5}+0.06Re^{0.66})\ Pr^{0.4}\ (\mu_s/\mu_\infty)^{0.25}$	--
Zuritz & Sastry (1987)	CMC	mushroom (aluminum)	$2+2.95Re^{0.21}\ Pr^{0.14}$	0.99
Chandrana *et al.* (1988)	starch	cubes (silicone)	$0.55Re^{0.44}\ Pr^{0.35}$	0.92
Chandrana *et al.* (1988)	water	cubes (silicone)	$0.85\ Re^{0.43}$	0.95
Chandrana *et al.* (1990)	starch	cubes (silicone)	$2+0.028Re^{1.6}\ Pr^{0.89}$	0.79
Chandrana *et al.* (1990)	water	cubes (silicone)	$2+0.0333\ Re^{1.08}$	0.89
Zuritz *et al.* (1990)	CMC	mushroom (aluminum)	$2+28.37Re^{0.23}\ Pr^{0.14}\ (d/D)^{1.79}$	0.96
Awuah *et al.* (1993)	CMC	cylinders (carrot)	$2.45(Pr\ Gr)^{0.108}$	0.80
Awuah *et al.* (1993)	CMC	cylinders (potato)	$2.02(Pr\ Gr)^{0.113}$	0.88
Astrom & Bark (1994)	silicon oil	spheres (lead)	$8+2.53Re^{0.54}$	--
Astrom & Bark (1994)	silicon oil	cubes (lead)	$8+2.25Re^{0.61}$	--
Bhamidipati & Singh (1995)	CMC	cylinder (temp. sensor)	$0.27Re^{0.2}\ Pr^{0.33}$	0.85
Kelly *et al.* (1995)	CMC	sphere, cube, cylinder (aluminum)	$2+19.36Re^{0.132}\ Pr^{-0.08}$	0.83
Baptista *et al.* (1997)	CMC	sphere (hollow aluminum)stationary	$Nu_s+0.64Re^{0.59}\ Pr^{0.28}$	--
Baptista *et al.* (1997)	CMC	sphere (hollow aluminum)rotating	$Nu_s+0.17Re^{0.71}\ Pr^{0.42}\ (r_p/R_t)^{0.28}$	--
			$Nu_s=2+0.025\ Pr^{0.33}\ Gr^{0.5}$	
Chakrabandhu & Singh (1998)	CMC	cubes (sodium alginate)-stationary	$18197Re^{0.29}\ Pr^{-1.52}\ (d/D)^{4.35}$	0.91
Chakrabandhu & Singh (1998)	CMC	cubes (sodium alginate)-rotating	$338Re^{0.86}\ Pr^{-0.22}\ (d/D)^{1.67}$	0.89

It is necessary to analyze and compare both the cases of: 1) an immersed particle moving in a stagnant fluid, a simulated tube-flow condition with the existence of a relative velocity and, 2) a free particle rotating and moving simultaneously in a moving fluid. The objectives of this study were, therefore, to develop dimensionless correlations for experimental data obtained from the particle oscillatory motion method, when the particle movement is limited to oscillatory motion and rotational movement was not provided, and data obtained from the calorimetric method with the free movement of a particle in a carrier fluid as well as using all data together.

THEORETICAL BACKGROUND

Heat transfer from liquid to particles in continuous processing of multi phase systems is affected by both liquid and particle thermophysical properties as well as system parameters. In the dimensional analysis of forced convection heat transfer, the fluid-to-particle heat transfer coefficient (h_{fp}) is expressed in terms of the Nusselt number (Nu), which is generally described as a function of other dimensionless numbers consisting of liquid, particle and system properties such as the Reynolds number (Re), Prandtl number (Pr), and Grashof number (Gr):

$$Nu = f\,(Re, Pr, Gr)$$

Different forms of dimensionless correlations have been published concerning the flow field and heat transfer to particles in tube-flow conditions. Kramers (1946), Ranz and Marshal (1952) and Whitaker (1972) probably were some of the early researchers who presented the following equations for forced convection conditions respectively:

Kramers (1946): $$Nu=2 + 1.3\ Pr^{0.15} + 0.66\ Pr^{0.31}\ Re^{0.5} \quad \text{Eq. (7.1)}$$

Ranz and Marshal (1952): $$Nu= 2 + 0.6\ Re^{0.5} + Pr^{0.33} \quad \text{Eq. (7.2)}$$

Whitaker (1972): $$Nu=2+(0.4\ Re^{0.5} + 0.06\ Re^{0.66})\ Pr^{0.4}\ (\mu_{\infty}/\mu_{s})^{0.25} \quad \text{Eq. (7.3)}$$

All the above correlations involve Reynolds number as dominant factor influencing h_{fp}. The velocity term in Reynolds number, however, has been employed differently by different researchers. Some researchers have defined Reynolds number based on either fluid or particle velocity while the others used the relative velocity between particle and fluid, also called slip velocity, which is the difference between fluid and particle velocities. The latter seems to be more related to the concept of the case of study, even though for using Whitaker's (1972) equations it was clearly mentioned that fluid velocity far-removed from the particle should be used to calculate Re number. The particle velocity is clear and easy to measure. However, the fluid velocity in the tube-flow conditions of a two-phase system is a source of differences among the researchers. In the case of tube-flow conditions with moving particles, many other factors also have significant influence on particle motion and thus fluid-to-particle heat transfer coefficient. Particle shape and size, thermophysical properties of both particle and carrier fluid as well as system parameters such as tube diameter and fluid flow rate can be named as some of the influencing factors. These parameters can be grouped as dimensionless numbers and correlated with Nusselt number. Therefore, to account for the other influencing factors associated with h_{fp}, recent studies have presented modified forms of the earlier equations. Further, to improve the prediction of the developed model, depending on the experimental conditions, some other groups of dimensionless numbers, such as: Pecelt , Froude, Rayleigh numbers, or dimensionless ratios such as: Gr/Re^2, d/D, α_f/α_p,and μ_∞/μ_s have been also included in the empirical equations. Some of the empirical equations including one or more of the above mentioned groups of numbers are presented in Table 7.1.

In the present study the Nusselt number and generalised forms of the Reynolds number, Prandtl number, and Grashof number were used and calculated as follows:

$$Nu = h_{fp}\, d_p / k_f \qquad \text{Eq (7.4)}$$

$$GRe = \rho\, V_s\, d_p / \mu \qquad \text{Eq (7.5)}$$

$$GPr = C_p\, \mu / k_f \qquad \text{Eq (7.6)}$$

$$GGr = g\, \beta\, \rho^2\, \Delta T\, d_p{}^3 / \mu \qquad \text{Eq (7.7)}$$

where:

$$V_s = V_f - V_p \quad \text{Eq (7.8)}$$

$$\Delta T = (T_f - T_{ip}) / 2 \quad \text{Eq (7.9)}$$

$$V_f = Q / \pi (R_t^{\,2} - R_p^{\,2}) \quad \text{Eq (7.10)}$$

$$Cp = 1.675 + 0.025\ (\%W) \quad \text{Eq (7.11)}$$

$$\mu = 2^{n-3}\ m\ (3n+1/n)^n\ (d_p/V_s)^{\ 1-n} \quad \text{Eq (7.12)}$$

$$k_f = [326.575 + 1.0412\ T - 0.000337\ T^2][(0.796 + 0.009346\ (\%W)] \quad \text{Eq (7.13)}$$

All the parameters are defined in the nomenclature at the beginning of the thesis.

MATERIALS AND METHODS

Data generated by the two previously developed methods: *"particle oscillatory motion method"* (detailed in chapters 3 and 4); and *"calorimetric method"* (chapter 5 and 6) on the convective fluid-to-particle heat transfer coefficient (h_{fp}) in tube-flow situation were used for the dimensionless modeling.

Data analysis

In the literature, the heat transfer coefficients associated with pure forced convection with unbounded flow is generally evaluated from the expression:

$$Nu = A + B\ Re^c\ Pr^d \quad \text{Eq (7.14)}$$

while, in the case of tube-flow conditions of a two-phase system, additional dimensionless terms are also added to the correlation as explained earlier. In the present study, with the set of calorimetric data, after logarithmic linearization of the variables, regression analyses were performed starting with the simplest form of correlations: Nu number as a function of just GRe number [Nu = f (GRe)]; and then as a function of both GRe and GPr numbers [Nu=f(GRe, GPr)]; as well as a function of three GRe, GPr and GGr numbers [Nu=f(GRe, GPr, GGr)]. To account for other influencing parameters, it was recognised that, in terms of modelling, the particle size as well as fluid and particle flow rate could have significant contribution to the model (specially in the case of tube-flow conditions with free particle movement). Hence, other parameters such as d/D, V_p/V_f and V_p/V_s were also added into the model to see the improvement of the model prediction.

After observing successful improvement of the model prediction by including other variables, multiple regression with backward elimination procedure was performed using SAS computing program to obtain the best model and indicate parameter estimate as well as their level of significant in the model. This procedure was also carried out for the set of data obtained from particle oscillatory motion method separately (considering other potential influencing parameters such as: α_f/α_p and GGr/GRe^2) as well as the combination of all data obtained from both methods over about 600 experimental data.

RESULTS AND DISCUSSIONS

Regression analysis between dimensionless groups resulted in a number of correlations with different coefficient of determinations (R^2) and coefficient of variations (CV) as indexes for quality of fit. Overall, these coefficients varied over the following ranges: $0.4<R^2<0.99$, $1<CV<15\%$. Depending on the complexity of the correlation and number of combinations of dimensionless groups to be considered in the equations, R^2 increased and CV decreased indicating general improvement of the model based on the goodness of fit.

As mentioned earlier, multiple regressions were performed for different models with sets of data obtained from the calorimetric method. Different correlations were obtained with quality of fit varying as follows:

$$Nu = 2 + 18.4\, GRe^{0.147} \qquad (R^2=0.60;\ CV=7.1) \qquad \text{Eq. (7.15)}$$

$$Nu = 2 + 0.25\ GRe^{0.601}\ GPr^{0.448} \quad (R^2=0.71;\ CV=6.1)$$ Eq. (7.16)

$$Nu = 2 + 0.035\ GRe^{0.440}\ GPr^{0.681}\ GGr^{0.191} \quad (R^2=0.73;\ CV=5.8)$$ Eq. (7.17)

$$Nu = 2 + 1.15\ GRe^{0.250}\ GPr^{2.180}\ GGr^{1.125}\ (d/D)^{4.508} \quad (R^2=0.91;\ CV=3.2)$$ Eq.(7.18)

$$Nu = 2 + 3.8\ GRe^{0.479}\ GPr^{-0.655}\ GGr^{-0.526}\ (d/D)^{2.293}\ (V_p/V_s)^{0.514} \quad (R^2=0.97;\ CV=1.8)$$ Eq.(7.19)

$$Nu = 2 + 6.53\ GRe^{0.528}\ GPr^{-0.776}\ GGr^{-0.610}\ (d/D)^{2.514}\ (V_p/V_s)^{0.948}\ (V_p/V_f)^{0.915} \quad (R^2=0.98;\ CV=1.6)$$ Eq. (7.20)

A logarithmic plot of Nu number: experimental versus predicted based on Eq. (7.15) presented in Figure 7.1, shows the fit of the simplest correlation. As can be seen from the figure, data are scattered and the R^2 is relatively low at 0.6 and the CV is high at about 7%. This was expected because the effects of the other influencing parameters were not included in the model. The second correlation [Eq.(7.16)] was tried in the form of Nu number as a function of just Re and Pr as commonly used in many published correlations including the well known Ranz and Marshal correlation. The R^2 improved somewhat (from 0.6 to 0.7) by including Pr number in the model (Figure 7.2). Adding Gr to the model [Eq. (7.17)] did not improve R^2 that much since the range of Gr/Re^2 is mainly less than one indicating that experimental conditions were more under forced convection situation rather than natural convection due to the flow system. Logarithmic plot of Eq. (7.17) is also shown in Figure 7.3. Adding the ratio of particle-to-tube diameter d/D into the model caused a good improvement of the model and R^2 increased from 0.7 to 0.9. This improvement can be seen in Figure 7.4. Including the ratio of particle-to-slip velocity (V_p/V_s) and particle-to-fluid velocity (V_p/V_f) also contribute to improving model prediction. The best resulting model has an R^2 greater than 0.98. Experimental values of Nu obtained from the calorimetric method versus predicted using Eq.'s (7.18), (7.19) and (7.20) are shown in Figures 7.4, 7.5 and 7.6 respectively showing an excellent goodness of fit by including several of the influencing parameters associated with h_{fp} in the model.

$$Nu = 2+18.4\ GRe^{0.147}$$

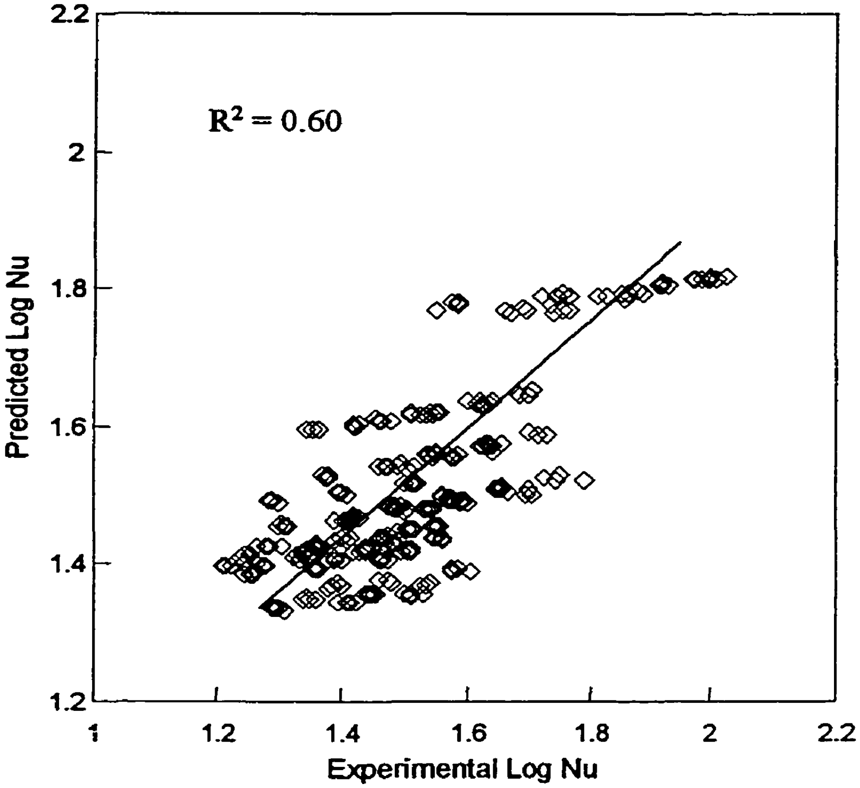

Figure 7. 1. Logarithmic plot of experimental values of Nu evaluated from calorimetric method versus predicted Nu using Eq. (7.15).

$$Nu=2+0.25\ GRe^{0.601}\ GPr^{0.448}$$

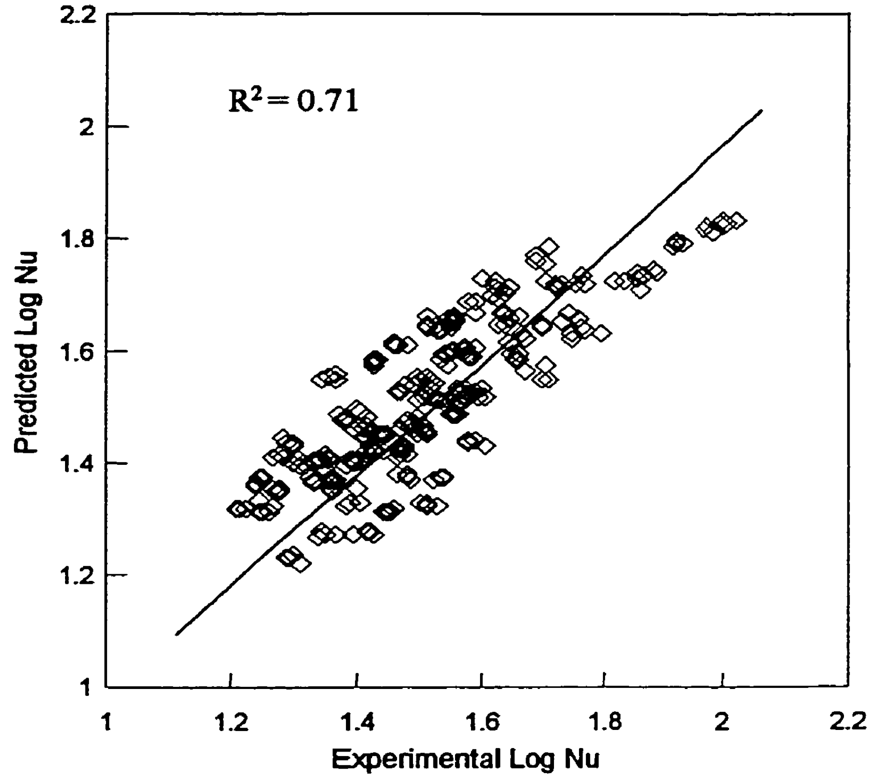

Figure 7. 2. Logarithmic plot of experimental values of Nu evaluated from calorimetric method versus predicted Nu using Eq. (7.16).

$$Nu = 2 + 0.035\ GRe^{0.440}\ GPr^{0.681} GGr^{0.191}$$

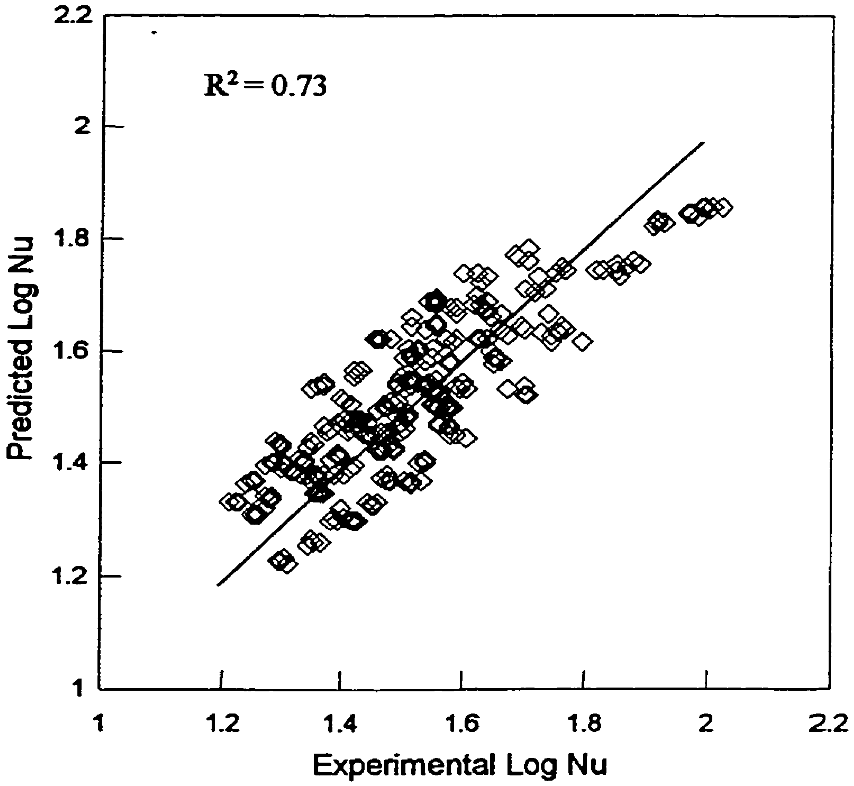

Figure 7. 3. Logarithmic plot of experimental values of Nu evaluated from calorimetric method versus predicted Nu using Eq. (7.17).

$$Nu = 2 + 1.15GRe^{0.250}\, GPr^{-2.180}\, GGr^{-1.125}\, (d/D)^{4.508}$$

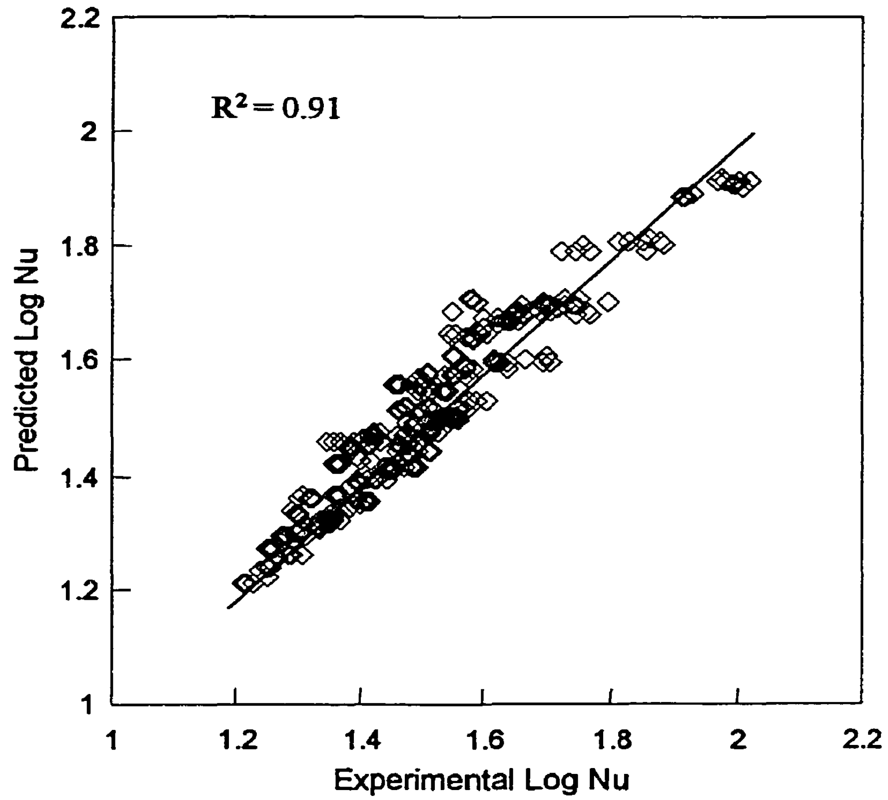

Figure 7. 4. Logarithmic plot of experimental values of Nu numbers evaluated from calorimetric method versus predicted Nu numbers using Eq. (7.18).

$$Nu = 2 + 3.8\, GRe^{0.479}\, GPr^{-0.655}\, GGr^{-0.526}\, (d/D)^{2.293}\, (V_p/V_s)^{0.514}$$

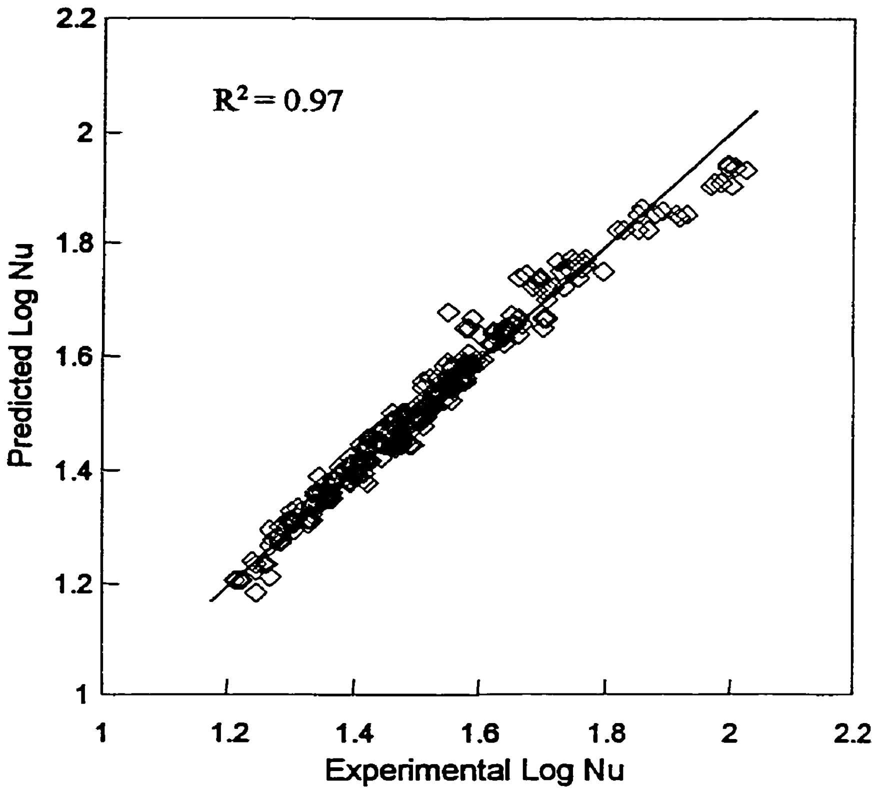

Figure 7. 5. Logarithmic plot of experimental values of Nu evaluated from calorimetric method versus predicted Nu using Eq. (7.19).

$$Nu = 2 + 6.53\ GRe^{0.528}\ GPr^{-0.776}\ GGr^{-0.610}\ (d/D)^{2.514}\ (V_p/V_s)^{0.948}\ (V_p/V_f)^{0.915}$$

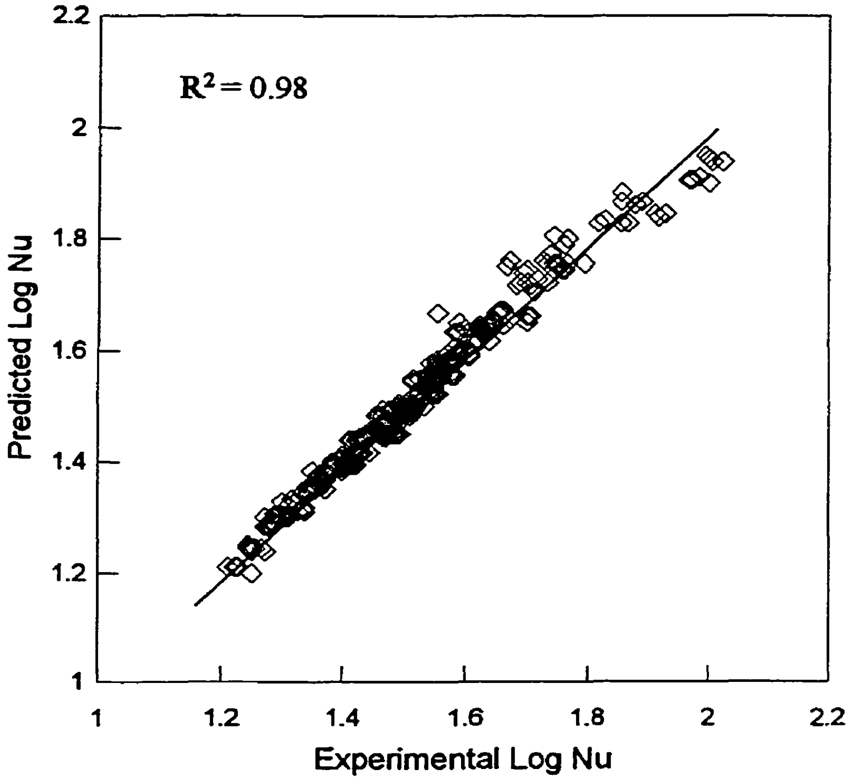

Figure 7. 6. Logarithmic plot of experimental values of Nu evaluated from calorimetric method versus predicted Nu using Eq. (7. 20).

After realising the effects of different parameters in the regressed model using a step wise procedure, to obtain the best model with the presence of all significant factors in the model, multiple regression with backward elimination procedure was performed. Results of the backward elimination procedures are given in Tables 7.2, 7.3 and 7.4 for the calorimetric method data, the particle oscillatory motion data and the combination of all data together respectively. For the set of calorimetric data, as it can be seen from Table 7.2 part C (the summary of backward elimination procedure) the groups of GGr/GRe^2 and d/D were not significant (p>0.1) in comparison with the other parameters and therefore these two were eliminated from the correlation. In fact, the effect of particle to tube diameter ratio is an important factor in tube-flow conditions since it can affect the flow behavior around the particle and hence the heat transfer coefficient. This fact was clearly observed earlier using a step wise procedure; when the parameter d/D was added into the model, the R^2 improved from 0.7 to 0.92 [Eq. (7.18)]. However, using a backward elimination procedure the effect of d/D is somehow presented in other forms of dimensionless group numbers such as V_p/V_f and/or V_p/V_s in the final correlation.

In general, regression analysis with the backward elimination procedure resulted in the following equation with the best fit (R^2=0.98) for about 300 number of experimental data obtained from the calorimetric method under different experimental conditions.

$$Nu = 2 + 24.77\ GRe^{0.589}\ GPr^{0.977}\ GGr^{0.231}\ (V_p/V_f)^{-0.607}\ (V_p/V_s)^{0.731}\ (\alpha_f/\alpha_p)^{-8.402} \qquad \text{Eq(7.21)}$$

The validity of the above equation is limited to the following ranges of the dimensionless group numbers: $2.5<GRe<5600$; $2.6<GPr<3100$; $4.3<GGr<1.6E7$; $0.30<V_p/V_f<0.77$; $0.43<V_p/V_s<3.37$ and $1800<\alpha_f/\alpha_p<1900$. Figure 7.7 shows the plot of Nusselt number calculated from the Eq. (7.21) versus experimental values of Nusselt numbers obtained from the calorimetric method.

Table 7.2. **Results of regression analysis for data obtained from *calorimetric method* showing all variables and corresponding estimated parameters, standard errors and levels of significant; a) all variables included ; b) lest significant variables eliminated ; c) summery of backward elimination and corresponding partial R^2 and model R^2.**

a) all variables entered in the model

Variable	Parameter Estimate	Standard Error	Sum of Squares	F	Prob>F
INTERCEPT	24.99329788	3.16200230	0.03608118	62.48	0.0001
Re	0.56607801	0.42114548	0.00104339	1.81	0.1800
Pr	0.99936442	0.29099115	0.00681155	11.79	0.0007
Gr	0.25339604	0.23014275	0.00070010	1.21	0.2718
d/D	-0.03116292	0.41945486	0.00000319	0.01	0.9408
V_P/V_F	-0.60299843	0.18220816	0.00632491	10.95	0.0011
V_P/V_S	0.72873804	0.09161385	0.03654084	63.27	0.0001
Gr/Re^2	-0.01202746	0.21013983	0.00000189	0.00	0.9544
α_f/α_p	-8.49876650	1.32703113	0.02368686	41.02	0.0001

b) the least significant variables removed from the model

Variable	Parameter Estimate	Standard Error	Sum of Squares	F	Prob>F
INTERCEPT	24.76832090	1.24036386	0.22864799	398.74	0.0001
Re	0.58925738	0.01926941	0.53622327	935.13	0.0001
Pr	0.97768917	0.01963232	1.42210224	2480.04	0.0001
Gr	0.23105016	0.01298849	0.18145454	316.44	0.0001
V_P/V_F	-0.60745776	0.16904669	0.00740442	12.91	0.0004
V_P/V_S	0.73155263	0.08294934	0.04460029	77.78	0.0001
α_f/α_p	-8.40161400	0.39093392	0.26484466	461.87	0.0001

All variables left in the model are significant at least at the 0.1 level.

c) summary of backward elimination procedure for dependent variable Nu

Step	Variable Entered	Variable Removed	Number In	Partial R^2	Model R^2	C(p)	F	Prob>F
1	V_P/V_F		1	0.6904	0.6904	4147.6512	637.7274	0.0001
2	d/D		2	0.1807	0.8710	1563.8689	399.2418	0.0001
3	Gr/Re^2		3	0.0453	0.9163	918.1064	153.5461	0.0001
4	Pr		4	0.0488	0.9651	221.2083	396.2037	0.0001
5	α_f/α_p		5	0.0070	0.9721	123.5199	70.3648	0.0001
6	V_P/V_S		6	0.0074	0.9795	19.1968	101.9001	0.0001
7	Re		7	0.0009	0.9804	8.2123	12.9747	0.0004
8	Gr		8	0.0001	0.9805	9.0000	1.2123	0.2718
9		Gr/Re^2	7	0.0000	0.9805	7.0033	0.0033	0.9544
10		d/D	6	0.0000	0.9805	5.0107	0.0075	0.9312

C(p): Compute Mallows' static=$(SSE/\sigma^2)+(2\rho-n)$; where σ is the estimate of pure error variance and ρ is the number of parameters in the model and n is the number of observations.

Table 7.3. Results of regression analysis for data obtained from *particle oscillatory motion* method showing all variables and corresponding estimated parameters, standard errors and levels of significant; a) all variables included; b) lest significant variables eliminated; c) summery of backward elimination and corresponding partial R^2 and model R^2.

a) all variables entered in the model

Variable	Parameter Estimate	Standard Error	Sum of Squares	F	Prob>F
INTERCEPT	-7.98657447	1.04068533	0.36874534	58.90	0.0001
Re	-1.60926219	1.51218383	0.00709069	1.13	0.2882
Pr	2.11026066	0.23545024	0.50294240	80.33	0.0001
Gr	1.96382908	0.80123006	0.03761293	6.01	0.0149
d/D	-1.95076625	0.36883798	0.17513926	27.97	0.0001
Gr/Re^2	-1.12409475	0.75897694	0.01373387	2.19	0.1398
α_f/α_p	0.30660959	0.02711805	0.80038460	127.84	0.0001

b) the least significant variable removed from the model

Variable	Parameter Estimate	Standard Error	Sum of Squares	F	Prob>F
INTERCEPT	-7.64398905	0.98989754	0.37353125	59.63	0.0001
Pr	2.03180397	0.22366783	0.51692066	82.52	0.0001
Gr	1.11971637	0.11323848	0.61248479	97.78	0.0001
d/D	-1.84290966	0.35473116	0.16907396	26.99	0.0001
Gr/Re^2	-0.31658448	0.01651158	2.30287058	367.62	0.0001
α_f/α_p	0.30467996	0.02706431	0.79389129	126.73	0.0001

All variables left in the model are significant at least at the 0.1 level.

c) summary of backward elimination procedure for dependent variable Nu

Step	Variable Entered	Variable Removed	Number In	Partial R^2	Model R^2	C(p)	F	Prob>F
1	Re		1	0.6568	0.6568	485.3636	501.5090	0.0001
2	Pr		2	0.1398	0.7967	183.6846	179.4499	0.0001
3	α_f/α_p		3	0.0524	0.8491	71.7675	90.3642	0.0001
4	Gr		4	0.0197	0.8688	30.9730	38.8941	0.0001
5	d/D		5	0.0119	0.8807	7.1936	25.6608	0.0001
6	Gr/Re^2		6	0.0010	0.8817	7.0000	2.1936	0.1398
7		Re	5	0.0005	0.8812	6.1325	1.1325	0.2882

C(p): Compute Mallows' static=$(SSE/\sigma^2)+(2\rho-n)$; where σ is the estimate of pure error variance and ρ is the number of parameters in the model and n is the number of observations.

Table 7. 4. Results from regression analysis for all data obtained from both *particle oscillatory motion* and *calorimetric* methods, showing all variables and corresponding estimated parameters, standard errors and levels of significant; a) all variables included ; b) lest significant variables eliminated; c) summery of backward elimination and corresponding partial R^2 and model R^2.

a) all variables entered in the model

Variable	Parameter Estimate	Standard Error	Sum of Squares	F	Prob>F
INTERCEPT	2.71004198	0.57416392	0.13762429	22.28	0.0001
Re	1.50278068	0.98140982	0.01448456	2.34	0.1263
Pr	-0.30845096	0.13086326	0.03432034	5.56	0.0188
Gr	-0.83341758	0.50162479	0.01705227	2.76	0.0972
d/D	1.64359029	0.20120715	0.41220682	66.73	0.0001
V_P/V_F	1.73773575	0.22711306	0.36165801	58.54	0.0001
V_P/V_S	-0.52608404	0.11360411	0.13247595	21.44	0.0001
Gr/Re^2	0.47577758	0.49233728	0.00576896	0.93	0.3343
α_f/α_p	0.22649787	0.02089589	0.72580723	117.49	0.0001

b) the least significant variable removed from the model

Variable	Parameter Estimate	Standard Error	Sum of Squares	F	Prob>F
INTERCEPT	2.64975159	0.57072956	0.13314094	21.56	0.0001
Re	0.55475145	0.02744655	2.52338528	408.53	0.0001
Pr	-0.29442011	0.13004742	0.03165873	5.13	0.0240
Gr	-0.35247796	0.06278990	0.19464640	31.51	0.0001
d/D	1.62777954	0.20052866	0.40700554	65.89	0.0001
V_P/V_F	1.74820816	0.22684058	0.36686547	59.39	0.0001
V_P/V_S	-0.53281359	0.11338358	0.13639935	22.08	0.0001
α_f/α_p	0.22748350	0.02086972	0.73388624	118.81	0.0001

All variables left in the model are significant at least at the 0.1 level.

c) summary of backward elimination procedure for dependent variable Nu

Step	Variable Entered	Variable Removed	Number In	Partial R^2	Model R^2	C(p)	F	Prob>F
1	d/D		1	0.5333	0.5333	2390.1426	628.4460	0.0001
2	Re		2	0.2972	0.8305	521.0171	962.7286	0.0001
3	α_f/α_p		3	0.0295	0.8600	337.4690	115.3534	0.0001
4	Gr		4	0.0281	0.8881	162.4665	137.4378	0.0001
5	V_P/V_F		5	0.0207	0.9088	33.9267	124.1879	0.0001
6	V_P/V_S		6	0.0040	0.9128	11.0587	24.6842	0.0001
7	Pr		7	0.0008	0.9136	7.9339	5.1254	0.0240
8	Gr/Re^2		8	0.0001	0.9137	9.0000	0.9339	0.3343
9		Gr/Re^2	7	0.0001	0.9136	7.9339	0.9339	0.3343

C(p): Compute Mallows' static=(SSE/σ^2)+(2ρ-n); where σ is the estimate of pure error variance and ρ is the number of parameters in the model and n is the number of observations.

$$Nu = 2+24.77\, GRe^{0.589}\, GPr^{0.977}\, GGr^{0.231}\, (V_p/V_f)^{-0.607}\, (V_p/V_s)^{0.731}\, (\alpha_f/\alpha_p)^{-8.402}$$

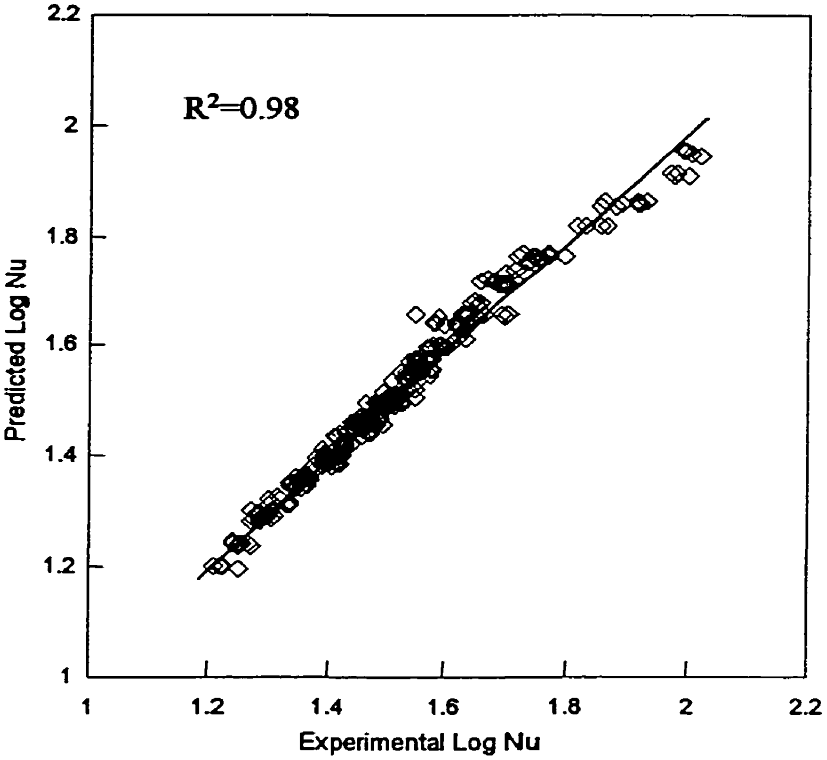

Figure 7.7. Logarithmic plot of experimental values of Nu evaluated from calorimetric method versus predicted Nu using Eq. (7. 21) obtained from multiple regression and backward elimination procedure .

The same procedure, backward elimination, was also performed for data obtained using particle oscillatory motion method, and the best model ($R^2 = 0.88$) was found as:

$$Nu = 2 - 7.64\ GPr^{2.032}\ GGr^{1.120}\ (d/D)^{-1.843}\ (GGr/GRe^2)^{-.0316}\ (\alpha_f/\alpha_p)^{0.305} \qquad \text{Eq. (7.22)}$$

The validity of the above equation is limited to the following ranges of the dimensionless group numbers: $3.5<GRe<7660$; $3<GPr<1606$; $6.3<GGr<3.5E7$; $0.2<d/D<0.4$; $0.06<GGr/GRe^2<0.94$; and $0.33<\alpha_f/\alpha_p<1.02$. Contributions from natural convection were accounted for by introducing both GGr and GGr/GRe^2 ratio in Eq. (7.22). The magnitude of Gr/Re^2, describes the ratio of buoyant to inertia forces indicating free, forced and mixed convection regimes (Chapman, 1989). Yuge (1960) indicated that forced convection dominates for flow over a sphere when condition $Gr/Re^2 <0.01$ is satisfied. According to Johnson *et al.* (1988), mixed convection occurs when the ratio falls between 0.08 and 5.1. Figure 7.8 shows the logarithmic plot of Nusselt number calculated from the Eq. (7.22) versus experimental values of Nusselt numbers obtained from the particle oscillatory motion method.

Multiple regression and backward elimination for all the 600 experimental data obtained from both methods resulted in the following model ($R^2 = 0.91$) after including all the possible influencing factors associated with h_{fp}:

Eq. (7.23)

$$Nu = 2 + 2.64\ GRe^{0.555}\ GPr^{-0.294}\ GGr^{-0.352}\ (d/D)^{1.628}(V_p/V_f)^{1.748}\ (V_p/V_s)^{-0.533}\ (\alpha_f/\alpha_p)^{0.227}$$

The validity of the above equation is limited to the following ranges of the dimensionless group numbers: $2.9<GRe<7660$; $2.5<GPr<3077$; $4.15<GGr<1.5E7$; $0.2<d/D<0.6$; $0.30<V_p/V_f<1$; $0.43<V_p/V_s<3.37$; and $0.33<\alpha_f/\alpha_p<1892$. Figure 7.9 shows the logarithmic plot of Nusselt number calculated from the Eq. (7..23) versus experimental values of Nusselt numbers obtained from the pooled data including both calorimetric and particle oscillatory motion methods.

$$Nu = 2 - 7.64\, GPr^{2.032}\, GGr^{1.120}\, (d/D)^{-1.843}\, (Gr/Re^2)^{-0.316}\, (\alpha_f/\alpha_p)^{0.305}$$

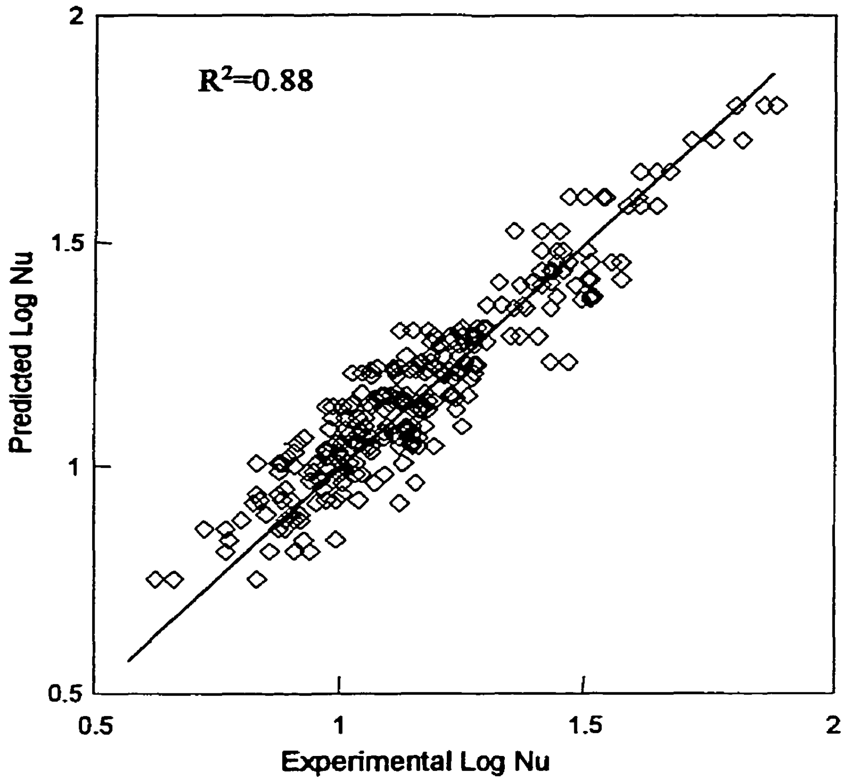

Figure 7. 8. Logarithmic plot of experimental values of Nu evaluated from particle oscillatory motion method versus predicted Nu using Eq. (7.22) obtained from multiple regression and backward elimination procedure .

$$Nu = 2 + 2.64\ GRe^{0.554}\ GPr^{-0.294}\ GGr^{-0.352}\ (d/D)^{1.628}\ (V_p/V_f)^{1.748}\ (V_p/V_s)^{-0.533}\ (\alpha_f/\alpha_p)^{0.227}$$

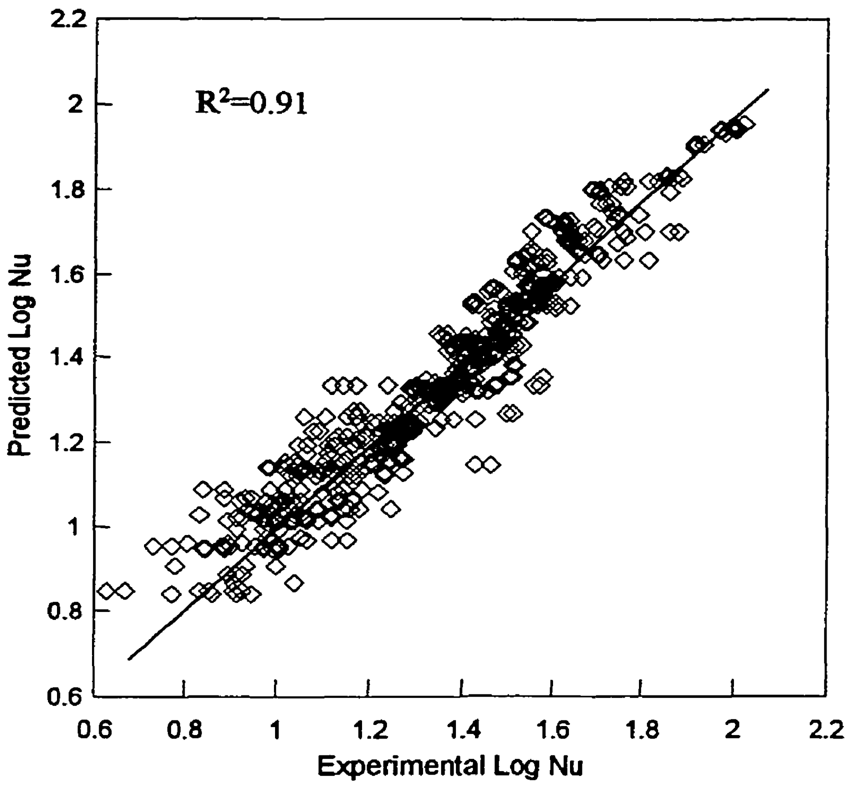

Figure 7. 9. Logarithmic plot of experimental values of Nu evaluated from both methods versus predicted Nu using Eq. (7.23) obtained from multiple regression and backward elimination procedure .

It is worth mentioning that, in the heat transfer literature, the convective heat transfer coefficient in the form of the Nusselt number is correlated to Reynolds and Prandtl numbers due to the influence of properties associated with the carrier fluid which can affect the boundary conditions. The constant value of 2 has been reported in the developed correlations to be considered as a limiting Nusselt number value for the steady state heat conduction between fluid and sphere. This number may vary for different particle geometry (Whitaker, 1976). In the present study, particle-to-tube diameter ratio (d/D), and thermal diffusivity ratio (α_f/α_p) as well as velocity ratios (V_p/V_f or V_p/V_s) were found to be appropriate for h_{fp} correlations under tube-flow situations investigated.

Dimensionless numbers as well as the coefficients of determination for the above models are different from those reported in the literature. Attempts to compare the above model with others in the literature resulted in either over-estimate or under-estimate the Nusselt number. Comparison with well-known correlations such as Ranz and Marshal (1952) or Whitaker (1972) is not possible because these equations were derived for an unbounded flow situation. In general, it is not appropriate to compare the empirical equations in the literature because of differences in experimental procedures, and most importantly differences in the range of Re number and other dimensionless numbers which might differ from the experimental condition for the present study.

CONCLUSION

Convective fluid-to-particle heat transfer coefficients (h_{fp}) for spherical particles under tube-flow conditions were evaluated using two different methods as influenced by all parameters. Dimensionless correlations between Nusselt number and other dimensionless numbers were developed for data obtained from particle oscillatory motion method and calorimetric approach separately as well as the combination of all data together. SAS computing program with multiple regression analysis and backward elimination procedure were used to obtain the best model with statistically significant parameters associated with h_{fp}. Heat transfer to the particle from the carrier medium was modelled using Reynolds number, Pr number and Grashof number. Their relationship were attributed to the carrier fluid and various parameters affecting the boundary condition. In addition particle-to-tube diameter ratio (d/D), and thermal diffusivity ratio (α_f/α_p) as well as velocity ratio (V_p/V_f) were found to be appropriate for h_{fp} correlations under tube-flow and force convection situations investigated in the present suede. Nusselt numbers estimated from the developed equations showed a good agreement with experimental data obtained from the particle oscillatory motion method (R^2>0.88) and an excellent goodness of fit with experimental data obtained from the calorimetric approach (R^2> 0.98). In general, using all data, a very good correlation (R^2> 0.91) was obtained between Nusselt numbers predicted from developed empirical equation and observed data evaluated from both experimental methods.

CHAPTER 8

GENERAL CONCLUSIONS

Aseptic processing which is a technique for high-temperature short-time (HTST) processing of particulate food under continuous tube-flow conditions is one processing technique with the potential for producing high-quality products. Aside from the residence time distribution (RTD), design of thermal processes of particulate foods depends strongly on the value of fluid-to-particle heat transfer coefficient (h_{fp}). Having a precise knowledge of h_{fp} is important from both safety and quality point of view to ensuring adequate lethality and minimizing the loss of nutrients and overall quality. However, evaluation of h_{fp} is a difficult task due to the monitoring the temperature of a moving particle suspended in a continuously moving fluid. Therefore, estimating h_{fp} from the empirical models developed under the simulated conditions is a useful technique.

Different means and methods have been used for evaluation of h_{fp} in tube-flow situations. Basically, these methods can be classified into two categories: I) direct time-temperature measurement of a particle processed under simulated conditions, and II) indirect measurement of the temperature of a moving particle in a more realistic tube-flow system. In the present work a comprehensive study of both techniques of temperature measurements have been used to evaluate the associated tube-flow fluid-to-particle heat transfer coefficient.

1. A new technique, involving particle oscillatory motion during processing with the existence of a relative velocity between the particle and fluid, was developed for measurement of convective heat transfer coefficient associated with particles subjected to a stagnant fluid of higher temperature . A specific experimental setup was designed and fabricated to satisfy the purpose; being able to record the temperature history of a particle while it was not in a stationary position. An oscillatory approach was used for imparting particle motion in a model holding tube. The conventional thermocouple approach and analytical solution to partial

differential equation governing heat transfer phenomena, were used for evaluating h_{fp} in tube-flow conditions. The experimental setup designed permitted easier investigation of the effect of some parameters affecting h_{fp} because of the better control on factors such as particle velocity and particle location inside the tube.

2. Using the "*particle oscillatory motion*" method, experiments were carried out to obtain data under different experimental conditions with both Newtonian and non-Newtonian fluids, which are commonly used in food processing systems. Some of the influencing factors on h_{fp} associated with both particle and carrier medium such as particle size, material and velocity as well as different concentration of carboxymethyl cellulose (CMC) solution at various temperatures were investigated using this technique. A full factorial experimental design was used to study the effect of influencing factors on h_{fp} associated with spherical particles made of Aluminum epoxy and Nylon. Depending on the experimental conditions, values of h_{fp} varied from 350 to 2000 W/m^2K. Statistical analysis of experimental data indicated that all the above mentioned factors had significant ($p<0.0001$) effect on h_{fp}. Conventional trends of increasing heat transfer coefficient with particle velocity, fluid temperature and decreasing fluid viscosity were observed. However, with respect to the effect of particle size a decrease in h_{fp} values was found as particle size increased in contrast to some studies and in agreement with others. Values of h_{fp} were also found to be higher for Aluminum epoxy particles than for the Nylon particles.

3. Attempts to evaluate h_{fp} associated with a freely moving particle, which is not attached to a thermocouple, and to account for the contribution of particle rotation, were succeeded with a "*calorimetric method*". Conventional methods of direct temperature measurement of a particle ignore the contribution of particle rotation to heat transfer in tube-flow conditions. Using a calorimetric method the mass average or bulk temperature of a moving particle in tube-flow conditions was measured instead of recording center point temperature for the subsequent

evaluation of the h_{fp} using a finite difference model. Since the medium temperature, particle initial temperature, exposure time and thermophysical properties were known, the associated h_{fp} was computed using an iterative numerical technique for the evaluated bulk temperature of the particle. The calorimetric approach was successfully standardized, verified and validated for the case of study using thermocouple equipped particles subjected to various time-temperature treatments. The h_{fp} values thus obtained from the calorimetric approach were comparable to those from conventional techniques involving thermocouple equipped particles. Values of h_{fp} increased with increasing flow rate, particle size and decreasing viscosity. Higher values of h_{fp} were found for moving particles than those for the stationary particle under the same experimental conditions. The calorimetric method showed good potential for evaluating h_{fp} in continuous tube-flow applications because it permits the evaluation of h_{fp} under the natural movement of particles in a carrier fluid without any interference.

4. Convective fluid-to-particle heat transfer coefficient was evaluated, using the previously developed calorimetric technique, under tube-flow conditions without interfering the particle motion. Experiments were carried out using Aluminum spherical particles with water and various concentration of CMC solution as the carrier fluid. Factors influencing h_{fp} such as fluid flow rate, concentration and temperature as well as the particle size were investigated. Values of h_{fp} varied from 650 to 2660 W/m^{2}K for different experimental conditions and followed the conventional trends of increasing with increasing fluid flow rates or decreasing CMC concentration. With respect to the effect of particle size values of h_{fp} increased with particle size. It was also found that the values of h_{fp} decreased as the fluid temperature increased. This is due to the fact that the particle velocity decreased at higher fluid temperature or lower viscosity due to the diminishing drag force. Particle velocity is one of the influencing factors associated with h_{fp} under tube-flow conditions with freely moving particles.

5. Dimensionless correlations between Nusselt number and other dimensionless numbers were developed for data obtained from particle oscillatory motion method and calorimetric approach separately as well as the combination of all data together. SAS computing program with multiple regression analysis and backward elimination procedures were used to obtain the best model with statistically significant parameters associated with h_{fp}. Heat transfer to the particle from the carrier medium was modelled using Reynolds number, Prandtl number and Grashof number. Their relationship were attributed to the carrier fluid and various parameters affecting the boundary condition. In addition, the material properties, particle size and velocity were found to have significant effects on the heat transfer coefficient and hence Nusselt number. A series of correlations were developed in the form of Nusselt number as a function of other influencing dimensionless numbers. Introduction of diffusivity ratio defined as the ratio of fluid-to-particle thermal diffusivity, particle-to-tube diameter ratio and particle-to-fluid velocity ratio were found to improve the developed models. Nusselt numbers estimated from the developed equations showed a good agreement with experimental data obtained from the particle oscillatory motion method (R^2>0.88) and an excellent goodness of fit with experimental data obtained from the calorimetric approach (R^2> 0.98). In general, using all data, a good correlation (R^2> 0.91) was obtained for the Nusselt number using the pooled data evaluated from both experimental methods.

RECOMMENDATIONS FOR FUTURE RESEARCH

Methods have been developed for evaluation of convective fluid-to-particle heat transfer coefficients (h_{fp}) under tube-flow conditions. This work has shown interest in the area of heat transfer involving particle motion in tube-flow systems. Due to time limitations it was not possible to study some other interesting parameters associated with h_{fp}. The following are recommendations for future research in this area:

1. Study the effect of particle location in the tube, particle shape and the effect of particle concentration using "*particle oscillatory motion*" method.

2. Use of this technique is also possible for evaluating heat transfer to particulate liquids in cans subjected to oscillatory agitation.

3. Study the effect of factors affecting particle rotation and linear velocity and hence heat transfer coefficient using "*calorimetric*" approach.

4. Use the calorimetric approach for evaluation of fluid-to-particle heat transfer coefficient with multiple particle or different concentration of particles.

5. Compare other methods of h_{fp} evaluation involving particle motion such as moving thermocouple approach or using thermo-chromic liquid crystal (TLC) material with calorimetric approach.

6. Extend the work to heat transfer with other carrier fluids and real food particles of different shapes using both "*particle oscillatory motion*" and "*calorimetric*" methods.

7. Biological validation of thermal processing using predicted h_{fp} from the developed dimensionless empirical correlations.

REFERENCES

Abbatemarco C. and Ramaswamy H. S., 1993. Heating behavior and quality factor retention in a canned model food as influenced by thermal processing in a rotary retort. J. Food Quality, 16: 273-285.

Abdelrahim K. A., Ramaswamy H. S., Marcotte M. and Toupin, C., 1993. Residence time distribution of carrot cubes in starch solutions in a pilot scale aseptic processing system. Food Res. Int. 26:431-442.

Abdelrahim K. A, 1994. Residence time distributions of food particles and rheological properties of carrier fluids under aseptic processing conditions. Ph.D. thesis, Dept. of Food Science, McGIll university.

Abdelrahim K. A. and Ramaswamy H. S., 1995. High temperature/pressure rheology of carboxymethyl cellulose (CMC). Food Res. Int. 28(3):285-290.

Alhamdan A. and Sastry S. K., 1990. Natural convection heat transfer between non-Newtonian fluids and an irregular shape particle. J. Food Process Engineering, 13:113-124.

Astrom, A., and Bark, G., 1994. Heat transfer between fluid and particles in aseptic processing. J. Food Engineering, 21: 97-125

Awuah, G. B., Ramaswamy, H. S. and Simpson B. K. 1995. Comparison of two methods for evaluating fluid-to-surface heat transfer coefficients. Food Res. International, 28(3):261-271.

Awuah, G. B. and Ramaswamy, H. S. 1996. Dimensionless correlations for mixed and forced convection heat transfer to spherical and finite cylindrical particles in an aseptic processing holding tube simulator.

Awuah, G. B., Ramaswamy H. S., Simpson B. K. and Smith J. P., 1996. Fluid to particle convective heat transfer coefficient as evaluated in an aseptic processing holding tube simulator. J. Food Process Engineering, 19(3):241-267.

Balasubramaniam, V. M. 1993. Liquid-to-particle convective heat transfer in aseptic processing systems. Ph.D. Dissertation, The Ohio State University, Columbus.

Balasubramaniam, V. M., and Sastry S. K. 1994a. Convective heat transfer at particle interface in continuous tube flow at elevated fluid temperatures. J. of Food Science 59(3):675-681.

Balasubramaniam, V. M., and Sastry S. K. 1994b. Liquid-to-particle convective heat transfer in non-newtonian carrier medium during continuous tube flow. J. of Food Engineering, 23:169-187.

Balasubramaniam, V. M., and Sastry S. K. 1995. Use of liquid crystal as temperature sensors in food processing research. J. of Food Engineering, 26:219-230.

Balasubramaniam, V. M., and Sastry S. K. 1996a. Liquid-to-particle heat transfer in continuous tube-flow: Comparison between experimental techniques. J. Food Process Engineering, 31:177-187.

Balasubramaniam, V. M., and Sastry S. K. 1996b. Fluid to particle convective heat transfer coefficient in a horizontal scraped surface heat exchanger determined from relative velocity measurement. J. Food Process Engineering, 19:223-240.

Balasubramaniam, V. M., and Sastry S. K. 1996c. Estimation of convective heat transfer between fluid and particle in continuous flow using remote temperature sensor. J. Food Process Engineering, 19: 223-240.

Ball, C. O. and Olson, F. C. W. 1957. Sterilization in Food Technology, McGraw Hill Book. Co., New York, NY.

Baptista, P. N., Oliveira, F. A. R., Oliveira, J. C., and Sastry S. K., 1997a. The effect of translational and rotational relative velocity components on fluid-to-particle heat transfer coefficients in continuous tube flow. Food Res. Int., 30(1): 21-27.

Baptista, P. N., Oliveira, F. A. R., Oliveira, J. C., and Sastry S. K., 1997b. Dimensionless Analysis of fluid-to-particle heat transfer coefficients. J. Food Engineering, 31:199-218.

Bhamadipati, S. and Singh R. K. 1995. Determination of Fluid-Particle Convective Heat Transfer Coefficient. Trans. ASAE 38 (3):857-862.

Bourne, M. C., 1982. Food Texture and viscosity: concept and measurement. Academic Press. New York.

Brown, K. L. 1991. Principle of heat preservation. In "Processing and Packaging of Heat Preserved Foods. J. A. G. Rees and J. Bettison (eds.) Van Nostrand Reinhold. New York. pp. 72-91.

Brown K. L., Ayres C. A., Gaze J. E. and Newman, M. E. 1984. Thermal destruction of bacterial spores immobilized in food / alginate particles. Food Microbiology 1:187-198.

Brown, R. B. and Otten, L., 1992. Thermal conductivity and convective heat transfer coefficient for soybean and white bean seeds. Canadian Agricultural Engineering 34(4):337-341.

Buchner, N. 1993. Aseptic processing and packaging of particulates. In "Aseptic Processing and Processing of Particulate Foods". E. M. A. Willhoft (ed.). Blackie Academic and professionals. London. pp. 1-21.

Burfoot, D. and james, S. J., 1988. The effect of spatial variations of heat transfer coefficient on meet processing time. J. Food Engineering 7:41-61.

Carslaw, H. S. and Jaeger, J. C. 1959. Conduction of heat in solids. 2nd ed. Oxford University. Press. London. England.

Chakrabandhu K. and Singh R. K. 1998. Determination of fluid-to-particle heat transfer coefficients for rotating particles. J. of Food Process Engineering, 21: 327-350.

Chandarana, D. I. and Gavin, A. 1989a. Modeling and heat transfer studies of heterogeneous foods processed aseptically. In "Innovations in aseptic processing of particulates". J. V. Chambers. (ed). 1st Int. congress on aseptic processing technologies. Indianapolis, IN. USA, March 19-21.

Chandarana, D. I. and Gavin, A. 1989b. Establishing thermal process for heterogenous foods to be processed aseptically: a theoretical comparison of process development methods. J. Food Science, 54:198-204.

Chandarana, D. I., Gavin, A and Bernard D. T. 1987. Aseptic processing of particulates: Approval procedure. In " Food protection Technology " (C.W. Felix, Ed.), p. 387. Lewis Publishers, Inc. Chelsea, Michigan.

Chandarana, D. I., Gavin, A. and Wheaton, F. W. 1988. Particle/fluid interface heat transfer during aseptic processing of food. ASAE Paper No. 88-6599. American Society of Agricultural Engineers, St Joseph, MI.

Chandarana, D. I., Gavin, A. and Wheaton, F. W. 1989. Simulation of parameters for modelling of aseptic processing of food containing particulate. Food Technology, 43 (3): 137-143.

Chandarana, D. I., Gavin, A. and Wheaton, F. W. 1990. Particle/fluid interface heat transfer under UHT conditions at low particle/fluid relative velocity. J. of Food Process Engineering, 13: 191-206.

Chandarana, D. J. 1992. Acceptance procedure for aseptically processed particulate foods. In advances in aseptic processing technologies, (R. K. Singh and P. E. Nelson, eds.) Elsevier Applied Science, London.

Chandra P. K. and Singh, R. P. 1995. Applied numerical methods for food and agricultural engineers. CRC Press Inc., Florida, U.S.

Chandrana, D. I 1992. Acceptance procedure for aseptically processed particulate foods. In "Advances in Aseptic Processing Technologies." R. K. Singh and P. E. Nelson. Elsevier Applied Science. London & New York. pp 261-278.

Chang, S.Y. and Toledo, R. T. 1989. Heat transfer and simulated sterilization of particulate in continuously flowing system. J. Food Science, 54(4): 1017-1024.

Chang, S.Y. and Toledo, R. T. 1990. Simultaneous determination of thermal diffusivity and heat transfer coefficient during sterilization of carrot dices in a packed bed. J. Food Science, 55:199-205.

Chapman, A. J. 1989. Heat Transfer. 4th edition. Macmillan publishing Co. New York.

Chau, K.V. and Synder, G.V. 1988. Mathematical model for temperature distribution of thermally processed shrimp. Trans. ASAE. 31:608-612.

Chen, S. L., Yeh, A, and Swi-Bea Wu, J. 1997. Effects of particle radius, fluid viscosity and relative velocity on the surface heat transfer coefficient of spherical particles at low Reynolds numbers. J. of Food Eng. 31: 473-484.

Cousin, M. A. 1993. Microbiology of aseptic processing and packaging. In "Principles of Aseptic Processing and Packaging" , 2nd edition. pp. 47-86. P. E. Nelson and J. V. Chambers (eds.). The Food Processors Institute, Washington, D. C.

De Ruyter, P.W. and Brunet, R. 1973. Estimation of process conditions for continuous sterilization of foods containing particles. Food Technol. 27(7):44-51.

Deniston, M. F., Hassan, B. H., and Merson, R. 1987. Heat transfer coefficients to liquids with food particles in axially rotating cans. J. Food Science, 52:962-966.

Digeronimo, M., Garthright, W. and Larkin, J. W. 1997. Statistical design and analysis. Food Technology. 51:(10)52-56.

Dignan, D. M., Berry, M.R., Pflug, I.J. and Gardine, T.D. 1989. Safety considerations in establishing aseptic processing for low-acid foods containing particulates. Food Technology, 43:118-121.

Dutta, B. and Sastry, S.K. 1990a. Velocity distribution of food particle suspensions in holding tube flow: experimental and modeling studies on average particle velocities. J. Food Science, 55: 1448-1453.

Dutta, B. and Sastry, S.K. 1990b. Velocity distribution of food particle suspensions in holding tube flow: characteristics and fastest-particle velocities. J. Food Science, 55: 1703-1710.

Fichtail, J. 1990. Production f casein using extrusion technology. Ph.D. Thesis, McGill University, Montreal, Canada.

Gaze, J. E., Seen ce, L. E., Brown, C. D. and Holdsworth, S. D. 1990. Microbiological assessment of process lethality using food alginate particles. Tech. Memo. No. 580. Camden Food and Drink Research Assoc. Chipping Campend. pp. 1-47.

Grigull, U. and Sandner, H. 1984. Heat conduction. Hemisphere Publication Co. New York.

Grabowski, S. and Ramaswamy H. S. 1995. Characterization of single particle tube-flow behavior at elevated temperate. J. Food Process Engineering, 18:343-361.

Gun, D. J. and Narayanan, P. V. 1981. Particle-fluid heat transfer and dispersion in fluidized beds. Chem. Eng. Sci. 36: 1985-1995.

Hassan, B. H. 1984. Heat transfer coefficient for particles in axillary rotating cans, Ph.D. theses, Department of Agricultural Eng. University of California, Davis, CA.

Heisler, M. P. 1947. Temperature charts for induction and constant temperature heating. Trans ASME 69:227-236.

Heldman, D. R. 1989. Establishing aseptic processing for low-acid foods containing particulates. Food Technology 43(3):122-125.

Heppel, N. J. 1985. Measurement of the liquid-solid heat transfer coefficient during continuous sterilization of food stuffs containing particles. Presented at the 4th Congress on Engineering and Foods, Edmonton, AB, Canada, July 7-10.

Hinton, J., Driver, A., Silverman, M. G. and Taub, I. A., 1989. Validation of the thermal sterilization of particulates processed at elevated temperature. Activities Report of the R&D Associates. 41(1):39-49.

Holman, J. P. 1990. Heat Transfer. McGraw-Hill, Inc., New York, U.S.

Hunter, G. M. 1972. Continuous sterilization of liquid media containing suspended particles. Food Technol. Aust. 24: 158-165.

IFT Staff Report. 1989. Top 10 food science innovations: 1939-1989. Food Technology. 43 (9):309.

Incropera, F. P. and de Witt, D. P. 1990. Introduction to Heat Transfer, 2nd ed.. John Wiley & Son. New York.

Johnson, A. G. and Kirk, G., and Shin, T. 1988. Numerical and experimental analysis of mixed forced and natural convection about a sphere. Trans. ASAE Vol. 31(1): 293-299.

Kantt C. A., Schmidt S. J. and Sizer C. E. 1998. Temperature mapping of particles during aseptic processing with magnetic resonance imaging. J. Food Science 63(2):305-311.

Kelly, B. P., Megee, T. R. A. and Ahmed, M. N. 1995. Convective heat transfer in open channel flow: effect of geometric shape and flow characteristics. Trans IChem, Vol 73, part C.

Kramers, H. 1946. Heat transfer from spheres to flowing media. Physica. 12:61. Cited in Fluidization and fluid particle systems". F. A. Zenz and D. F. Othmer (eds). Reinhold Pub. Corp., New York., 1960.

Larkin, J. W. 1990. Mathematical analysis of critical parameters in aseptic particulate processing systems. J. Food Process Engineering, 13: 155-167.

Larkin, J. N. 1989. Use of modified Ball's formula method to evaluate aseptic processing of foods containing particulates. Food Technology, 43(3):124-131.

Lee, J. H. and Singh R. K., 1990. Mathematical models of scraped surface heat exchangers in relation to food sterilization. Chem. Eng. Commun., 87:21-51.

Lee, J. H., Singh R. K. and Larkin, J. W. 1990. Determination of lethality and process time in continuous sterilization system containig particulates. J. Food Eng. 11: 67-92.

Lens, M. K. and Lund, D. B. 1978. The lethality-Fourier number method. Heating rate variations and lethality confidence intervals for forced-convection heated foods in containers. J. Food Process Engineering, 2:227-271.

Leonard, S. J., Merson, R. L., Marsh, G. L. and Heil, J. R. 1986. Estimating thermal degradation in processing of food. J. Agri. Food Chem. 34 (3): 392-396.

Lopez, A. 1987. A complete course in canning: Book II. Canning Trade, Inc. Baltimore, MD.

Luikov, A. V. 1968. Analytical heat diffusion theory. Academic press, New York.

Lund, D. B. 1982. Influence of processing on nutrients in foods. J. Food Protection 45 (4): 367-373.

Lund, D. B. 1977. Design of thermal process for maximizing nutrient retention. Food Technology, 31 (2):71-78.

Lund, D. B. and Singh, R. K. 1993. The system and its elements. In " Principle of Aseptic Processing and Packaging". J. V. Chambers and P. E. Nelson (Eds.) pp: 3-30.

Maesmans, G., Hendrickx, M., Decordt, S., Fransis, A, and Tobback, P. 1992. Fluid-to-particle heat transfer coefficient determination of hetergenious foods: A review. J. Food Process and Preservative, 16:29-69.

Mankad, S., Nixon, K. M., and Fryer, P. J. 1997. Measurements of particle-liquid heat transfer in systems of varied solid fraction. J. Food Engineering, 31: 9-33.

Manson, J. E. and Cullen, J. F. 1974. Thermal process simulation for aseptic processing of food containing discrete particulate matter. J. Food Science, 39:1084-1089.

Marcy, J. E. 1997. Biological validation. Food Technology, 51(10):48-52.

Merson, R. L., Singh, R. P. and Carroad, P. A. 1978. An evaluation of Ball's formula method of thermal process calculations. Food Technology, 32(3):66-78.

Mitchel, E. L. 1988. A review of aseptic processing. Advances in Food Rese. 32:1-37.

Moffat, R. J. 1990. Some experimental method for heat transfer studies. Experimental Thermal and Fluid Science, 3: 14-32.

Mohsenin, N. N. 1980. Determination of thermal conductivity, thermal diffusivity, and unit surface conductance. In thermal properties of food and agricultural materials. Gordon and Breach, New York.

Murakami, E. G. and Okos, M. R. 1987. Heat transfer property studies of composite food, Paper 87-6541, American Society of Agricultural Engineers, St. Joseph, MI.

Mwangi, J. M, Datta, A. K and Rizvi, S. S. 1992. Heat transfer in aseptic processing of particulate foods. In "Advances in Aseptic Processing Technologies." R. K. Singh and P. E. Nelson. Elsiver Applied Science. London & New York. pp 73-102.

Mwangi, J. M., Rizvi, S. S. H. and Datta, K. A., 1993. Heat transfer to particles in shear flow: application in aseptic processing. J. Food Engineering 19:55-74.

Palaniappan S. and Sizer C. E. 1997. Aseptic process validated for foods containing particulates. Food Technology, 51(8):60-68.

Palmieri, L., Cacace, D., Dipollina, G and Dall Aglio, G. 1992. Residence time distribution of food suspensions containing large particles when flowing in tubular system. J. Food Engineering (17):225-239.

Ramaswamy, H. S., Lo, K. V., and Tung, M. A. 1982. Simplified equations for transient temperatures in conductive foods with convective heat transfer at the surface. J. Food Science, 47, 2042-7.

Ramaswamy, H. S., Tung, M. A. and Stark, R. 1983. A method to measure surface heat transfer from steam/air mixtures in batch retorts. J. Food Science, 48, 900-904.

Ramaswamy, H. H. and Gazala, S. 1990. Centerpoint nutrient degradation in heat processed conduction heating food model. J. Food Process Engineering, 12:159-169.

Ramaswamy, H. S., Abdelrahim, K. A., 1991. Thermal processing and food quality. In "Encyclopedia of food science and technology". pp:2538-2552, H. Y. Hue (Edt.) John Willey & Sons, New York.

Ramaswamy, H. S., Abdelrahim, K. A. and Smith, J. 1992a. Thermal processing and computer modelling. In "Encyclopedia of Food Science and Technology". Y. H. Hui (Edt.) John-Wiley & Sons, Inc. New York. NY, 2538-2552.

Ramaswamy, H. S., Pannue, K., Simpson, B. K. and Smith, J. P. 1992b. An apparatus for particle-to-fluid-relative velocity measurement in tube-flow at various temperatures under nonpressurized flow conditions. Food Research International, (25):227-284.

Ramaswamy, H. S., Abbatemarco, C., and Sablani, S. S. 1993. Heat transfer rates in a canned food model as influenced by processing in an end-over-end rotary steam/air retort. J. Food Process Preservation, 17, 269-286.

Ramaswamy, H. S., Abdelrahim, K. A ., Simpson, B. K., and Smith, J. P. 1995. Residence time distribution (RTD) in aseptic processing of particulate foods: a review. Food Research International, 28 (30):291-310.

Ramaswamy, H. S., Awuah, G. B. and Simpson, B. K. 1996. Influence of Particle characteristics on fluid-to-particle heat transfer coefficient in a pilot scale holding tube simulator. Food Research International, 29(3-4):291-300.

Ramaswamy, H. S., Awuah, G. B. and Simpson, B. K. 1997. Heat transfer and lethality consideration in aseptic processing of liquid/particle mixture: a review. Critical reviews in food science and nutrition 37(3):253-286.

Ranz, W. E. and W. R. Marshall, 1952. Evaporation from drop. Chem. Engineering Progress, 48: 141-147, 173-180.

Rao, M. A. 1992. Aseptic processing of foods. In "Biotechnology and Food Process Engineering". H. G. Schwaetzberg and M. A. Rao (eds.). Marcel Dekker, Inc. New york. pp. 247-268.

Richardson, P. and Holdworth, S.D., 1989. Characteristics of flow of food mixtures comprising liquids and particles, in Symp. Proc.: Recent development in aseptic technology, Camden Food and Drink Research Association, Chipping Campden, U.K., Dec.4-6.

Ronner, U. 1990. A new biological indicator for aseptic sterilization. Food Technology International Europe, 90:43-46.

Sablani, S. S. and Ramaswamy, H. S. 1995. Fluid-to-particle heat transfer coefficients in cans during end-over-end processing. Lebensm-Wiss. u.-Technol, 28:56-61.

Sablani, S. S., 1996. Heat transfer studies of particulate liquids in cans subjected to End-Over-End Processing. Ph.D. thesis submitted to faculty of graduate studies and research, McGill University, Montreal Canada.

Sablani, S. S. and Ramaswamy, H. S. 1996. Particle heat transfer coefficients under various retort operating conditions with end-over-end rotation. J. Food process Engineering, 19:403-425.

Sablani, S. S. and Ramaswamy, H. S. 1997. Heat transfer to particles in cans with end-over-end rotation: influence of particle size and concentration (V/V). J. Food Processing Engineering, 20:265-283.

Sablani, S. S., Ramaswamy, H. S. and Mujumdar, A. S. 1997. Dimensionless correlations for convective heat transfer to liquid and particles in cans subjected to end-over end rotation. J. Food Engineering, 34:453-472.

Sablani, S. S., and Ramaswamy, H. S. 1998. Multi-particle mixing behavior and its role in heat transfer during end-over-end agitation cans. J. Food Eng., 38:141-152.

Sastry, S. K. 1986. Mathematical evaluation of process schedules for aseptic processing of low-acid foods containing discrete particulates. J. Food Science, 51: 1323-1328.

Sastry, S. K. 1989. Aseptic technology for particulate foods: problems, issues and some potential solutions. Presented at the 1st International congress on aseptic processing technologies. Indianapolis, In, USA. March 19-21.

Sastry, S. K., 1992. Liquid-to-particle heat transfer coefficient in aseptic processing, in "Advances in Aseptic Processing Technologies", Singh, R. K. and Nelson, P. E., Eds., Elsevier Applied Science, London.

Sastry, S. K., 1993. Momentum and heat transfer in particulate sterilization. Paper No. B.2.3 presented at Third Conference of Food Engineering, CoFE'93,, Chicago, IL.

Sastry, S. K., 1997. Measuring residence time and modeling the system. Food Technology, 51:(10):44-48.

Sastry, S. K., Li, S. F., Patel, M., Konanayakam, M. Bafna, P., Doores, S. and Beelman, R. B. 1988. A bioindicator for validation of thermal process for particulates food. J. Food Science, 53:1528-1536.

Sastry, S. K. and Zuritz, C.A., 1987. A review of particle behaviour in tube flow: applications to aseptic processing. J. Food Process Engineering, 10:27-52.

Sastry, S. K., Heskitt, B. F, and Blasidel, J. L. 1989. Experimental and modeling studies on Convective heat transfer at particle-liquid interface in aseptic processing system. Food Technology, 43 (3): 132-136,143.

Sastry, S. K., Lima, M., Brim, J., Brunn, T. and Heskitt B. F. 1990. Liquid-to-particle heat transfer during continuous tube flow : influence of flow rate and particle to tube diameter ratio. J. of Food Process Engineering, 13: 239-253.

Segner, W. P., Ragusa, T. J., Marcus, C. L. and Soutter, E. A. 1989. Biological evaluation for sterilizing low acid large particulate foods for aseptic packaging. J. Food Proc. Preserv. 13:257-274.

Silva, C., Hendrickx, M., Oliveira, F. and Tobback, P. 1992. Critical evaluation of commonly used objective functions to optimize overall quality and nutrient retention of heat-preserved foods. J. Food Eng. 17:241-258.

Simpson, S. G. and Williams, M. C. 1974. An analysis of high temperature short time sterilization during laminar flow. J. Food Science, 39:1047-1054.

Singh, R. K. 1982. Thermal diffusivity food processing. Food Technology. 36(2):87-91.

Singh, R. K. 1987. Residence time distributions in aseptic processing. In "Principles of aseptic processing and packaging" pp 17-27, P. E. Nelson , J.V. Chambers and J. H. Rodgriguez (Eds), The Food Processors Institute, Washington D. C.

Singh, R. K. and Lee, J. H. 1992. Residence time distribution of foods with/without particulates in aseptic processing systems. In advances in aseptic processing technologies. R.K. Singh and P.E. Nelson. (Eds.) Elsevier Applied Science Publication, London.

Singh, R. P. and Heldman, D. R. 1993. Introduction to Food Engineering. 2nd Edn. Academic Press Inc. New York.

Stevenson, K. E., and Ito, K. A. 1991. Aseptic processing and packaging of heat preserved foods. In "processing and Packaging of Heat Preserved Foods". J. A. G. Rees and J. Bettison (eds.) Van Nostrand Reinhold. New York. pp. 72-91.

Stoforos, N. G. 1988. Heat transfer in axially rotating canned liquid/particulate food systems. Ph.D. thesis. Dept. of Agricultural Engineering University of California, Davis, CA.

Stoforos, N. G., Park, K. L. and Merson, R. L. 1989. Heat transfer in particulate foods during aseptic processing. Presented at the 1989 IFT Annual Meeting, Chicago, IL, USA.

Stoforos, N. G. and Merson, R. L., 1990. Estimating heat transfer coefficient in liquid/particulate canned food using only liquid temperature data. J. Food Science 55:478-483, 521.

Stoforos, N. G. and Merson, R. L., 1991. Measurement of heat transfer coefficient in rotating liquid/particulate system. Biotechnol. Prog. 7:267-271.

Stoforos, N. G., 1992. An overview of aseptic processing of particulate foods. In "Food Science and Human Nutrition." G. Charalambous, 1992. Elsevier Sc. Publishers. pp 665-677.

Stumbo, C. R. 1973. Thermobacteriology in Food Processing. Second edition, Academic Press, New York, NY.

Teixeira, A. A., Dixon, J. R. Zahradnik, J. W. and Zinsmeister, G. E. 1969a. Computer determination of spore survival distribution in thermally-processed conduction heated foods. Food Technol. 23, 352-354.

Teixeira, A. A., Dixon, J. R., Zahradnik, J. W. and Zinsmeister, G. E. 1969b. Computer optimization of nutrient retention in the thermal processing of conduction-heated foods. Food Technology, 23: 845-850.

Tewari, G. and Jayas, D. S. 1997. Heat transfer during thermal processing of liquid foods with or without particulate: a review. International Agricultural Engineering Journal, 6(1):1-27.

Toledo, R. T. and Chang, S.Y. 1990. Advantages of aseptic processing of fruits and vegetables. Food Technology, 44(2):72-76.

Weng, Z., Hendrickx, M., Maesmans, G. and Tobback, P. 1992. The use of time-temperature integrator in conjunction with mathematical modeling for determining liquid/particle heat transfer coefficients. J. Food Engineering, 16:197-214.

Weres, J., Jayas, D. S. and Ryniecki, A. 1999. An inverse heat transfer method for the estimation of convective heat transfer coefficient. International Agricultural Engineering Journal 8(1):45-55.

Whitaker, S., 1976. Elementary Heat Transfer Analysis. Pergamon Press Inc. New York.

Whitaker, S., 1972. Force convection heat transfer calculations for flow in pipes, past flat plates, single cylinder, single sphere and for flow in packed beds and tube bundles. J. AIChe. 18: 361-371.

Yuge, T, 1960. Experiments on heat transfer from spheres including combined and forced convection. J. Heat Transfer (82):214-220.

Zareifard M. R., S. Grabowski and H. S. Ramaswamy. 1996. Comparison of three methods of fluid-to-particle heat transfer coefficient evaluation under continuous flow conditions. Canadian Institute of Food Science and Technology (CIFST). Guelph, ON. August 19-22.

Zareifard M. R. and Ramaswamy, H. S. 1997. A new technique for evaluating fluid-to-particle heat transfer coefficients under tube-flow conditions involving particle oscillatory motion. J. of Food Process Engineering, 20(6): 453-475.

Zareifard M. R. and Ramaswamy, H. S. 1998. A calorimetric approach for fluid to particle heat transfer coefficient evaluation under tube-flow condition. Lebensm.-Wiss.u.-Technol. (*submitted*).

Zitoun, K. B. and Sastry, S. K. 1994a. Determination of convective heat transfer coefficient between fluid and cubic particles in continuous tube flow using noninvasive experimental techniques. J. Food Process Engineering, 17: 209-228.

Zitoun, K. B. and Sastry, S. K. 1994b. Convection heat transfer coefficient for cubic particles in continuous tube flow using the moving thermocouple method. J. of Food Process Eng. 17: 229-241.

Zuritz, C. A., McCoy, S. and Sastry, S. K. 1990. Convection heat transfer coefficients for irregular particles immersed in non-newtonian fluids during tube flow. J. Food Engineering, 11:159-174.